Rational Structural Diversification and Application of DalPhos Ligands for use in Challenging C-N Cross-Coupling Reactions

by

Mark A. MacLean

Submitted in partial fulfilment of the requirements
for the degree of Master of Science

at

Dalhousie University
Halifax, Nova Scotia
April 2013

DALHOUSIE UNIVERSITY

DEPARTMENT OF CHEMISTRY

The undersigned hereby certify that they have read and recommend to the Faculty of Graduate Studies for acceptance a thesis entitled "Rational Structural Diversification and Application of DalPhos Ligands for use in Challenging C-N Cross-Coupling Reactions" by Mark A. MacLean in partial fulfilment of the requirements for the degree of Master of Science.

Dated: April 22, 2013

Supervisor: _____

Readers: _____

_____

_____

Departmental Representative: _____

DALHOUSIE UNIVERSITY

DATE: April 22, 2013

AUTHOR: Mark A. MacLean

TITLE: Rational Structural Diversification and Application of DalPhos Ligands for use in Challenging C-N Cross-Coupling Reactions

DEPARTMENT OR SCHOOL: Department of Chemistry

DEGREE: MSc CONVOCATION: October YEAR: 2013

_____

Signature of Author

TABLE OF CONTENTS

LIST OF TABLES

LIST OF FIGURES

LIST OF SCHEMES

ABSTRACT

Transition-metal catalyzed transformations have revolutionized modern chemical synthesis; the 2001, 2005, and 2010 Nobel prizes in Chemistry attest to their broad applicability in academia and industry. To this end, advances in transition metal catalysis are rooted in the development of ancillary ligands that are capable of supporting electronically and coordinatively unsaturated metal centers. The Pd-catalyzed cross-coupling of amines and (hetero)aryl (pseudo)halides (Buchwald-Hartwig amination), to afford synthetically useful arylamines, has benefitted greatly in this regard.

The use of highly efficient P,N-phenylene ('DalPhos') ligands in challenging C-N cross-coupling reactions (e.g. hydrazine and ammonia monoarylation), has recently been disclosed by the Stradiotto group. Herein, a Pd/Mor-DalPhos catalyst system has been exploited for the preparation of a diverse range of (hetero)aryl hydrazines, useful synthons for the synthesis of myriad heterocyclic scaffolds, including *N*-aryl pyrazolones. These compounds have been identified as a potent class of anti-aggregants that may prevent the formation of toxic Aβ oligomer species, serving as candidates for the treatment of Alzheimer's Disease. Employing a tandem monoarylation/condensation protocol, 25 examples of structurally diverse Edaravone derivatives were afforded in good yield. Biological testing allowed for the identification of several compounds highly active toward inhibition of Aβ-40 and biotin-Aβ42 formation; their IC_{50} values were also determined.

Given the literature precedent for improved catalyst activity arising from subtle changes to the ancillary ligand framework, rational structural diversification of Mor-DalPhos has been achieved in an effort to improve efficiency. Eight new DalPhos variants prepared in good to excellent yield, featuring substitution of the phenylene-backbone with electron-withdrawing and donating groups, thiomorpholino substitution, and two structural isomers where the phenylene-backbone has been replaced with pyridine. New variants were combined with $[Pd(cinnamyl)Cl]_2$ to yield coordination complexes which may allow for a greater understanding of the catalytic cycle for BHA. Finally, new ligands were screened in a series of challenging C-X (X = N, C, O) cross-coupling reactions; a pyridine-bridged ligand variant displays unparalled activity in acetone arylation.

LIST OF ABBREVIATIONS AND SYMBOLS USED

Å	angstrom
δ	chemical shift
η	hapticity (contiguous donor atoms)
κ	hapticity (non-contiguous donor atoms)
1–Ad	1-adamantyl
AD	Alzheimer's Disease
app	apparent
aq	aqueous
BDE	bond dissociation energy
BHA	Buchwald-Hartwig Amination
BINAP	2,2'-bis(diphenylphosphino)-1,1'-binaphthalene
Bn	benzyl
br	broad
*n*Bu	*n*-butyl
*t*Bu	*tert*-butyl
BrettPhos	dicyclohexyl(2',4',6'-triisopropyl-3,6-dimethoxybiphenyl-2-yl)phosphine
cataCXium® A	di(1-adamantyl)-*n*-butylphosphine
cataCXium® ABn	di(1-adamantyl)benylphosphine
cataCXium® PtB	2-(di-*tert*-butyl-phosphino)-1-phenyl-1*H*-pyrrole
cataCXium® PIntB	2-(di-*tert*-butyl-phosphino)-1-phenylindole
cataCXium® PICy	2-(dicyclohexylphosphino)-1-(2,4,6-trimethyl-phenyl)-1*H*-imidazole
CM-phos	2-[2-(dicyclohexylphosphino)phenyl]-1-methyl-1*H*-indole
COSY	homonuclear shift correlation spectroscopy
Cy	cyclohexyl
d	doublet(s) *or* day(s)
DavePhos	2-dicyclohexylphosphino-2'-(*N,N*-dimethylamino)biphenyl
dba	dibenzylideneacetone

dd	doublet of doublet
ddd	doublet of doublets of doublets
DiPAMP	ethane-1,2-diylbis[(2-methoxyphenyl)phenylphosphane]
DPEPhos	(oxydi-2,1-phenylene)bis(diphenylphosphine)
DPPE	1,2-bis(diphenylphosphino)ethane
DPPF	bis(diphenylphosphino)ferrocene
DPPP	1,3-bis(diphenylphosphino)propane
D*i*PPF	1,1'-bis(diisopropylphosphino)ferrocene
DMSO	dimethyl sulfoxide
EDG	electron-donating group
ee	enantiomeric excess
equiv	equivalent
ESI	electrospray ionization
Et	ethyl
EWG	electron-withdrawing group
GC	gas chromatography
H	hour(s)
HRMS	high-resolution mass spectrometry
Hz	Hertz
IC_{50}	half maximal inhibitory concentration
$^{n}J_{xx'}$	n bond coupling constant between atom X and atom X'
JohnPhos	(2-biphenyl)di-*tert*-butylphosphine
JosiPhos	(*R*)-(-)-1-[(*S*)-2-(dicyclohexylphosphino)ferrocenyl]ethyldi-*tert*-butylphosphine
L-DOPA	L-3,4-dihydroxyphenylalanine
L	neutral 2-electron donor ligand
L_n	generic ligand set
M	generic transition metal or mol/L or molecular ion
m	multiplet *or* meta (if in italics)
m/z	mass-to-charge ratio

Me	methyl
Me-DalPhos	2-(di-1-adamantylphosphino)-*N,N*-dimethylaniline
min	minute(s)
mol	mole(s)
Mor-DalPhos	*N*-[2-di(1-adamantylphosphino)phenyl]morpholine
NaO*t*Bu	sodium *tert*-butoxide
NHC	*N*-heterocyclic carbene
NIS	*N*-iodosuccinimide
NMR	nuclear magnetic resonance
SAR	structure-activity relationship
ORTEP	Oak Ridge thermal ellipsoid plot
OAc	acetate
OMs	mesylate (methanesulfonate)
OTf	triflate (trifluoromethanesulfonate)
OTs	tosylate (*p*-toluenesulfonate)
o	ortho
p	para
Ph	phenyl
iPr	iso-propyl
ppm	parts per million
q	quartet
Rh	rhodium
rt	room temprature *or* reaction time
Ru	ruthenium
RuPhos	dicyclohexyl(2',6'-diisopropoxybiphenyl-2-yl)phosphine
sat	saturated
s	singlet
S_NAr	nucleophilic aromatic substitution
t	triplet
THF	tetrahydrofuran
TLC	thin-layer chromatography

TOF	turnover frequency
TFA	trifluoroacetic acid
T-20	Tween-20 (polyoxyethylene sorbitan monolaurate)
TMS	trimethylsilyl
TON	turnover number
X	generic anion *or* anionic ligand
Xantphos	4,5-bis(diphenylphosphino)-9,9-dimethylxanthene
XPhos	dicyclohexyl(2',4',6'-triisopropylbiphenyl-2-yl)phosphine

ACKNOWLEDGMENTS

First and foremost I would like to thank Dr. Mark Stradiotto for his invaluable leadership and assistance over the past two years. Mark's work ethic and passion for his career is nothing short of inspirational and has greatly contributed to my developing understanding of what it takes to be successful as a scientist and a professional. I will always remain grateful for being given the opportunity to pursue interesting research with such a talented chemist.

I would like to thank my parents Stuart and Charlotte for their understanding, patience, and overwhelming support. Also, Stradiotto group member Chris Lavery has not only become one of my best friends, I am thankful for his mentorship in the laboratory. Countless black gold and visits to see Gail made it all the more enjoyable. Thanks Wz.

I extend appreciation to those who have greatly assisted me in accomplishing the work detailed within this thesis. Dr. Craig Wheaton generously solved the crystal structures presented throughout Chapter 3, and was always available for helpful discussions. Dr. Sarah Crawford performed the screening reactions detailed in Section 3.3.3. Dr. Mike Lumsden (NMR-3) assisted in collection of the saturation transfer experiments presented in Section 3.3.2. Dr. Xiao Feng collected the mass-spectrometry data presented in throughout. I thank Drs. Mark Reed (Treventis Corporation) and Donald Weaver (Dalhousie) for their collaboration on the work disclosed in Chapter 2.

During my BSc I was lucky to have gained knowledge and experience from Dr. Roland Roesler (U of C) and Dr. Gonzalo Cosa (McGill), whom I thank for taking me on as a summer researcher. I would like to thank Dr. Laura Turculet for supervision during my honours project research, and for the very enjoyable courses I have taken with her. During my honours project I was fortunate to work under the supervision of Erin Morgan. Erin is an amazing individual and I wish her success in her future endeavors. Drs. Aleman, Burnell and Schepp are all excellent professors; I thank them greatly for their guidance in and out of the classroom over the past six years.

I thank the Natural Sciences and Engineering Research Council (NSERC) Canada who have provided me on multiple occasions with funding to conduct research I am passionate about.

CHAPTER 1. INTRODUCTION

1.1. THE UTILITY OF TRANSITION METAL CATALYSIS IN MODERN CHEMICAL SYNTHESIS

1.1.1. General Introduction

Transition metals have played a valuable role in advancing modern chemical synthesis over the past century. These are often employed in the form of organometallic complexes featuring one or more metal-centers supported by peripheral ancillary ligand(s). A systematic understanding of the principles that govern trends in structure and bonding for organometallic complexes is of utmost importance as these principles allow chemists to explain and predict the behavior of such complexes. In this context, the classification of ligands and metal-ligand bonding has allowed chemists to understand the influence of orbital interactions on reactivity; the field of transition metal catalysis has benefited greatly from this understanding.[1] Furthermore, the foundation upon which reaction chemistry featuring organometallic complexes has been developed depends on the ability to 'tune' their steric and electronic properties to enhance both activity and selectivity.

A diverse set of chemical transformations, such as alkene hydrogenation and methane oxidation, are thermodynamically favorable but suffer from limited reactivity under ambient conditions.[2] Transition metal catalysts have drastically increased the rate of reaction for such pathways, often maintaining mild and direct conversion without the requirement for stoichiometric amounts of precious metals. Sub-stoichiometric amounts of catalyst, as low as 1 ppm, have been reported for well-developed catalytic systems.[3] Effective systems that can be employed in low loading are desirable for their industrial applications. Originally developed on gram-scale in an academic setting, they are frequently applied in the ton-scale production of pharmaceuticals, natural products, optical devices, and fine-chemicals.[3c] Considering various hetero- and homogenous organometallic complexes, enzymes, and organic molecules may bear the ambiguous title of "catalyst", its use henceforth will be reserved for homogenous organometallic complexes.[4]

The impact of chemical processes on the environment started to receive increased attention during the early 1990's when many laboratories began placing an emphasis on

environmental sustainability.[5] It was during this period that the term 'green chemistry', which embodies clean and efficient chemical processes, was coined. Concepts such as atom economy, the ratio of molecular weight of desired produced to that of all products, were also introduced during this period.[6] As natural resources become further depleted, green chemistry will rely more heavily on synthetic methods that feature (metal) catalyzed reactions. Today, process research and development rely heavily on sustainable practices. Waste prevention instead of remediation, use of renewable raw materials, and a decrease in high waste-to-product ratios (5:1-100:1 by mass) are ways in which transition metal catalysis has revolutionized modern chemical synthesis.[5b,7]

It is now common to find metal-catalyzed transformations in most multi-step synthetic sequences. These processes demonstrate a streamlining effect on synthesis, allowing for the construction of complex organic frameworks in fewer steps than traditional stoichiometric reactions. The applicability of these reactions toward synthetic applications has been recognized by the 2001, 2005 and 2010 Nobel Prizes in Chemistry (Scheme 1.1). These awards are briefly described in the following sections and highlight important examples of transition metal catalyzed reactions made possible by the strategic design of catalysts.[1,3c]

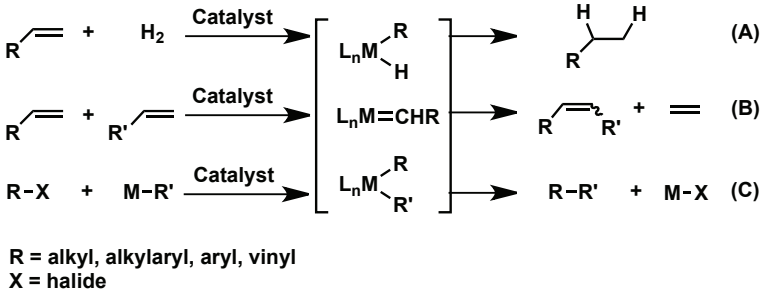

Scheme 1.1 Nobel prize winning transition-metal catalyzed reactions: hydrogenation (A), metathesis of olefins (B) and C-C cross-coupling (C).

1.1.2. The 2001 Nobel Prize in Chemistry: Asymmetric Hydrogenation

Asymmetric transformations, especially those that are catalytic, are relevant to a wide variety of biological transformations. Constituents of biological systems, such as the DNA and proteins of living organisms often exist in a single enantiomeric form. In this regard, a molecule is considered to be homochiral if its components are identical in chirality.[8] These concepts are important to consider in synthesis, specifically the

preparation of molecules applied in biological systems, where each enantiomer of a chiral molecule may draw a unique biological response. As the majority of products arising from the pharmaceutical industry are applied in biological settings, advances in this field have to a great extent resulted from the development of asymmetric catalysis.

Asymmetric catalysis was recognized for its broad applicability in synthetic chemistry via the 2001 Nobel Prize, half of which was awarded to William S. Knowles and Ryoji Nyori for their efforts toward asymmetric hydrogenation. No other method is as frequently employed for the construction of tertiary chiral stereocenters in an industrial setting. In 1968, Knowles discovered that Rh, among other late transition metals, was valuable in chiral-ligand supported metal complexes toward asymmetric hydrogenation. Specifically, Knowles used the (*R,R*)-enantiomer of DiPAMP in the first industrialized asymmetric hydrogenation reaction, synthesis of the Parkinson's treatment L-DOPA (Scheme 1.2).[9]

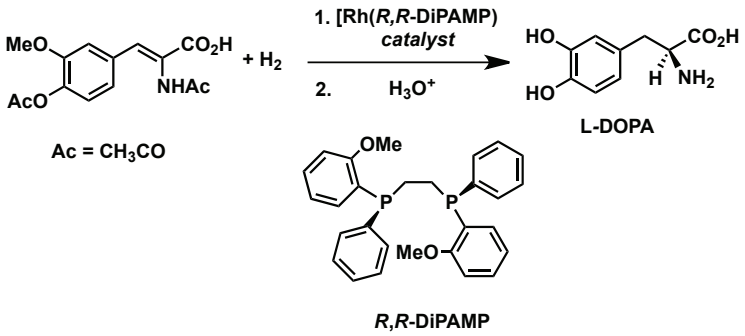

Scheme 1.2 Knowles enantioselective preparation of L-DOPA.

The classification of ligands and metal-ligand interactions plays a role in understanding the novel activity of catalysts. Indeed, Noyori's studies on metal-BINAP complexes have illustrated the importance of an atropisomeric, biaryl ligand backbone in chirality transfer.[10] Atropisomerism refers to ligands employed as a single stereoisomer, displaying axial chirality due to hindered rotation about the biaryl axis. The C_2-chiral BINAP ligand is available as either the (*R*)- or (*S*)- enantiomer (Figure 1.1). Through bisphosphines chelation, BINAP imparts a strong steric and electronic influence on transition metal centers. Tuning of the ligands by substitution at phosphorus or the aromatic backbone affords catalysts which actively impart chirality upon prochiral substrates.[10b]

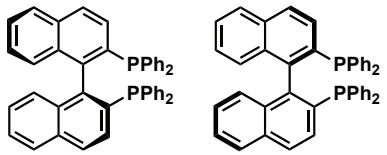

(*S*)-BINAP (*R*)-BINAP

Figure 1.1 Noyori's aromatic bisphosphine ligands, (*S*)- and (*R*)-BINAP.

In summary, the 2001 Nobel Prize in Chemistry has recognized enantioselective hydrogenation as an important transition metal catalyzed reaction. Furthermore, it highlights an excellent example of how strategic catalyst design can afford improved activity. Selectivity in challenging reactions (enantiomeric excess), decreased catalyst loadings, and simpler routes for ligand preparation may make this a cleaner more efficient process. Other notable research efforts include the design of various classes of chiral ligands. Aromatic bisphosphine, ferrocenyl backbone, aliphatic bisphosphine, *P*-chiral phosphines, and P,N ligands have been employed with success (Figure 1.2).

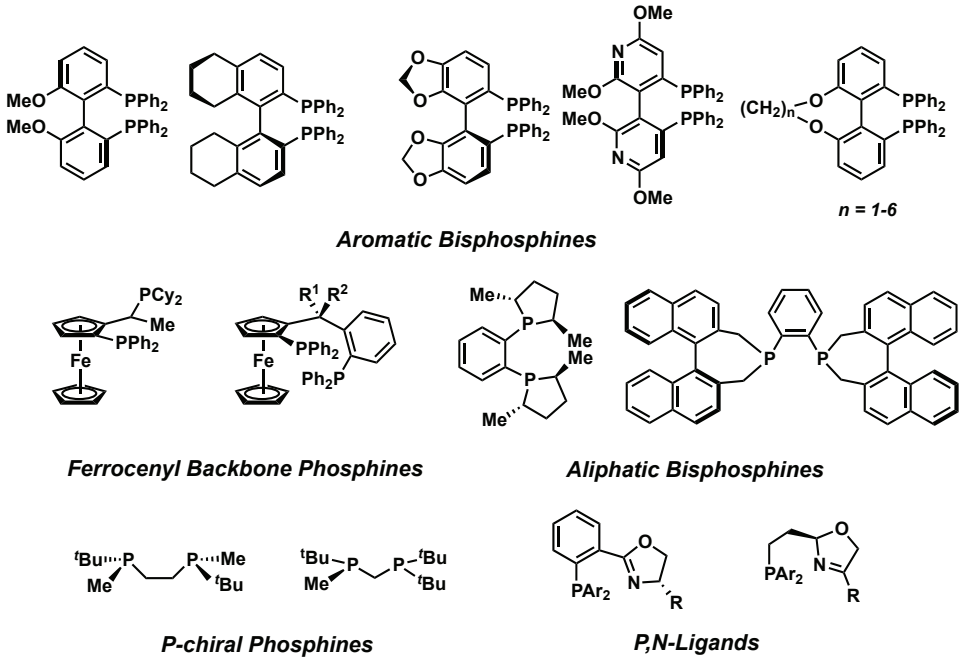

Figure 1.2 A selection of active ligands for asymmetric hydrogenation.

1.1.3. The 2005 Nobel Prize In Chemistry: Olefin Metathesis

The importance of transition metals in chemical synthesis was highlighted for a second time in 2005 with the Nobel Prize awarded to Yves Chauvin, Richard Schrock

and Robert Grubbs. These researchers jointly contributed to the development of the olefin metathesis process, a useful method for the cleavage and formation of carbon-carbon multiple bonds, catalyzed by organometallic complexes featuring early or late transition metals.[11] Chauvin is recognized for proposing the widely accepted mechanism of this process, featuring metallocarbene and metallocyclobutane intermediates. Following his studies, a variety of highly active and selective metallocarbene catalysts were designed by Schrock[11b] and Grubbs[11c] and are now commercially available for use in organic synthesis.

Karl Ziegler, a 1963 Nobel Laureate for polymerization studies, came across the first serendipitous finding regarding metathesis processes. A series of unexpected results and incorrect mechanisms reported by others involved in the field of polymerization (Scheme 1.3) [11a,12] led up to Chauvin's correct mechanistic proposal in the early 1970's. Today, Chauvin is recognized not only for the mechanism of olefin metathesis, but also for developing the Dimersol process, the first homogenous catalytic method in which coordination chemistry was used in refining gasoline. His processes for dimerizing small organic hydrocarbons have a combined annual output of 4.5 million tonnes.[11a]

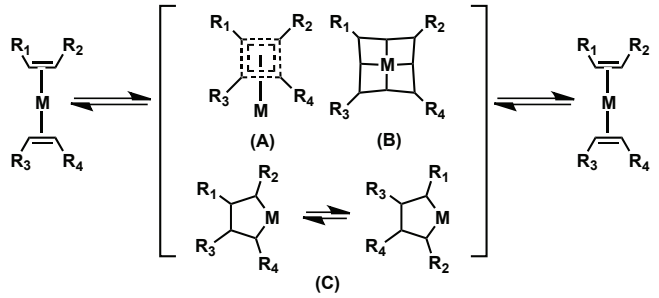

Scheme 1.3 Rejected intermediates for the olefin metathesis mechanism; (A) "quasicyclobutane" complex (B) tetramethylene complex (C) metallocyclopentane isomers.

In the early 1950's, prior to the discovery of metal-carbon double bonds, Ziegler was studying organometallic complexes in ethylene polymerization when he unexpectedly identified 1-butene as a reaction product as opposed to the expected longer-chain hydrocarbons; upon closer examination he detected the presence of nickel species.[13] Although these salts were not characterized at the time, nickel catalysts have since been exploited in various catalytic applications, for example, in the Shell higher

olefin process for the production of linear α-olefins.[14] Nearly a decade after Ziegler's finding, researchers at DuPont attempted polymerization of norbornene when they discovered a product resulting from an unexpected ring-opening process [15] Subsequently, Phillips Petroleum Co.,[16] and Goodyear Tire and Rubber Company,[17] detailed the conversion of propylene, to ethylene and 2-butene (olefin disproportionation). While these findings did not appear related, they were consistent with a pair-wise mechanism invoking diolefin intermediates.[11c]

Despite the aforementioned findings that supported pair-wise olefin disproportionation, Chauvin reported on a non-pair-wise process involving metal-carbene intermediates (Scheme 1.4). Schrock used the alkoxide-ligated tantalum-alkylidene complex, [Ta(=CH*t*Bu)Cl(PMe$_3$)(O*t*Bu)$_2$] to catalyze the metathesis of *cis*-2-pentene, validating intermediates required by Chauvin.[18] Grubbs used a ring-closing metathesis reaction and examined the statistical distribution of reaction products, a distribution that varies for pair-wise and non-pair-wise mechanisms.[19] Schrock and Grubbs have independently developed highly active homogenous catalysts featuring molybdenum and ruthenium, respectively (Figure 1.3).

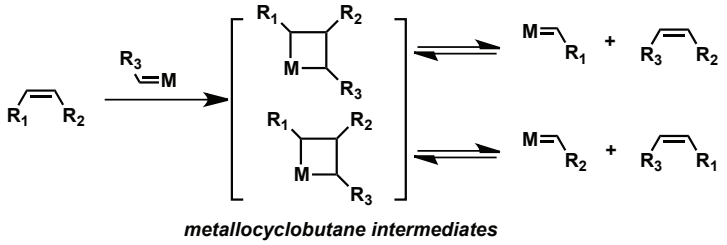

Scheme 1.4 Chauvin's non-pair-wise mechanism for olefin metathesis.

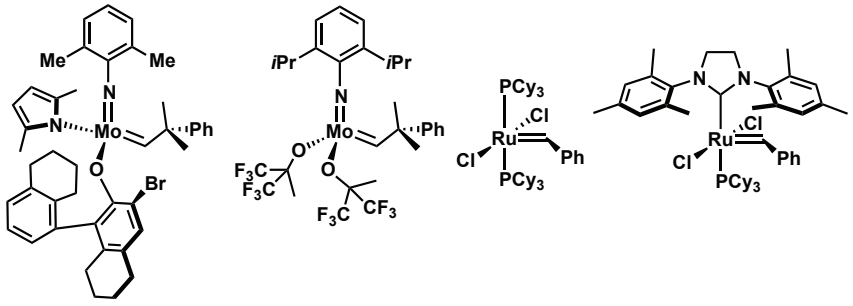

Figure 1.3 Highly active olefin metathesis catalysts featuring molybdenum (Schrock) and ruthenium (Grubbs).

Grubbs catalysts for olefin metathesis provide an excellent example of how mechanistic studies may correlate catalyst structure and activity. First-generation catalysts rely upon Ru(II) supported by electron rich tertiary phosphine ligands, undergoing mono-phosphine dissociation *in situ* to afford a highly active 14-electron species. To improve catalyst stability and activity, a second-generation catalyst was prepared by exchange of a tertiary phosphine ligand for a strongly electron donating, sterically bulky *N*-heterocylic carbene (NHC). It was eventually discovered that the increase in activity owed to a preference for the binding of π-acids over dissociated phosphine. [20]

Grubbs and Schrock catalysts are now employed in all known classes of olefin metathesis, including those that are enantioselective. Their uses range from the opening of strained rings to produce polymers, to application in cross-metathesis to form unsymmetrical olefins.[12b,21] Current research efforts involve the strategic design of catalysts with improved air and moisture stability, as well as excellent kinetic selectivity for *E* and *Z* isomers and cross-metathesis products.[22]

1.1.4. The 2010 Nobel Prize in Chemistry: Palladium-Catalyzed Carbon-Carbon Bond Formation in Organic Synthesis

Cross-coupling reactions involve aryl, and vinyl, (pseudo)halide electrophiles substituted by a nucleophile in the presence of a transition-metal complex. Recently, the viability of heteroatomic coupling partners and sp^3-hybrized nucleophiles and electrophiles has been demonstrated. In this regard, the preparation of enantio-enriched coupling products is of interest in medicinal and process chemistry.[9] The broad applicability of these reactions in synthesis is rigorously documented in the chemical literature and they have been featured in a variety of special themed journal issues.[23]

Perhaps there is no better example that demonstrates the utility of homogenous catalysis toward highly selective synthetic procedures, than that of palladium-catalyzed cross-couplings to afford carbon-carbon (C-C), and carbon-heteroatom bonds (C-X; X = N, O, S, F, etc).[24] Richard F. Heck, Ei-ichi Negishi, and Akira Suzuki pioneered the field of C-C cross-coupling and were recognized for their contributions in the form of the 2010 Nobel Prize in Chemistry. Synthetic chemists now exploit these reactions (Scheme 1.5) as alternatives to the existing array of protocols for C-C bond formation. As of the 21st

century Pd-catalyzed cross-coupling has become an indispensable tool for the synthesis of pharmaceuticals and natural products in both academia and industry.[3c,25]

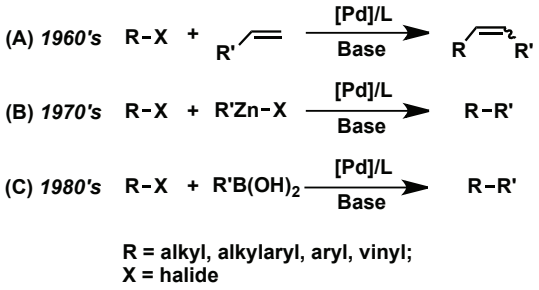

Scheme 1.5 Significant advances in Pd-catalyzed C-C bond forming reactions: (A) Heck (B) Negishi and (C) Suzuki coupling reactions.

Heck, Negishi and Suzuki reactions employ carbon-based nucleophiles featuring olefins, zinc, or boron, respectively. Suzuki reactions couple aryl, alkyl, alkenyl and allyl carbon-boron reagents with aryl, alkenyl or alkyl halide electrophiles. Negishi couplings are similar in terms of mechanism and electrophiles employed, however, nucleophilic coupling partners are delivered via organozinc compounds. Heck coupling was the first of these reactions to be reported in the late 1960's and affords substituted olefins by the direct functionalization of their C-H bonds with aryl or alkenyl halides.[26] The development of these reactions into synthetically useful tools is realized in complex pharmaceutical and natural product design featuring biaryl motifs (Scheme 1.6).[27]

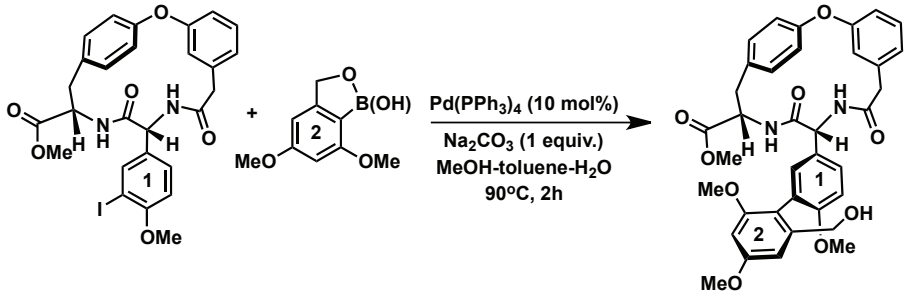

Scheme 1.6 Pd-catalyzed Suzuki coupling: generating a key intermediate in the total synthesis of the antibiotic Vancomycin.

An understanding of how ligated-metal complexes perform in stoichiometric reactions may allow chemists to establish organometallic principles that relate to the viability of intermediates present in catalytic cycles.[28] Regarding cross-coupling, this rationale may be applied to substantiate intermediate steps such as oxidative addition,

transmetalation, and reductive elimination (Scheme 1.7 left). The catalytic cycle for Heck coupling bears similarity to Negishi and Suzuki reactions, proceeding via oxidative addition and reductive elimination components. However, the transmetalation step does not involve the delivery of a nucleophilic component using stoichiometric organo-metal reagents. Instead, a palladium-alkyl species is generated upon olefin coordination and migratory insertion into the Pd-electrophile bond. Following C-C bond rotation of the alkyl fragment this species undergoes β-hydride elimination to afford the desired product, dehydrohalogenation by base regenerates the low-valent Pd(0) catalyst (Scheme 1.7 right).[1,29]

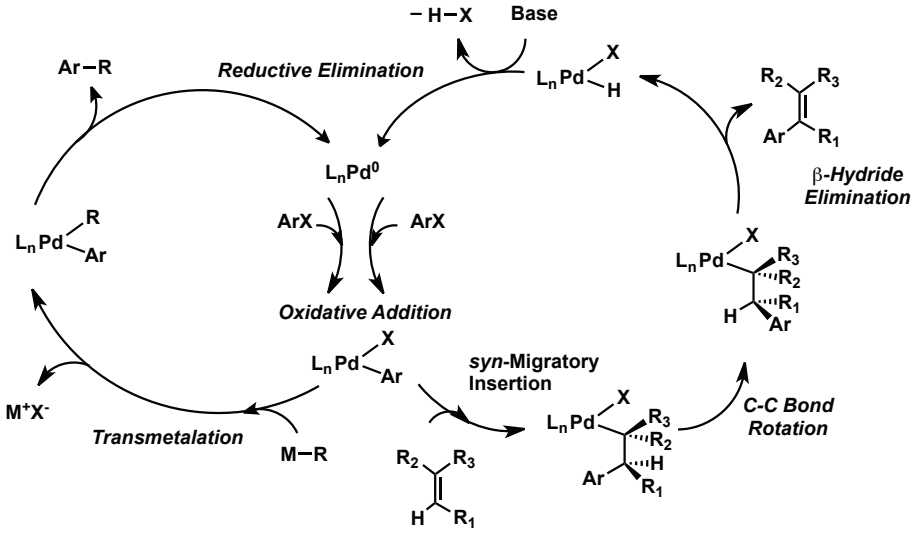

Scheme 1.7 Prototypical catalytic cycles for Negishi and Suzuki (left), and Heck (right) cross-coupling reactions.

To expand the broad applicability and cost-effectiveness of Pd-mediated processes, decreasing the cost of ligand and metal catalyst components, reducing reaction times, and developing robust complexes to prevent aggregate 'palladium-black' formation are the focus of current research efforts. Strategic alterations to the ligand set has enabled robust systems to operate with high efficiency, in some cases catalyst turn-over numbers are as high as 10^6.[24f,30] In process chemistry, removal of Pd-residue from final products is essential. This procedure is assisted by high turn-over numbers, typically between 1000-10000 are required before a precious-metal catalyzed route will be

implemented in the production of fine chemicals; palladium remains the most commonly employed metal for these catalytic transformations.[24f,31]

The discovery and development of transition metal-mediated C-C bond forming reactions by Heck, Negishi and Suzuki have inspired the development of many other synthetically useful C-X cross-coupling reactions. In this context, the cross-coupling of aryl or vinyl (pseudo)halides and N-H containing compounds (Buchwald-Hartwig amination) has emerged as an important method in both academia and industry for the construction of C-N bonds over the past two decades. Mechanistic studies of structure and bonding for ligated-palladium complexes in C-N cross-coupling has inspired the development of highly active catalysts. Ligand design has been key to this endeavor, allowing chemists to validate a relationship between the structure of metal-ligand complexes and observed catalytic activity in challenging metal-catalyzed reactions.[32]

1.2. CONVENTIONAL C-N BOND FORMING METHODOLOGIES

Classic reactions that rely on organometallic complexes to form C-C and C-H bonds have dominated the focus of research efforts throughout the 20th century. In the previous section (1.1), Pd-catalyzed cross-coupling chemistry was highlighted as an important replacement for stoichiometric alternatives to C-C bond formation, offering improved atom economy and broad applicability in a variety of important synthetic transformations. Today, Pd-catalyzed carbon-nitrogen (highlighted in this section),[28,33] carbon-oxygen,[34] carbon-sulfur,[35] and carbon-halide[36] bond forming strategies are available to the synthetic chemist. Despite many advances in cross-coupling methodologies that exploit Pd, it is not the only useful transition-metal for cross-coupling reactions. The following section describes conventional and alternative non-Pd based bond forming strategies, with a particular focus on the use of Cu in Ullmann coupling.

1.2.1. Stoichiometric Methods for the Construction of C-N Bonds

Cross-coupling methodologies have emerged as alternatives to a variety of classic methods (Scheme 1.8) for the construction of C-N bonds. Most of these classic reactions lack scope, call for harsh reactions conditions, or use inconvenient reagents. This is certainly the case regarding the preparation of valuable nitrogen-containing aromatics by the well-known nitration-reduction reaction.[29] The electrophilic aromatic substitution (nitration) of benzene with HNO_3 and H_2SO_4 serves as a precursor to aniline, afforded by

subsequent treatment of nitrobenzene with an acidic solution of tin or iron, or alternatively, H_2 in the presence of heterogeneous Pd/C. Alternatively, nucleophilic aromatic substitution (S_NAr) of aryl halides is also frequently used to substitute arenes with amine coupling partners; limited scope (EWG groups are required for substitution on the aryl halide) inhibit practicality. A variety of other methods, such as aliphatic nucleophilic substitution to generate alkyl-amines, reductive amination and the well-known Mannich reaction, are still applied in organic synthesis but are not useful when working with sensitive, functionalized substrates.[14]

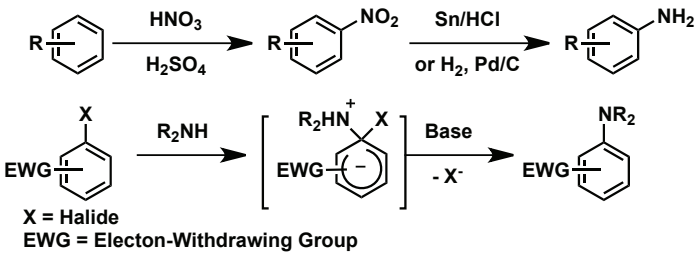

Scheme 1.8 Well-known C-N bond forming methods: electrophilic (top) and nucleophilic (bottom) aromatic substitution.

1.2.2. Cu-Catalyzed Cross-Coupling

The use organometallic complexes featuring coinage-metals for cross-coupling reactions spans the 20th century. Iron,[37] copper[24d,31b,34f,38] and nickel[39] began garnishing attention far before precious metals such as palladium were recognized as being advantageous. Ullmann-Goldberg chemistry represents the first metal-mediated C-N bond formation process, discovered in the early 1900's. These reactions allow the stoichiometric[40] and catalytic[41] preparation of aryl amines (Scheme 1.9). High loadings and temperature (> 200 ^{o}C) are typically required for such reactions. Despite representing the first route to biaryl amines, limited scope and intolerance toward the coupling of electron-rich arenes limit the utility of these processes. Furthermore, this methodology does not typically tolerate the coupling of aryl chloride substrates.

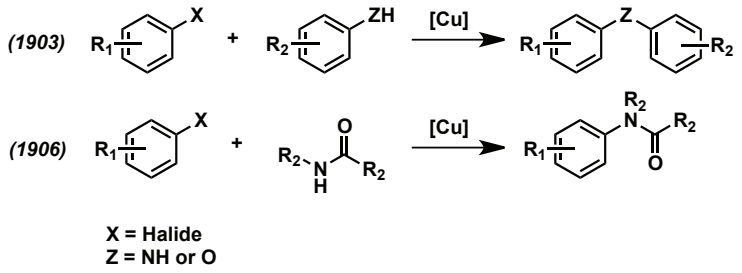

Scheme 1.9 Cu-catalyzed Ullmann (1903) and Goldberg (1906) reactions.

The use of ligated-Pd complexes in C-N cross-coupling reactions have received far more attention than those employing Cu. Pd often supersedes first-row (3*d*) metal alternatives by enabling milder reaction conditions, higher yields, and the conversion of less reactive coupling partners such as hindered and electron-rich aryl chloride electrophiles.[24e,24g,38c] It should be noted that Pd-catalyzed reactions are more efficient for nucleophiles that yield higher rates of reductive elimination; a balance of free amine nucleophilicity and NH acidity of the bonded nucleophile must be considered.[24d] In this regard, Pd-systems work well with strongly nucleophilic alkyl-amines as well as aromatic amines, which represent a middle-ground between NH-acidity and nucleophilicity of the free amine. Cu-catalyzed systems are better suited to strongly NH-acidic substrates such as sulfonamide, amide and azoles,[42] while working poorly for aromatic or aliphatic amines, where bases strong enough to deprotonate these substrates are not commonly employed. Considering substrate preference in C-N cross-coupling relies on electronic and steric preferences from the perspective of amine and aryl electrophiles, it is not surprising that only loose trends for Cu have been determined.

Recent reviews highlight a growing, renewed interest in Ullmann-Goldberg chemistry and suggest that a deficit in mechanistic understanding of the catalytic processes employing Cu has contributed to their slower development compared to Pd.[24d] The difficulty in studying Cu-catalyzed mechanisms is largely due to the instability of viable catalytic intermediates. It is proposed that Cu(I)/Cu(III) oxidation states may be called for *in situ*, isoelectronic (d^8/d^{10}) with well known Pd(0)/Pd(II) cycles. Cu(III) complexes are known to be difficult to isolate and highly oxidizing; reported instances where they are stabilized by ancillary ligands are often limited to those bearing polyfluoroalkyl groups.[38c,43]

Although "ligandless" Cu(I) precatalysts are frequently employed in catalysis, considering the potential viability of reactive Cu(III) species in catalytic cycles, ancillary ligands capable of stabilizing these intermediates are desirable. Cu(I) is isoelectronic with Ni(0) and prefers ligands featuring hard donors like N and O as opposed to bulky tertiary phosphines like those preferred by 4*d* complexes (Figure 1.4).[1] This preference owes partially to a smaller coordination sphere, limiting the ability for ligand tuning. The vast number of strategically ligated-Pd complexes characterized, compared to a lack of those supported by Cu, sheds light on the importance of ligand design toward successful catalyst developments with Pd. To this end, differences in activity between Pd and Cu in the cross-coupling of NH-containing nucleophiles owes to precise control of the Pd coordination sphere using ancillary ligands and differing soft/hard bonding preferences (Section 1.4).[43a]

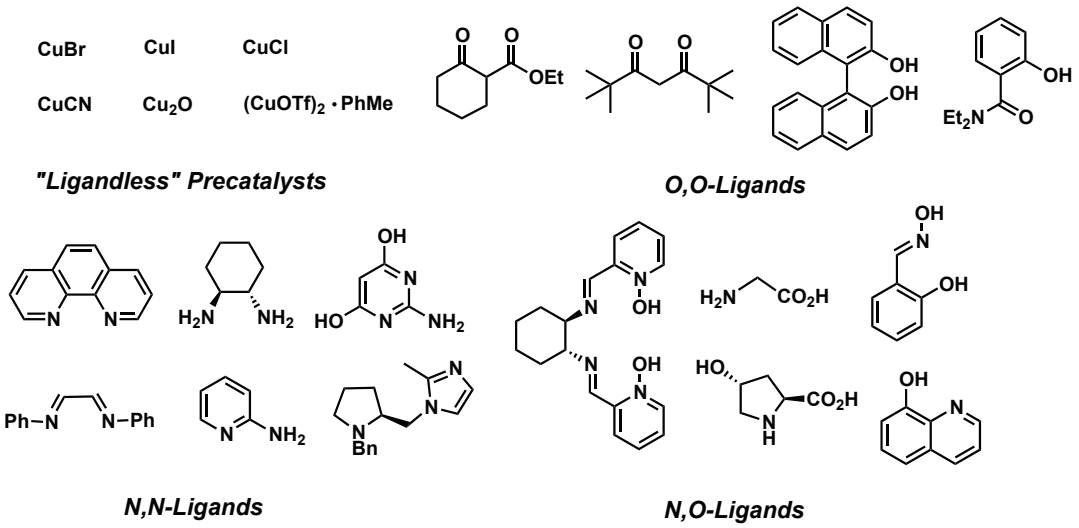

Figure 1.4 Selected ligand classes and precatalysts for Cu-catalyzed C-N cross-coupling reactions.

Current research efforts are focused on allowing for milder reaction conditions, ideally room temperature reactions.[24d] In this regard, Cu-catalyzed formation of Ullmann condensation products have benefited greatly from tuning of reaction conditions such as solvent, base, and other additives that may serve as ligands *in situ*. Studies examining Cu(III) intermediates via reductive elimination from Cu-halide species,[44] and the use of aryl boronic acid coupling partners[45] have been useful toward achieving milder

conditions and broadening scope. The groups of Buchwald and Hartwig have used Cu in amidation reactions, and for the coupling of nitrogen-containing heterocycles.[38d,46] Seminal work published in 2012 by Peters and Fu established photo-induced Cu-catalyzed methods for *N*-arylation and *N*-alkylation reactions (Scheme 1.10) under extraordinarily mild conditions (room temperature to -40 ^{o}C).[38a]

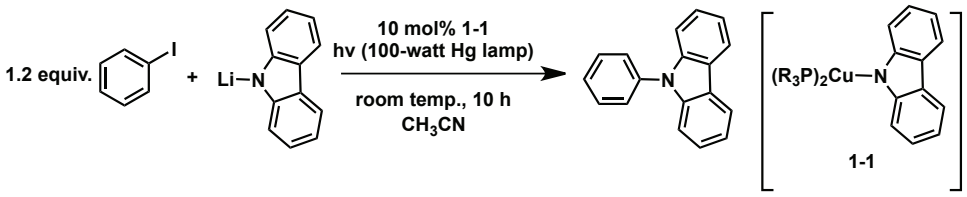

Scheme 1.10 Photo-induced Ullmann coupling catalyzed by **1-1**.

Capitalizing on the photoluminescence of Cu-carbazolide complexes, this work has provided an inroad to practical Ullmann coupling methods and the long sought after mechanism of this classic reaction. While concerted oxidative addition following amine coordination has been proposed for Cu catalyzed C-X bond cleavage, evidence is presented substantiating a photo-induced radical intermediate. While the authors report this single-electron-transfer mechanism is not necessarily indicative of a general mechanism by which Ullmann couplings proceed, they do confirm that a carbon-centered radical leads to C-N bond formation under mild reaction conditions.[38a]

In summary, the synthesis of complex organic frameworks from sensitive, functionalized substrates could conceivably benefit from the discovery of C-N bond forming systems that employ economically advantageous Cu sources. However, further work regarding identification of reactive intermediates and Cu-complexes supported by ancillary ligands is needed. In this regard, Pd-catalyzed C-N bond formation remains the state-of-the-art and is addressed in the following section.

1.3. BUCHWALD-HARTWIG AMINATION

Buchwald-Hartwig amination (BHA) is a Pd-catalyzed cross-coupling methodology that affords novel products from aryl or vinyl pseudo(halides) and N-H containing reagents. BHA has emerged as a useful synthetic carbon-heteroatom bond forming strategy as it allows for diversification of complex molecules via connection of functionalized substrates. Although it was noted in the previous section that Cu sources

may be employed toward the selective monoarylation of aryl and alkyl nucleophiles, they typically require high loading and temperature.[24d,40-41] No other transition-metal catalyzed processes are as broadly applicable in C-N cross-coupling as those featuring ligated-Pd species.

Various concepts are used to assess the applicability of catalysts, including those for BHA in industrial settings; two recurrent examples include catalyst productivity (TON) and activity (TOF). Perhaps just as important are chemo-, regio-, and stereoselectivity (collectively referred to as 'selectivity') which also determine the ability of catalysts to expedite the synthesis of pharmaceuticals, natural products, organic materials, as well as electronics, polymers and liquid crystals.[31c,47] Furthermore, high levels of selectivity allow synthetic chemists to prepare small libraries of compounds (arrays) and establish their structure-activity relationships (SARs) against biological targets (presented in Chapter 2).[31c] Historical developments, mechanistic consideration, and the evolution of catalysts for the BHA reaction are discussed below.

1.3.1. Historical Developments: Aminostannane Coupling Partners

To place the historical development of BHA into context, it is important to credit C-C bond forming strategies such as Stille coupling. In 1977 John Stille discovered a general, selective Pd-catalyzed method for ketone synthesis from acid chlorides and organo-tin compounds, bypassing the need for organo-lithium or Grignard reagents which react with the product ketone.[48]

This seminal discovery likely gave rise to the first Pd-catalyzed C-N cross-coupling reaction published using similar conditions only 5 years later by Migita and co-workers (Scheme 1.11), describing the mild coupling of aryl bromides and the toxic (*N,N*-diethylamino)tributyltin. Catalyzed by $PdCl_2[P(o\text{-tolyl}_3)]_2$, this process was considered to be inconsistent with other well-known C-N bond forming mechanisms invoking nonregiospecific benzyne, or reducing radical ($S_{RN}1$), intermediates.[49]

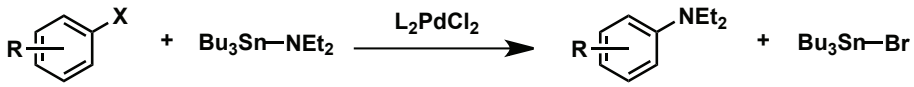

Scheme 1.11 Migita's palladium-catalyzed aromatic amination of aryl bromides with (*N,N*-diethylamino)tributyltin.

After going un-referenced for nearly a decade, Buchwald expanded Migita's work by generating aminostannanes *in situ*. This route accommodated 1° and 2° anilines, as well as 2° aliphatic amines[50]. Unfortunately, this reaction was intolerant of *o*-substitution on the aryl halide, and aryl bromides were the only viable aryl halide coupling partner. The best ancillary ligand tested for promoting these transformations was P(o-tolyl)$_3$, a result consistent with those found by Migita. The importance of ligand choice became obvious as $PdCl_2L_2$ catalysts (where L = PPh_3, DPPF, or DPPE) did not generate the desired arylamine with the same efficiency.[50] Concurrent studies by Hartwig detailed catalytic turnover for the cross-coupling of aryl halides and tin-amides as well as key intermediates in the catalytic cycle.[51]

In order to eliminate the requirement for stoichiometric quantities of tin and allow for coupling of primary amines, Buchwald sought other main-group reagents capable of performing transmetalation. The delivery of amine coupling partners via aminoboron derivatives temporarily served this purpose.[52] Aminoboron and aminostannane derivatives were rendered useless when Buchwald[52] and Hartwig[53] revealed catalytic systems for the coupling of secondary amines with electron rich-, and poor-aryl bromides in the presence of stoichiometric sodium *tert*-butoxide (NaO*t*Bu) or bis(trimethylsilyl)amide bases, respectively. Other palladium sources being explored at this time, such as $Pd(dba)_2$ and $PdCl_2$, allowed Pd(II) sources to be accommodated as viable starting materials, requiring pre-activation by a reductant.

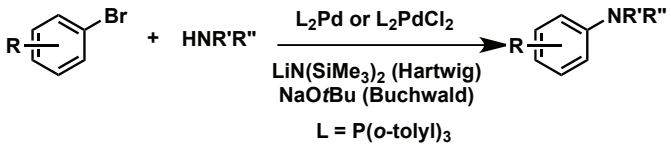

Scheme 1.12 Base-assisted Pd-catalyzed amination in the absence of tin reagents.

Despite these advances, aryl iodides and aryl chlorides remained unsuitable coupling partners; less expensive aryl chlorides represent ideal substrates as they are

available in great diversity.[24g] Advancing the scope and applicability of the Buchwald-Hartwig amination reaction to allow challenging aryl halides and 1^{o} amines to serve as viable coupling partners has required a detailed understanding of the reaction mechanism. This understanding has been developed through careful examination of the components that comprise the catalytic system, discussed in Section 1.3.2 and 1.3.3.

1.3.2. The Mechanism for Buchwald-Hartwig Amination

In Migita's early report on the coupling of aryl bromides and Sn-amides he proposed a mechanism that invoked oxidative addition, transmetalation and reductive elimination. Subsequent investigation, revealed in a surge of publications a decade later from the groups of Hartwig and Buchwald, validated this mechanistic proposal.[50-54]

In 1994, Hartwig revisited Migita's results and identified crystallographically, kinetically competent intermediates of a catalytic cycle for the synthesis of *N,N*-dialkylanilines using a $PdX_2[P(o\text{-tolyl}_3)]_2$ (X = Cl or Br) catalyst (Scheme 1.13). It was determined that reversible dissociation of phosphine occurs to generate mono-ligated Pd(0), whereas excess phosphine inhibits catalytic turnover. Also, dimeric species irreversibly dissociate to monomeric Pd(0) in the presence of Sn reagents, suggesting Sn transmetalation to be rate-limiting (consistent with Stille coupling).[51,54] Although these findings are useful toward rationalizing the behavior of ligated-Pd species, carrying out BHA reactions with stoichiometric quantities of base, foregoing the use of highly toxic main-group transmetalating reagents requires an alternative mechanism.

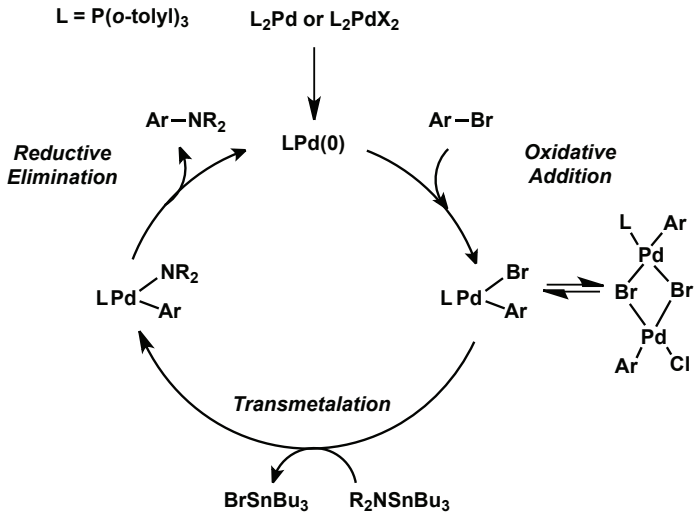

Scheme 1.13 Hartwig's proposed catalytic cycle for the Pd-catalyzed cross-coupling of aryl halides and aminostannes.

Entering the catalytic cycle (Scheme 1.14) calls for either ligand dissociation from a Pd(0) precatalyst, or *in situ* reduction of a L_nPdX_2 complex (L_n = supporting ancillary ligand(s), X = halide or organic leaving group). Each pathway similarly affords a 12- or 14-electron $L_nPd(0)$ species, depending upon denticity of the chosen ancillary ligand. The first step of the cycle proceeds via oxidative addition of aryl (pseudo)halide to Pd(0). Considering the activated Pd(0) species represents the resting state of the catalyst, the oxidative addition step is often rate-limiting (refer to section 1.5.2 for an exception) and is affected by a variety of electronic and steric factors. In contrast to the transmetalation of tin-amides, there are two primary routes by which the Pd(II)aryl(amido) intermediate may be generated following oxidative addition, when using alkoxide bases.

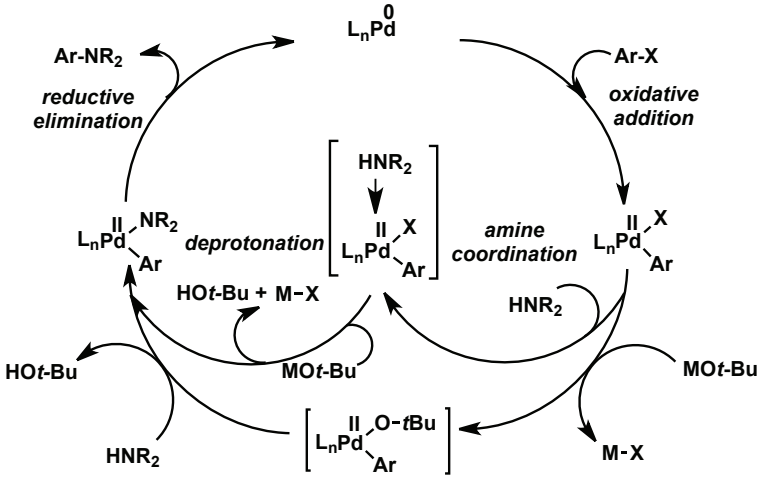

Scheme 1.14 Proposed catalytic pathways for the Buchwald-Hartwig amination reaction.

The first route invokes formation of a Pd(II)aryl(alkoxide) with loss of the respective metal-salt (M-X). Subsequent addition of amine results in protonation and displacement of the alkoxide fragment as alcohol. In the majority of cases however where the amine N-H is of low acidity, it is likely that amine coordination occurs following oxidative addition, and the complexed amineundergoes subsequent deprotonation. Regardless of the mechanism by which the Pd(II)aryl(amido) complex is formed, reductive elimination has a major effect on reaction scope and yield, and in many systems represents the rate-limiting step.[1]

1.3.3. Catalyst Considerations

The general mechanism (Section 1.3.2) for BHA depends on numerous interplaying factors, and it is likely for this reason a universal set of conditions does not exist. Carefully designed experiments (a statistical Design of Experiment approach)[32] are employed in order to facilitate optimization of reaction conditions such as Pd source, ligand, base, solvent and temperature, all of which depend on substrate choice. Also, amine substrates may influence key steps in the catalytic cycle, depending specifically upon on a balance of free-amine nucleophilicity and N-H acidity of the bonded nucleophile.

Electronic and steric effects are both factors that must be considered when rationally designing catalysts for BHA. Generally speaking, electron-rich catalysts promote aryl (pseudo)halide oxidative addition, while catalysts bearing sterically encumbering ligands promote reductive elimination via relief of steric strain.[1,55] The

latter is also favored for electron-poor complexes; evidently a balance must be struck to optimize catalyst activity. From the perspective of the substrate, characteristics of the amine and aryl (pseudo)halide coupling partners are frequently used to rationalize reaction rates.[56] Sterically hindered aryl (pseudo)halides bearing bulky *ortho*-substituents tend to undergo oxidative addition slower than those that are unhindered. Similarly, sterically hindered amines may exhibit weaker binding to the catalyst, resulting in reduced reaction rates. Electron-rich aryl (pseudo)halides are commonly referred to as "deactivated" toward oxidative addition, while those that are electron-poor are "activated" substrates. The opposite can be said for the amine coupling partner; the rate of reductive elimination from Pd(II)aryl(amido) species is fastest for electron-rich amines (and electron-poor aryl moieties).[57]

The Hartwig group has studied in detail oxidative addition[55-56,58] and reductive elimination[57b] for well-known ligated-Pd species; their results underscore the value of isolated complexes toward mechanistic examination of stoichiometric reactions that may take place within a catalytic process. General trends corresponding to the catalytic turnover of aryl(pseudo)halide have been noted as follows; Br > OTf > I > Cl. This trend is inconsistent with the Ar-X bond dissociation energies for the phenyl-halides which typically effect the rate of oxidative addition (BDE in kcal mol^{-1}: Cl = 96, Br = 81, I = 65).[24g] Another factor contributing to the relative order of reactivity for aryl(pseudo)halides that was not initially understood is poisoning of the active catalyst by iodide ion.[59] This may occur via formation of stable Pd-iodide dimers or in some cases high levels of hydrodehalogenation (*vide infra*). Monomeric Pd(0) promotes the room temperature amination of aryl iodides and may be assisted by the use of chelating ancillary ligands or crown-ether additives.[60]

Buchwald's group discovered that electron-poor arenes and electron rich aminostannes react more quickly than their electron-rich and electron-poor analogues, respectively. Also, primary amines would only couple in good yield with electron-deficient and/or *ortho*-substituted substrates and would often afford hydrodehalogenation (arene) by-products. These findings are consistent with the aforementioned trends and have helped researchers to understand how to overcome deleterious side-reactions that could lead to decreased efficiency. Studies examining reductive elimination from

Pd(II)aryl(amido) complexes have been important toward the identification of such processes, including hydrodehalogenation. This process involves β-hydride elimination to generate imine and a Pd(II)aryl(hydride) which may reductively eliminate arene. Other commonly encountered issues include: amine displacement of ligand (typically phosphines), poly-arylation of amine substrates, and coordination of strongly lewis basic hetero-atom lone pairs to afford inactive Pd species.

Aryl pseudohalides represent useful aryl halide surrogates for cross-coupling chemistry that have been exploited successfully in Suzuki and Stille coupling. Specifically, Hartwig employed phenol-derived sulfonates including aryl triflates (and tosylates shortly thereafter) in BHA. These substrates, like those bearing carbonyl-containing functionality, are prone to cleavage by strong-bases, and were not suitable for coupling using the P(*o*-tolyl)$_3$ ligated-Pd catalyst useful for amination of aryl bromides. Employing mechanistic rationale, a new class of bidentate ancillary ligands enabled this transformation.[60c,61] The relative strength of base intrinsically determines functional group tolerance.[62]

Imparting a dramatic influence on reactivity, mechanistic understanding, scope, and generality for the Buchwald-Hartwig amination reaction, ancillary ligand design offers the most promise for continued success in addressing remaining challenges. Although universally applicable parameters have not been developed, "task-specific" ligands support catalysts capable of cross-coupling given substrate classes in a highly efficient manner.

1.4. TASK-SPECIFIC CATALYSTS: ADVANCING BUCHWALD-HARTWIG AMINATION VIA LIGAND DESIGN

Over a decade ago, Buchwald and co-workers proposed goals for the development of catalyst systems, many of which have been achieved.[63] These goals include operation under mild conditions, in some cases without the requirement for an inert atmosphere, the coupling of challenging coupling partners, and systems that tolerate scale-up for use in industrial settings. A focus on the design of ancillary ligands capable of supporting electronically and coordinatively unsaturated metal centers has allowed researchers to see the success of these endeavors. Highly active catalysts supported by novel ancillary ligands are now capable of amination of challenging arene substrates, including

deactivated (hetero)aryl chlorides,[24g] iodides, and less reactive (pseudo)halides such as tosylates (OTs)[61,64] and mesylates (OMs).[65] Significant progress has also been made toward the selective monoarylation of challenging amine coupling partners. Along with base-sensitive,[66] poorly nucleophilic,[67] heteroatom-functionalized,[68] and small nucleophilic amines (e.g. NH_3 or H_2NMe).[69] These substrate classes often require the use of a task-specific ancillary ligand.

Monodentate phosphines have suffered from reduced reactivity toward certain substrates, as exemplified via P(*o*-tolyl)$_3$ ligands ineffectively coupling primary amines. The presence of a second phosphine, other secondary stabilizing moiety such as the *ipso*-carbon of an aryl, or (N- or O-) heteroatoms may drastically increase reaction rates and prevent catalyst decomposition.[33c,35] Tertiary phosphines and NHCs represent the most commonly employed monodentate ligands in amination chemistry.[1,3a,32] Monodentate trialkylphosphines,[24c,24e,56,70] biaryldialkylphosphines,[32,33c] and bidentate bisphosphines[35,71] are discussed herein. Analogs of these phosphine classes, such as N- or O- functionalized phosphines[65a,72] are also presented depending upon the type of interaction they exhibit (monodentate vs. bidentate).

1.4.1. Monodentate Phosphines and Carbenes

Pd complexes ligated by the aryl-substituted ligand P(*o*-tolyl)$_3$ were found to exhibit higher catalytic activity than less bulky analogues, demonstrating how ligand choice may effect optimal catalytic turnover. Simple triarylphosphines such as PPh_3 were even thought to inhibit oxidative addition processes. Limitations exhibited by conventional monodentate-ligated catalysts have been overcome by use of more elaborate ligand systems. While both Buchwald and Hartwig began examining the use of bidentate bisphosphines (Section 1.4.2); these advanced ligands were still incapable of coupling acyclic secondary amines.[63] More highly evolved ligands capable of broadening the scope of BHA were sought by a variety of research groups; specifically efforts were directed toward preparation of bulkier monodentate ligands.

A variety of tertiary phosphine characteristics are necessary to achieve significant catalytic activity in cross-coupling reactions, including high Lewis basicity (pKa > 6.5) and having a Tolman Cone Angle > ca. 160^{o}.[73] Furthermore, monodentate phosphines must be directly substituted with at least one or two tertiary carbon atoms to maintain

these characteristics. One of the most widely useful monodentate ligands to meet these requirements is P*t*Bu$_3$. Hartwig[70c] and Fu[24g] have reported versatile methods that rely on the utility of P*t*Bu$_3$ for the amination of deactivated aryl chloride substrates, and Beller[74] has summarized many of these results with respect to the class of ligand employed.

Although simple trialkylphosphines suffer from limited ability to be sterically and electronically tuned by substitution, Beller opted to include adamantyl substitution to benefit from large steric volume and structural rigidity.[24c] Two of the first commercially successful PAd$_2$-ligands of this kind to be broadly employed in cross-coupling chemistry[70e,75] are Ad$_2$P*n*Bu and Ad$_2$PBn, sold under the trade names CataCXium® A and CataCXium® ABn, respectively (Figure 1.5). [68e,73] Beller *et al.* have also prepared a series of novel *N*-heterocycle tethered phosphines that are capable of supporting active complexes for ammonia monoarylation.[69b] However these systems suffer from limited scope and require high temperature (>120 ^{o}C) and high pressure (10 bar N_2) for optimal performance.[69b,76]

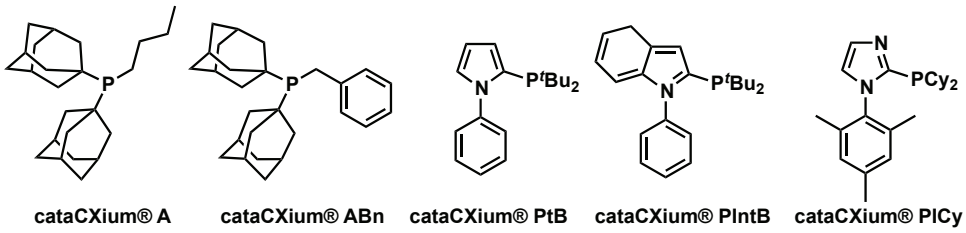

Figure 1.5 Selected cataCXium® ligands applied in Pd-catalyzed cross-coupling.

Maintaining a sterically demanding tertiary alkyl and aryl phosphine motif, the Buchwald group explored monodentate ligands supported by rigid ferrocenyl backbones. This work, inspired by their work with the chelating bisphosphine bis(diphenylphosphino)ferrocene (DPPF), identified a variant capable of cross-coupling (heteroaryl)aryl (pseudo)halides and acyclic secondary amines. Unfortunately, the cross-coupling of other substrate classes, such as primary amines, was not as efficiently accommodated; other chelating bisphosphines better served this purpose.[63] These results led the Buchwald group toward developing a new class of monodentate dialkylbiarylphosphine ligands benefitting from the secondary support of a biphenyl group. The ability to use these ligands in reactions that proceed with low catalyst loading, mild reaction conditions and short reaction times has contributed to their commercial

viability and continued applicability in industry. Furthermore, they benefit from ease of synthesis and stability on the bench-top, both of which are important for successful commercialization. Numerous structural variants (Figure 1.6; more than 10 ligands are commercially available) have been introduced as a result of the modularity afforded via their preparatory routes.[33c]

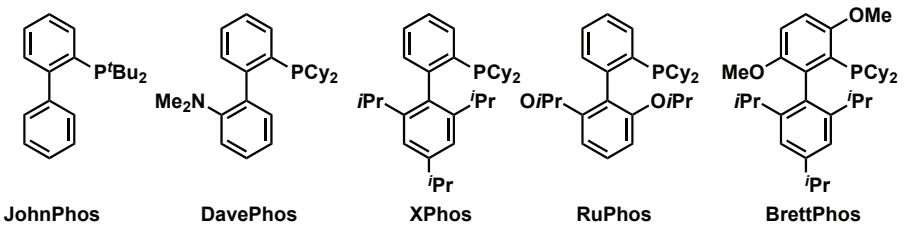

Figure 1.6 Select examples of dialkylbiarylphosphine (Buchwald) ligands.

JohnPhos and DavePhos are popular examples of dialkylbiarylphosphine ligands capable of stabilizing highly active catalysts for the amination of deactivated aryl chlorides. Considering its structure, DavePhos was prepared under the assumption it would bind to the metal-center in a κ^2-P,N-bidentate fashion; however this was not observed. Similar to other Buchwald ligands, a secondary *ipso*-carbon arene-Pd interaction has been found to improve active catalyst lifetime, increase electron density at the metal center, and promote reductive elimination. Furthermore, the lower arene ring may prevent oxidation at phosphorus by O_2, and *ipso*-substitution may prevent cyclometalation while promoting formation of the active LPd(0) catalyst.[32] This interaction is not observed for simple trialkylphosphines, and may explain divergent reactivity between the two ligand classes (Figure 1.7).

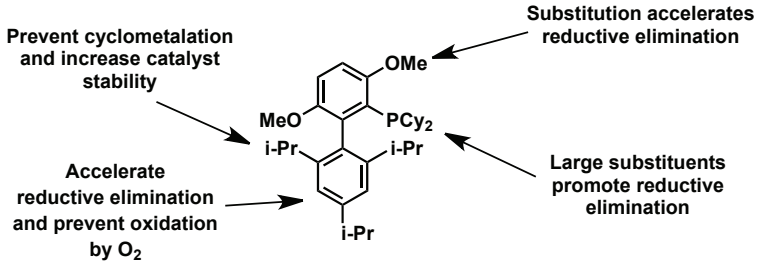

Figure 1.7 BrettPhos exemplifies dialkylbiarylphosphine ligand characteristics responsible for promoting enhanced catalyst activity.

The Buchwald ligand XPhos has been used extensively for coupling of aryl sulfonates,[77] and has found application in 'green' reactions carried out under aqueous

conditions which usually require ligand modification to improve solubility. RuPhos is the most highly active Buchwald ligand for coupling secondary alkyl amines and aniline nucleophiles.[60d,67b,78] BrettPhos, which features anisole substitution on the upper arene ring (thought to enhance reductive elimination), is the most active Buchwald ligand for the cross coupling of primary amine nucleophiles, including the selective monoarylation of small amines such as methylamine.[67a] The lower biaryl ring appears to sufficiently prevent both formation of dimeric species and displacement of the ancillary ligand by methylamine. Furthermore, BrettPhos efficiently couples aryl mesylates and Buchwald *et al*. reported on its use for the N-arylation of amides.[79] Aryl mesylates are not only cheap, but also benefit from the best atom economy and highest stability of the aryl sulfonates.[67a]

Kwong and co-workers have also contributed to mesylate arylation via application of benzimidazolyl phosphine-Pd complexes (Scheme 1.15).[65b,72f] Synthetically, their 2-arylindole ligand scaffold is prepared via Fischer indolization of acetophenones and arylhydrazines. As opposed to binding via the indole-N, the ligand prefers to cyclometalate with Pd via the indole C-2 position. The scope of their early work employing CM-Phos allowed N-arylation of nitrogen heterocycles and primary anilines and secondary cyclic and acyclic aliphatic amines. Reactions could alternatively be carried out in aqueous media, or free of solvent.[65]

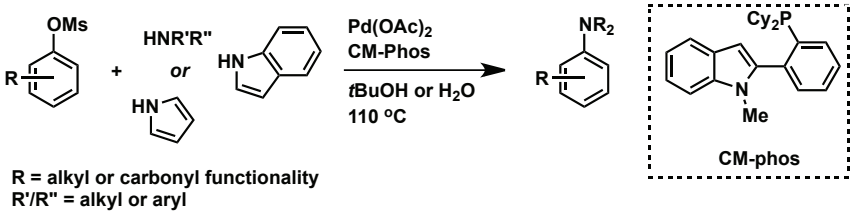

Scheme 1.15 CM-Phos, developed by Kwong for the arylation of mesylates.

While tertiary phosphines undoubtedly represent the most active and efficient ligands for BHA, monodentate N-heterocyclic carbenes (NHCs) have since been used to generate highly-active Pd-catalysts for the amination of challenging aryl (pseudo)halides. Initially explored as phosphine mimics, Hermann *et al.* successfully exploited NHCs in cross-coupling.[80] Similar to phosphine containing ligands, NHCs may be subtly tuned, both sterically and electronically, to observe unique reaction profiles. Organ *et al.* have prepared structurally diverse PEPPSI (pyridine-enhanced precatalyst preparation,

stabilization, and initiation; Figure 1.8) catalysts, perhaps the most active NHC-based catalysts known.

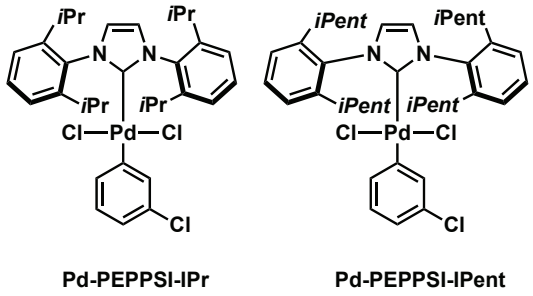

Pd-PEPPSI-IPr **Pd-PEPPSI-IPent**

Figure 1.8 Select Pd-PEPPSI precatalyst complexes supported by bulky monodentate NHC ligands.

Alteration to the steric profile of NHCs can lead to drastic changes in observed catalyst activity. Detailed rate studies have been conducted to examine these differences for Pd-PEPPSI-IPr and Pd-PEPPSI-IPent catalysts. In each case, the latter reached maximum turnover in a shorter time and was capable of coupling the most deactivated aryl chlorides, where Pd-PEPPSI-IPr failed.[3a] Pd-PEPPSI-IPent was effective for the coupling of primary anilines and both cyclic and acyclic secondary amines with deactivated aryl chlorides (including those bearing base-senesitive functionality) and in several cases, was used toward the preparation of tetra-*ortho* substituted products in good yield.[81]

1.4.2. Bidentate Bisphosphines

Considering the reluctance of the Pd/P(*o*-tolyl)$_3$ system to couple primary amines with aryl bromides, Buchwald and Hartwig concurrently developed 'second-generation' catalysts supported by bidentate bisphosphine ligation. In this regard, they explored aromatic bisphosphines and ferrocenyl-backbone phosphines that had been successfully exploited in transition-metal catalyzed processes such as asymmetric hydrogenation, prior to being revisited for use in cross-coupling. Their findings revealed a number of practical advantages and important concepts.[82] Bulky monophosphines are not necessary for high-yielding amination of aryl (pseudo)halides and chelation and bite-angle tuning may afford unexpected reactivity.

The Buchwald group pursued Noyori's ligand *rac*-BINAP, expecting strong chelation to provide an increase in the rate of reductive elimination over

hydrodehalogenation.[83] However, the success of this ligand came as a surprise considering the group's failed attempts at using the simple chelating bisphosphine DPPE and the evidence from studies of the P(*o*-tolyl)$_3$ system that suggested a singly bound phosphine is desirable as a catalytic intermediate. Catalyst mixtures generated from *rac*-BINAP and Pd_2dba_3 effectively promoted the monoarylation of primary amines, without displacement of ligand to afford inactive Pd(bis)amine species, and an overall minimized rate of formation of bridging halide complexes.[60b] Ultimately, an inability to couple acyclic secondary amines would ultimately lead the Buchwald group toward the development of dialkylbiarylphosphine ligands to address this shortcoming.

Hartwig and co-workers similarly discovered a second-generation Pd-DPPF catalyst for the coupling of primary amines with aryl bromides, and eventually expanded this system to include aryl iodides, chlorides and the first example of tosylates.[61] These findings arose from studies of late transition metal amido complexes, which demonstrated the effect of bite-angle on selectivity for monoarylated products. Given that the coupling of halopyridine substrates was not tolerated when employing P(*o*-tolyl)$_3$, Buchwald employe, separately, DPPP and BINAP to address this challenge. These ligands allowed the catalyst to withstand formation of inactive *trans*-bis(pyridyl)palladium complexes.[63] Finally, acyclic secondary amines still remained intolerable coupling partners, for all known catalyst systems. Several Hayashi-type ferrocenyl ligands, including (*rac*)-PPF-OMe and (*rac*)-PPFA, which are easily prepared and may be varied structurally for tuning of steric and electronic properties, overcame this challenge (Figure 1.9).[84]

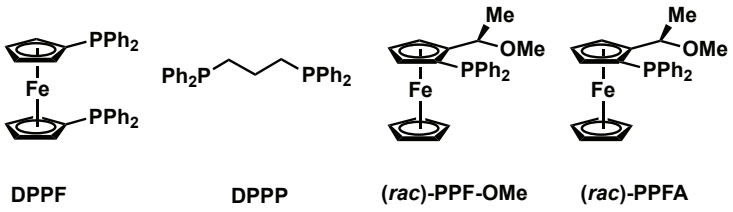

Figure 1.9 Early bidentate ligands explored by the Buchwald and Hartwig groups.

The ability to alter the bite angle of bisphosphines ligands offers a powerful tool to tune both the steric and electronic profile of a ligand, and to achieve unique catalyst activity. Specifically, a wider bite angle not only increases the effective steric bulk of the ligand itself, it may also disfavor particular coordination geometries of the metal complex. For example, favoring low-coordinate (zerovalent) species displaying trigonal

or tetrahedral ligand arrangements. Ancillary ligands featuring a xanthene backbone exemplify the ability to achieve small variations in bite angle, by varying substitution in the ligand backbone. The easily prepared Xantphos-type ligands which feature large bite angles, including DPEphos (104°) and Xantphos (108°), originally utilized in rhodium-catalyzed hydroformylation, hydroaminomethylation, and hydrocyanation, have been used in BHA (Figure 1.10).[85] This class of ligands is effective for the cross-coupling of primary (hetero)arylamines and aryl bromide or iodides; high monoarylation selectivity has been observed.[86] Kinetic studies on the amination of aryl (pseudo)halides using diphosphine ligands suggest that a larger bite angle leads to an increased initial reaction rate and higher concentrations of the active catalytic species.[87]

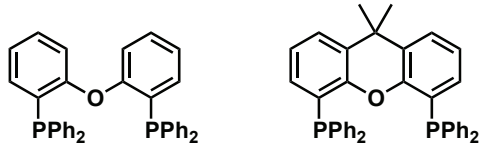

Figure 1.10 Wide bite angle bisphosphines ligands, DPEphos and Xantphos.

Hartwig further explored the task-specific nature of chelating bisphosphines and bite-angle effects in the cross-coupling of primary alkylamines with (hetero)aryl (pseudo)halides. The ligand 'JosiPhos' (Figure 1.11; **1-2**), developed by Solvias for use in asymmetric hydrogenation,[88] has been reported on extensively. Hartwig exploited this ligand for its combination of two strong phosphine donors and extreme steric bulk around Pd, as well as conformational rigidity enforced by a ferrocenyl backbone, disfavoring the binding of bulky substrates. Most notably, a palladium(II) precatalyst, [(**1-2**)$PdCl_2$], has been shown to promote the selective monoarylation of ammonia and lithium amide.[69a] This reaction attests to the ability of **1-2** to withstand displacement by small nucleophilic amines, formation of amide-bridged polynuclear complexes and unwanted polyarylated products. Despite the important consequences bidentate bisphosphine ligand studies have had on BHA, the requirement for high temperatures/harsh reaction conditions, poor substrate scope and in some cases the high cost of the ligand (e.g. **1-2**, ca. $600/g, has prompted the development of more active catalysts that feature one strongly binding P-donor, and a potentially hemi-labile N-donor, to generate active catalysts for challenging C-N cross-coupling reactions.

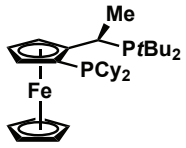

JosiPhos
1-2

Figure 1.11 Structure of the JosiPhos (CyPF*t*Bu; **1-2**) ligand, developed by Solvias.

1.5. DALPHOS LIGANDS FOR THE SELECTIVE MONOARYLATION OF CHALLENGING SUBSTRATES

In Section 1.4, the development of novel ancillary ligands capable of addressing challenging C-N cross-coupling reactions was discussed. Support of the metal center by ancillary ligands featuring one or two phosphine interactions, monodentate or bidentate respectively, enabled the majority of these developments. In many cases, the mechanistic findings and shortcomings of catalysts in such reactions inspired new task-specific systems capable of overcoming such limitations, although often at the expense of scope. This task-specific nature is exemplified by early work and limitations associated with the monophosphine P(*o*-tolyl)$_3$. These findings inspired the development of a variety of more effective monodentate and bidentate ligand sets capable of cross-coupling a broader scope of aryl or vinyl (pseudo)halides and primary and secondary N-H containing compounds.

In the field of BHA, the cross-coupling of abundant and inexpensive nitrogen sources such as small nucleophilic amines including ammonia and hydrazine have been largely unaddressed due to the inherent difficulty of cross-coupling these substrates.[33b] Nucleophilic coupling partners that do not sterically crowd the metal center, or are highly basic, may promote catalyst decomposition by forming deactivated bridging structures or displacement of ligand.[69d] The relief of steric strain from L_nPdaryl(amido) intermediates represents a significant driving force toward reductive elimination; small substrates are not only reluctant to undergo such reductive processes, they are also prone to undergo subsequent cross-coupling to form polyarylated products if they manage to do so.[33a] Small primary alkylamines such as methylamine, poorly nucleophilic or heteroatom-functionalized anilines, and base-sensitive substrates exemplify further challenges.[89] The design of ligands that modify the steric and electronic profile of the metal coordination

sphere so as to promote desirable reactivity in reactions involving these substrates represents an important goal.

1.5.1. The Development of DalPhos Ligands for Use in BHA

A research program initiated by the Stradiotto group in 2010 involved preparation of novel, yet structurally simple phenylene-bridged κ^2-P,N ligands to address issues such as catalyst deactivation and selectivity for monoarylation when employing small, nucleophilic N-H containing compounds. A ligand motif combining an electron rich and strongly binding phosphine donor, and a weaker amine donor was considered as a conceptual middle ground between the mono- and bidentate systems commonly reported in the chemical literature (Figure 1.12). A small number of research groups have benefitted from similar strong/weak donor motifs, including the groups of Beller[34c] and Kwong[65a]. The utility of their κ^2-P,N and P,C ligands has been demonstrated in hydroxide arylation and mesylate arylation reactions, respectively.

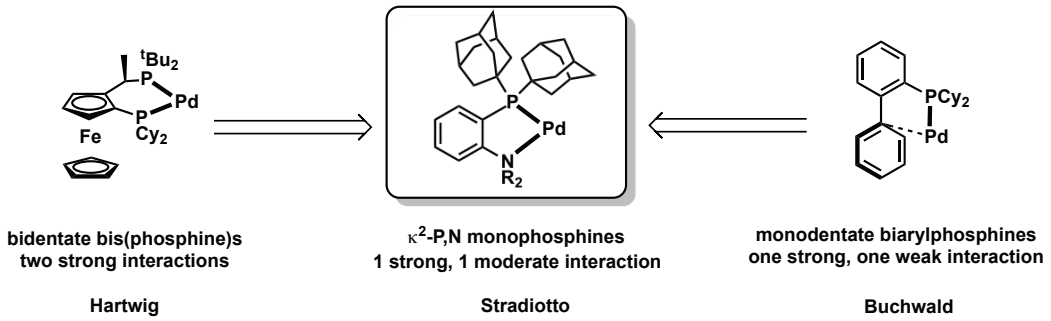

Figure 1.12 Comparing metal-ligand binding motifs; inspiration for the development of κ^2-P,N DalPhos ligands.

DalPhos ligands were prepared via procedures offering ease of synthesis relative to the most widely employed ligands for C-N cross-coupling reaction that often require handling of the product ligands under inert atmosphere and/or costly, less readily available reagents. The tuneable nature of the phenylene-based ligands allowed preparation of a series of structural variants, differing in substitution at phosphorus and nitrogen. Preliminary screens identified the importance of $[Pd(allyl)Cl]_2$ or $[Pd(cinnamyl)Cl]_2$, in combination with the ligand Me-DalPhos (**1-3**), as an optimal catalyst candidate for further screening in the cross-coupling of (hetero)aryl chlorides with ammonia and aniline. Ligands bearing less electron-rich and sterically demanding

substituents on phosphorus or lacking *ortho*-dimethylamino substitution resulted in inferior yields and selectivity.

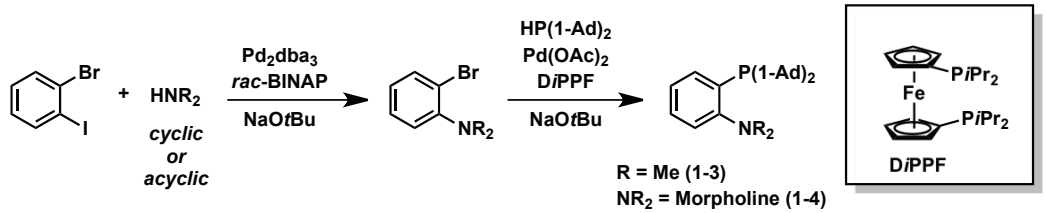

Scheme 1.16 Representative synthetic procedure for the synthesis of DalPhos ligands, including the highly efficient ligands **1-3** and **1-4**.

Ligand **1-3** (Figure 1.13) afforded good to excellent yields for a wide range of amine coupling partners, including primary aryl- and alkyamines, cyclic and acyclic secondary amines, lithium amide, N-H imines, hydrazones, and ammonia.[89] This substrate scope sharply contrasts that of nearly all other ancillary ligands developed to cross-couple primary or secondary amines exclusively. Further studies pertaining to the rational diversification of the DalPhos motif led to the development of the ancillary ligand Mor-DalPhos (Figure 1.13; **1-4**), demonstrating state-of-the-art performance toward challenging coupling reactions with ammonia (with improved monoarylation selectivity over **1-3**) and hydrazine. The development of BHA protocols that address these coupling partners are highlighted in Sections 1.5.1 and 1.5.2, respectively.

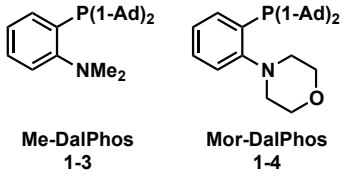

Figure 1.13 Me-DalPhos (**1-3**) and Mor-DalPhos (**1-4**), ligands capable of supporting highly active Pd-catalysts for the cross-coupling of challenging N-H containing substrates.

1.5.2. Selective Monoarylation of Ammonia

The rational, modular development of ancillary ligands capable of supporting catalysts to prevent deactivation and increase selectivity in challenging cross-coupling reactions has been the focus of many research programs. Unfortunately, findings that detail catalyst systems capable of achieving the selective monoarylation of the cheap and abundant commodity chemical ammonia are limited. While Cu-catalyzed protocols for

ammonia arylation have been reported,[38b,90] Pd-systems tend to be far more efficient for reasons previously outline (i.e low loadings, more mild conditions, broader scope; see Section 1.2). The Stradiotto group has developed DalPhos ligands, specifically **1-3**, and **1-4**, capable of achieving this task. These ligands represent but a few reported in the chemical literature that are capable of imparting the properties upon Pd necessary to achieve monoarylation.[33b] Ammonia and the amide anion (NH_2^-) present the ability to coordinate to Pd irreversibly via formation of stable bridging structures, to displace ancillary ligands (forming well-known Werner complexes) necessary to promote catalytic activity, to undergo polyarylation, and are reluctant to reductively eliminate from sterically unencumbered intermediates.[33a,b]

As mentioned previously, **1-3** allowed the cross-coupling of ammonia with aryl chlorides, albeit with harsh reactions conditions such as elevated temperature, catalyst loadings (2-4 mol%), and substrate excess (typically 10 equiv.). The substrate scope similarly suffered, restricted to 2-substituted aryl chlorides. These significant advances came only a few years following the first report on the selective monoarylation of ammonia using a [(**1-2**)$PdCl_2$] precatalyst, disclosed by Shen and Hartwig in 2006.[69a] A variety of other task specific ligands such as P(*t*Bu)$_3$, XPhos, DPPF, and BINAP were inferior, or provided no turnover under harsh conditions (24 h, 90 ^oC, 80 psi NH_3). Vo and Hartwig significantly advanced this protocol in 2009, reporting a [Pd(P(o-tolyl)$_3$)$_2$]-**1-2** precatalyst mixture that tolerates a series of aryl (pseudo)halides as well as base-sensitive functionality.[69d] These reactions were conducted without the requirement for high pressure; catalyst loadings as low as 0.1 mol% were sufficient to achieve desired activity (Scheme 1.16).

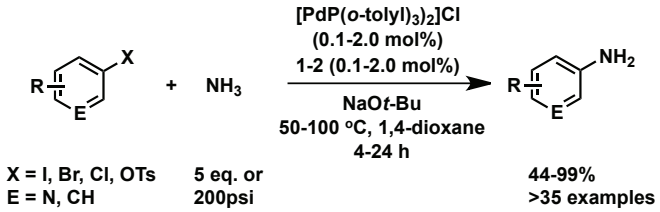

Scheme 1.17 A [Pd(P(*o*-Tol)$_3$)$_2$]-**1-2** precatalyst mixture for the monoarylation of ammonia with (hetero)aryl (pseudo)halides.

Interestingly, the resting state for Hartwig's catalyst system was later identified as [(**1-2**)Pd(aryl)(NH$_2$)], consistent with slow rates of reductive elimination. Generally speaking however, these findings do not align with established BHA trends. Not only are parent amido complexes of late transition metals rare to both stoichiometric and catalytic reactions, Hartwig's findings describe the thermodynamic stability of their arylpalladium amido complexes, affording a resting state inconsistent with Pd(0) and aryl-Pd(II) resting states for reactions involving most amines.[91]

The Buchwald group has also contributed to the monoarylation of ammonia, albeit with a limited substrate scope. The screening of ligands identified Pd$_2$(dba)$_3$ (2 mol% Pd) and *t*BuDavePhos (5 mol%) as an optimal combination, in terms of both substrate conversion (100%) and monoarylation selectivity (86%) employing chlorobenzene.[69c] The screening revealed that bulky substitution at phosphorus, and the presence of a dimethylamino group on the lower flanking arene ring are required to achieve desired activity. Similarly, no product was formed when the lower arene ring was left unsubstituted or when *t*Bu was replaced with Cy. While it can be assumed that heightened activity results from increased steric presence at Pd with *t*Bu phosphorus substitution, the role of the dimethylamino moiety has yet to be established. Buchwald and Tsvelikhovsky have recently applied this methodology to the synthesis of biologically active dibenzodiazepine heterocycles via intramolecular condensation reactions.[92]

Rational diversification of the DalPhos ligand structure allowed our research group to identify **1-4** as the most highly effective κ^2-P,N ligand for the cross-coupling of ammonia with electron-rich and electron-poor aryl (pseudo)halides (Scheme 1.17). In addition to a diverse substrate scope, which includes primary and secondary amines, excellent monoarylation selectivity and chemoselectivity in the presence of aminoaryl

fragments was identified for this particularly challenging substrate. Low catalyst loadings (as low as 0.3 mol%) and mild reactions conditions, including the first examples of room temperature arylation were disclosed.[93] Lastly, the screening of other DalPhos ligand variants gave poor results. Replacing $P(1\text{-}Ad)_2$ group with the less bulky PCy_2 did not afford monoarylated product, suggesting that the bulky rigid substitution at phosphorus is necessary to desired reactivity.

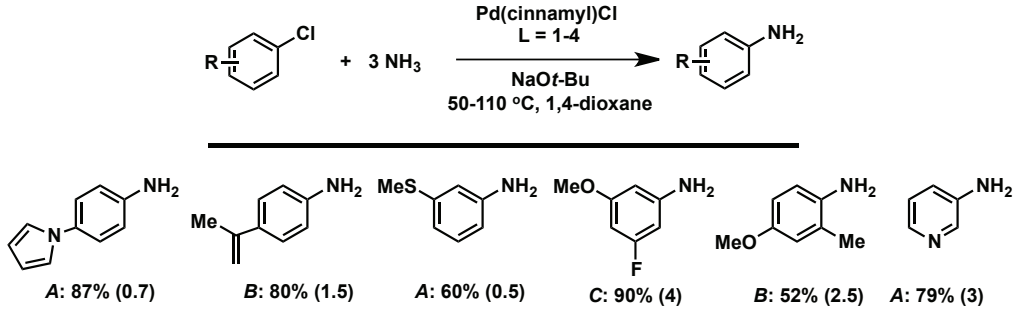

Scheme 1.18 Selected examples of the Pd-catalyzed cross-coupling of ammonia and aryl chlorides using the ligand **1-4**. Conditions (italicized): A: 110 °C; B: 65 °C; C: 50 °C. Pd loading (mol%) in parentheses.[94]

1.5.3. Selective Monoarylation of Hydrazine

Monoaryl hydrazines are broadly useful synthons in the assembly of heterocyclic scaffolds, notably indoles via Fischer indole synthesis, as well as pyrazoles and aryltriazoles.[95] Unfortunately, current preparatory methods for such synthons inherently restricts scope, both in terms of functional-group tolerance and atom economy. The most commonly relied upon synthetic methodology invokes oxidation of anilines to their corresponding diazonium salts, followed by reduction, or alternatively, direct nucleophilic aromatic substitution of electron-deficient aryl halides. Operationally simple methods by which aryl hydrazines are formed directly via Pd-catalyzed coupling of (hetero)aryl (pseudo)halides and convenient unprotected hydrazine sources (e.g. $NH_2NH_2{\bullet}H_2O$) have remained an important synthetic challenge that has only recently been addressed. Similar to ammonia, a variety of factors contribute to the difficulties associated with cross-coupling hydrazine, including: (i) the strongly reducing nature of hydrazine may lead to increased levels of hydrodehalogenation, and formation of inactive Pd-black; (ii) the N-N bond of hydrazine is susceptible to cleavage by Pd to form aniline

derivatives; (iii) similar to other small nucleophilic primary amines, further cross-coupling of the desired product may lead to unwanted polyarylated products.[96]

Following the success of **1-4** in the selective Pd-catalyzed monoarylation of ammonia, a ligand screen was performed by the Stradiotto group to assess the utility of various ligands in the Pd-catalyzed cross-coupling of 4-phenyl-chlorobenzene and hydrazine hydrate.[94,97] Various ligands such as Buchwald's biaryl monophosphines, bidentate bisphosphines, Beller's cataCXium phosphines, and monodentate carbenes were screened and found to be ineffective. Good results were obtained for the ligands **1-2**, **1-3**, and **1-4**. The cross-coupling of (hetero)aryl (pseudo)halides was found to be challenging, considering the sensitivity of the catalyst to varying reaction conditions; excess equivalents of hydrazine, use of aryl bromide substrates, and the use of milder alternatives to NaO*t*Bu lowered conversion and yield.

For the first time, a substrate scope (Scheme 1.18) was developed for the Pd-catalyzed hydrazine arylation of aryl chlorides and tosylates. Catalysts featuring ligand **1-4** tolerated *ortho*-substitution of the aryl chloride substrate, as well as the use of heteroaryl chlorides such as chloropyridine 3-, and 6-chloroquininoline. Chemoselective examples whereby aminoaryl chloride substrates were coupled selectively at the aryl halide position were also provided. Despite the breakthrough achieved by the Stradiotto group in developing this new protocol, challenges remain. Future improvements to this protocol will likely address low conversions and yields for electron-poor and electron-rich substrates such as 4-(trifluoro-methyl)chlorobenzene and 4-chloroanisole. Finally, this methodology was applied to the synthesis of NH-indazoles via a tandem hydrazine cross-coupling-condensation from 2-chlorobenzaldehydes. The application of this hydrazine monoarylation protocol to the modular assembly of novel Edaravone derivatives for use as potential Alzheimer's Disease (anti-aggregate) drug targets is discussed in Chapter 2.

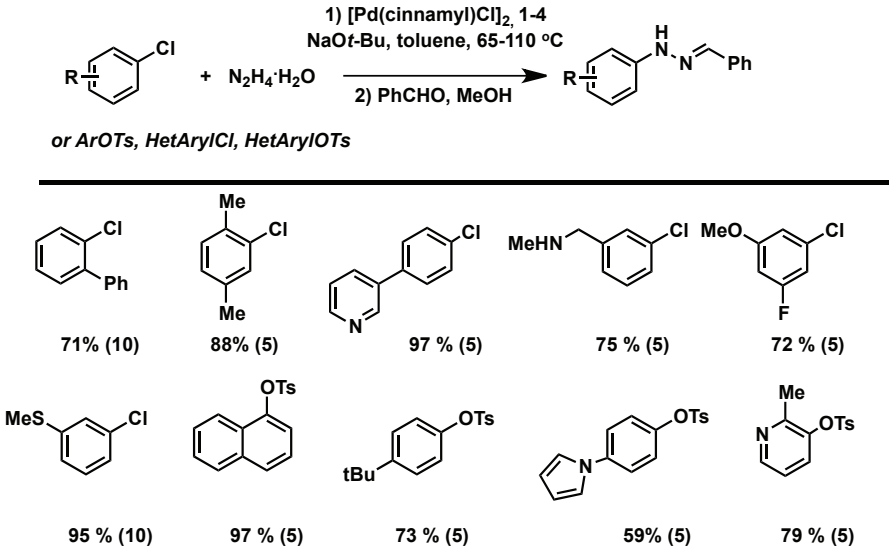

Scheme 1.19 Selected examples of the Pd-catalyzed cross-coupling of hydrazine and (hetero)aryl (pseudo)halides using the ligand **1-4**. Pd loading (mol%) in parentheses.

1.6. THESIS OVERVIEW

Research detailed in this thesis builds upon Stradiotto group efforts toward the application of phenylene-based P,N-ligands in the Pd-catalyzed cross-coupling of aryl halides and N-H containing nucleophiles (Buchwald-Hartwig Amination). As outlined in the previous Section, a Pd/**1-4** catalyst developed by the Stradiotto group has allowed the arylation of small nucleophiles such as ammonia and hydrazine. In Chapter 2, our efforts have extended the utility of this system to the modular synthesis of an array of nitrogen containing heterocycles, specifically pyrazolones, as potential drug targets for treatment of Alzheimer's Disease (AD). Section 2.2 provides an overview of the identification of Edaravone and related analogues as potential targets, and how our system may be utilized in their synthesis. Section 2.3 highlights application of these methods to the preparation of a small-molecule library, that with a small number of exceptions, contains structures not yet reported in the chemical literature (Scheme 1.19). The biological activity of these compounds will also be discussed briefly.

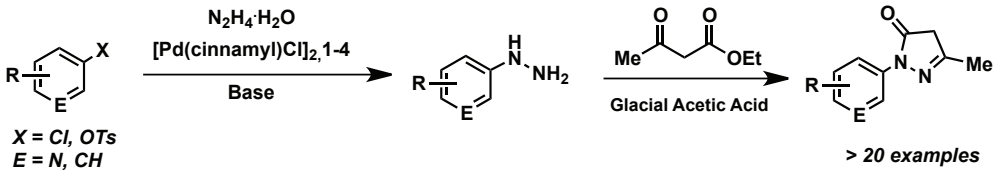

Scheme 1.20 Synthetic methodology for the preparation of Edaravone derivatives.

Many significant advances in the field of BHA have been made possible by the preparation and study of novel ancillary ligands and their Pd-complexes. Notwithstanding the success of Mor-DalPhos (**1-4**), further modification of this ligand framework may offer inroads to improved catalytic performance. In Chapter 3, rational diversification of the DalPhos ligand structure and screening of new structural ligand variants in challenging C-N, C-C, and C-O cross coupling reactions is presented. In Section 3.1, a brief outline of successful ligand diversification efforts, particularly subtle variations to the steric and electronic profile of ancillary ligands and the resulting effect on catalyst activity in challenging BHA reactions is provided. Section 3.2, describes the preparation of eight new structurally diverse variations of **1-4,** substituted with electron-donating or electron-withdrawing groups at various positions of the phenylene-backbone (Scheme 1.20). These groups vary with regard to their Hammett parameter (*para* and *meta* substituent constants) and will be discussed on a case-by-case basis. A variation of **1-4** is presented in which the *ortho*- position to phosphorus is substituted with a thiomorpholino group. The attempted synthesis of a P_2N_2 (dinuclear), and mononuclear nitro-substituted DalPhos variants are also disclosed.

To understand influences of ancillary ligand binding mode on reactivity, new ligands were combined with $[Pd(cinnamyl)Cl]_2$ to afford their Pd-complexes in excellent yield (Scheme 1.20). These results are described in Section 3.3 along with relevant NMR spectral data. Crystallographically determined ligand structures and respective Pd-complexes are examined to determine if significant changes to complex parameters (e.g. bond lengths/angles) result from alteration of electronic properties of the ligand. Section 3.4 describes preliminary screening of these ligands in cross-coupling reactions.

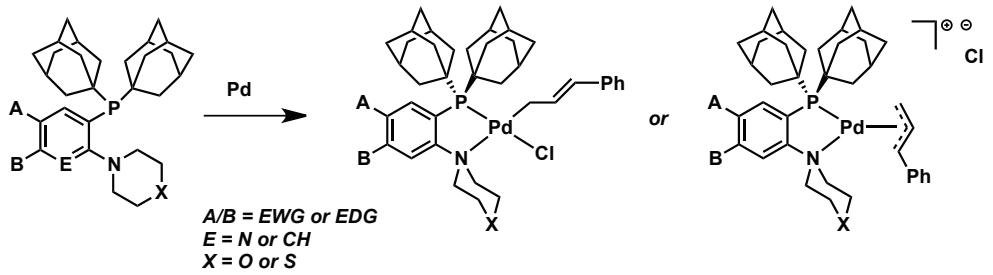

Scheme 1.21 Rational diversification of the DalPhos ligand structure and preparation of their coordination complexes.

To conclude, Chapter 4 presents a summary of the research efforts described herein, along with the future direction of research efforts aimed at the development of highly active catalysts supported by structurally diverse DalPhos ancillary ligands.

CHAPTER 2. MODULAR ASSEMBLY AND BIOLOGICAL SCREENING OF AN ALZHEIMER'S DISEASE DRUG TARGET ARRAY

2.1. INTRODUCTION AND CHAPTER OVERVIEW

Alzheimer's disease (AD) is a progressive neurodegenerative disorder that leads to dementia, cognitive impairment, and memory loss.[98] It is estimated that 25 million people worldwide were afflicted with AD in the year 2000, and that this number will more than quadruple by 2050.[99] While current treatments for AD can serve to manage the condition, effective therapies that can arrest the progression of and/or prevent AD are currently unknown. The aggregation of beta-amyloid (Aβ) peptides featuring 40 and 42 residues, which are generated via cleavage of amyloid precursor protein, has been shown to figure directly in the pathogenesis of AD.[98-99,100] As such, the development of drug molecules that can penetrate the blood-brain barrier and interfere with Aβ aggregation, thereby inhibiting the assembly of neurotoxic oligomers, represents a promising therapeutic strategy for addressing the challenge of AD.

As part of an on-going research program in collaboration with Dr. Mark Reed (Treventis Corporation),[101] and the Weaver research group (Dalhousie), the Stradiotto group has directed research efforts toward developing useful synthetic protocols for constructing new classes of drug-like molecules for the treatment of AD. In this regard, on the basis of *in silico* screening, functionalized *N*-aryl pyrazolones (including Edaravone, **2-1**, Scheme 2.1) were identified as representing a potent class of anti-aggregants that can inhibit aberrant misfolding and aggregation of amyloid peptides including Aβ. Notably, the neuroprotective characteristics of Edaravone are well-established; the potent anti-oxidant and free-radical scavenging properties of this compound are exploited therapeutically to reduce neuronal damage caused by acute brain ischemia.[102] Encouraged by these collective observations, including the knowledge that oxidative stress is known to figure prominently in the pathogenesis of AD,[103] I targeted the preparation of Edaravone and related variants, particularly those featuring alternative *N*-aryl substituents given that this position has emerged as an important locale for diversification as demonstrated by improved *in silico* docking scores where the aryl is a functionalized aromatic group. Following the modular preparation of such derivatives,

Treventis conducted assessment of their anti-aggregate potential. Whereas structural modification at the R_2 position can be achieved straightforwardly by use of established methods and commercial reagents (Scheme 2.1), variation at the sp^2-hybridized N-aryl position requires access to structurally diverse monoaryl hydrazine synthons of the type aryl-$NHNH_2$. Conventional protocols employed for the formation of monoaryl hydrazines include nucleophilic aromatic substitution involving an activated aryl halide,[104] as well as diazotization of aniline derivatives followed by reduction of the resulting diazonium salt.[105] While feasible, such protocols are plagued by limited substrate scope, harsh reaction conditions, and poor atom economy. Notably, a report examining structure–activity relationships within a small set of Edaravone derivatives with regard to radical scavenging activity has appeared very recently; however, the scope of *N*-aryl substituents examined was limited to four simple structural variants.[106]

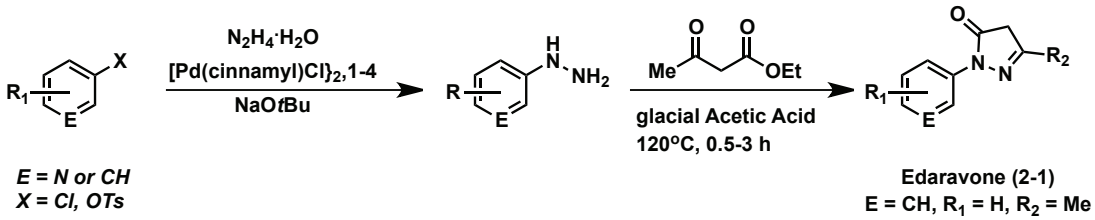

Scheme 2.1 Synthetic route to Edaravone and related *N*-aryl derivatives.

Given the broad utility of monoaryl hydrazines in the assembly of myriad heterocyclic scaffolds,[95] the identification of modular synthetic methods for the preparation of such synthons directly from (hetero)aryl (pseudo)halides and convenient hydrazine sources (e.g. $NH_2NH_2{\cdot}H_2O$) represents an important synthetic challenge that until very recently remained unaddressed. Whereas Buchwald-Hartwig amination methods would appear to be well-suited for such transformations, the strongly reducing nature of hydrazine presents a formidable challenge, both with respect to unwanted hydrodehalogenation of the (hetero)aryl (pseudo)halide reagent, as well as formation of catalytically inactive palladium black. Despite these considerations, the first reported protocol of this type was disclosed by the Stradiotto group in 2010.[97] Key to the success of this transformation was the use of $[Pd(cinnamyl)Cl]_2$/**1-4** catalyst mixtures, which were employed in the cross-coupling of inexpensive and readily obtained (hetero)aryl chlorides and tosylates, thereby affording structurally diverse monoaryl hydrazine

derivatives in good to excellent yield.[94,97] In this chapter, the application of this novel cross-coupling strategy toward the modular assembly of a small library of Edaravone derivatives featuring variation in the *N*-aryl substituent, and the subsequent assessment of the abilities of such *N*-aryl pyrazolones to inhibit Aβ aggregation, is reported.

2.2. MODULAR ASSEMBLY OF EDARAVONE DERIVATIVES

The protocol employed in preparing a small library of Edaravone derivatives is depicted in Scheme 2.2. This procedure makes use of the palladium-catalyzed cross-coupling of (hetero)aryl chlorides or tosylates with hydrazine hydrate to afford the requisite monoaryl hydrazine intermediate, followed by treatment with ethyl acetoacetate under acidic conditions using established literature protocols[107] to afford the desired pyrazolone. In exploiting this modular strategy, the expedient synthesis of Edaravone derivatives featuring a diversity of substitution patterns at the *N*-aryl position was achieved (Scheme 2.2). Edaravone itself (**2-1**) was prepared in this manner in good yield (76% from PhCl; 77% from PhOTs), as were isomeric *N*-tolyl (**2-2**-**2-4**) and naphthyl (**2-5** and **2-6**) compounds. *Ortho*-ethyl substitution was well accommodated (**2-7**), as was 2,5-dimethyl substitution (**2-8**, albeit in lower yield when employing the aryl tosylate). Edaravone derivatives featuring *N*-phenyl groups comprising a combination of methyl, fluoro, trifluoromethyl and/or methoxy substituents (**2-9**-**2-13**) were each prepared in acceptable isolated yield, as were derivatives featuring amine, ether, and thioether addenda (**2-14**-**2-18**). While heteroaryl (pseudo)halides in general proved to be challenging reaction partners in this cross-coupling chemistry (including heteroaryl chlorides derived from thiophene, imidazole, or quinoline), pyrazolones featuring pyridine or pyrimidine groups at nitrogen were prepared successfully in good isolated yield (**2-19**-**2-21**; 61-74%). Finally, given the privileged nature of the biaryl motif in pharmaceutical chemistry,[108] we directed our attention to the preparation of such Edaravone derivatives. *N*-(Hetero)biaryl pyrazolone derivatives featuring methoxy, pyridyl, and indolyl functionalities were all synthesized successfully (**2-22**-**2-25**; 50-83%). Notably, with a small number of exceptions (**2-1**-**2-4**, **2-11**), the Edaravone derivatives prepared herein represent new compounds that had not been reported previously in the chemical literature. In several cases, (**2-5**, **2-7**, **2-8**, **2-19**) compounds

identified in literature reports (or patents), lacked characterization (i.e. solution NMR spectroscopy) data.

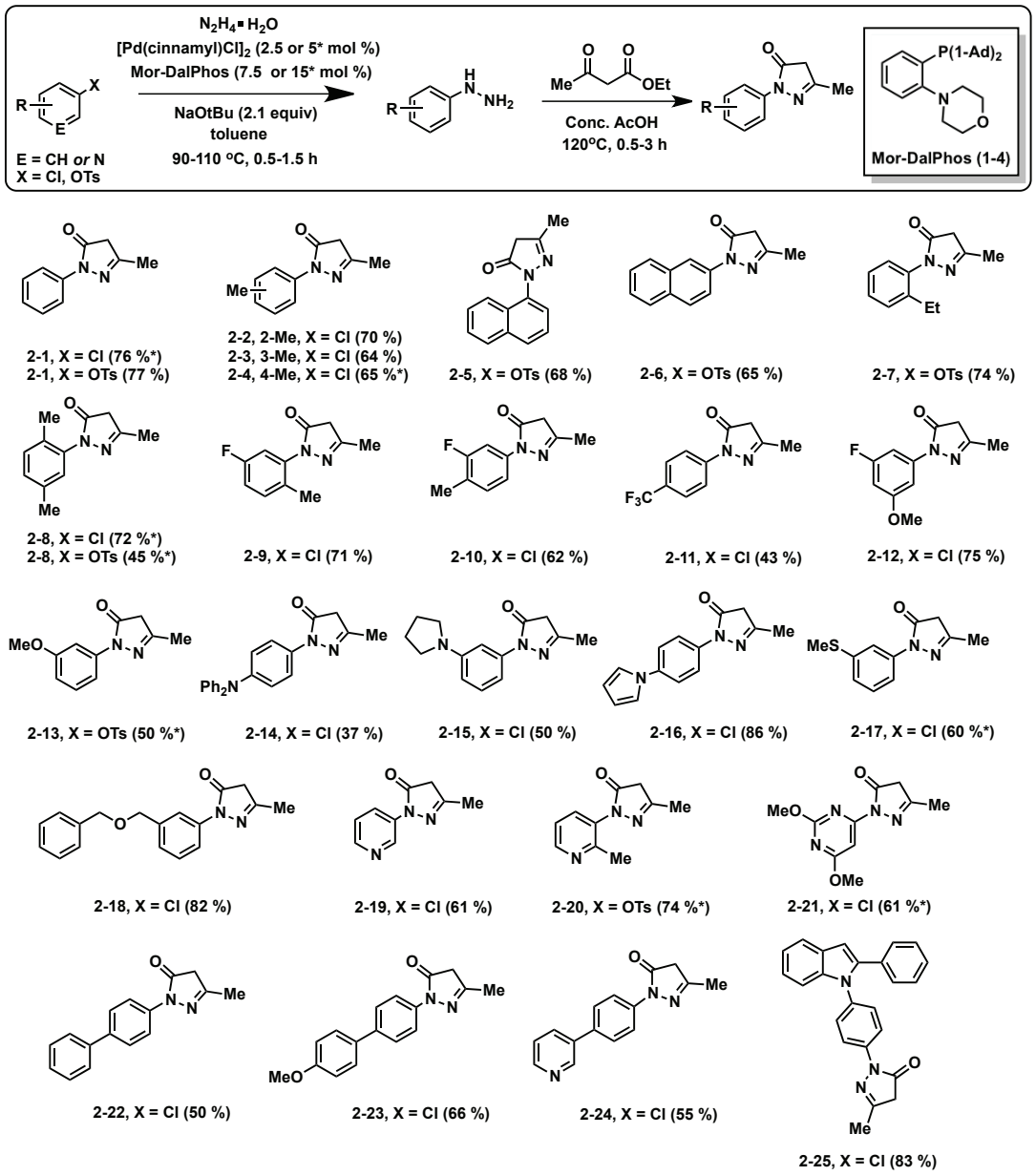

Scheme 2.2 Preparation of Edaravone derivatives employing palladium-catalyzed hydrazine cross-coupling.

Notwithstanding the broad substrate scope afforded using our modular synthetic strategy, several classes of (hetero)aryl (pseudo)halide substrates (Figure 2.1; **2-26**-**2-55**) proved to be incompatible; in most cases no pyrazolone product was isolated or a series of spots was observed by think layer chromatography (TLC) following condensation of

the intermediate aryl hydrazine. Notably, substrates **2-26**-**2-30** bear NH functionality, either pendant or as part of a heterocyclic ring system. While it is not clear at this time whether difficulties stem from the hydrazine arylation or condensation step, it should be noted that aminoaryl chlorides (such as **2-28**) have been cross-coupled in good yield without interference from this moiety (suggesting that condensation may be problematic). Despite the preparation of pyridine and pyrimidine substituted Edaravone derivatives **2-19**-**2-21**, heteroaryl chlorides in general proved to be challenging, including those derived from indole, imidazole, benzoxazole, quinoline and thiophene (**2-30**-**2-39**). As outlined in Chapter 1 (Sections 1.3 and 1.5), substrates that display a free lone pair, especially those in the 2-position relative to chloride or tosylate groups, may coordinate irreversibly to Pd, leading to catalyst decomposition. Although quinoline **2-37** was disclosed as a viable coupling partner in our group's initial report on hydrazine monoarylation,[97] **2-30**-**2-39** represent challenging coupling partners that will likely require further catalyst developments in order to be coupled successfully. Fluorinated (**2-40**-**2-43**), *ortho*-substituted (**2-38**, **2-42**, **2-44**, **2-45**, **2-47**) and base sensitive aryl chlorides (**2-47**-**2-50**), as well as several electron-poor (**2-51**) and electron-rich (**2-52**, **2-53**, **2-55**) aryl tosylates would similarly benefit from increased catalyst activity and milder conditions (e.g. weak base alternatives to NaO*t*Bu).

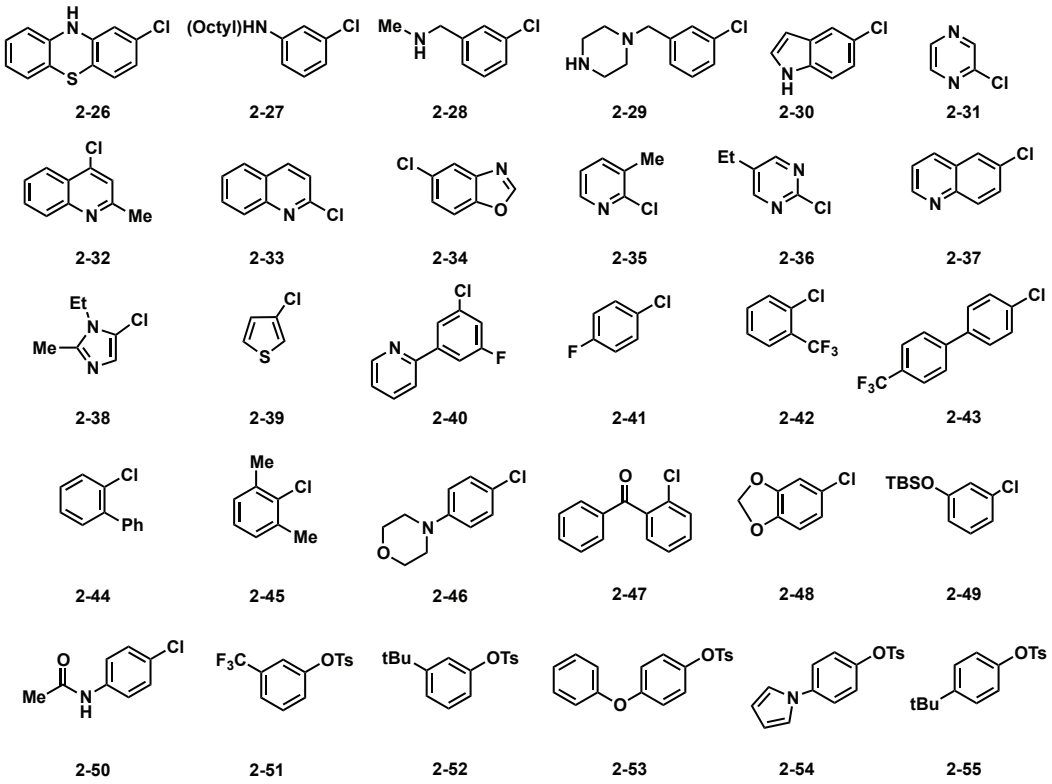

Figure 2.1 Aryl (pseudo)halides employed toward the preparation of Edaravone derivatives for which no desired pyrazolone product was isolated.

The condensation protocol employed was adapted from a literature report in which Edaravone (**2-1**) is prepared in 91 % isolated yield; this methodology was found to be reproducible. Given the general mechanistic simplicity in this step relative to that of hydrazine monoarylation, I was interested in determining if the efficiency of the reaction could be increased, exceeding 91% yield and forgo the use of hazardous materials such as glacial acetic acid (tedious work-up procedures). A methodology that would alleviate the need for harsh conditions (such as temperature upwards of 120 ^{o}C) and lengthy reaction times would be optimal. Seeking alternative strategies, I explored the use of the heterogeneous Bronstedt acid (-SO_3H) ion exchange resin, Amberlyst-15®. This catalyst is known to promote simple organic transformations, such as the acetylation of phenols and alcohols in combination with acetic anhydride. Furthermore, it is inexpensive, non-toxic, reusable, and would allow the use of bench-top organic solvents.[109] Screening various solvents, temperatures, and loadings of catalyst, the reactions were monitored via TLC. Although this catalyst did appear to promote the desired transformation (spotting

against an authentic sample of Edaravone), attempts at isolating the product were abandoned given that starting material was not fully consumed. In summary, improving the efficiency by which Edaravone deritives are prepared would perhaps benefit to a greater extent from advanced catalyst designs that allow for the preparation of (hetero)aryl hydrazines in greater yield. The Stradiotto group is currently investing research efforts in this area, particularly through the design of new structurally diverse DalPhos ligands. My research contributions in this area are discussed in Chapter 3.

Following the modular assembly of a small focused library of Edaravone analogs, the compounds were tested for their biological properties. The biological testing was conducted by collaborative partners (Treventis Corporation) of the Stradiotto group, as they investigated the Edarvone derivatives for their ability to inhibit aggregation of amyloid beta (Aβ). For this purpose, two functional biochemical assays were selected and utilized to study the compounds effect on both oligomer and fibril formation of Aβ. Analogs were first screened using a fluorescent dye-binding agent Thioflavin T (ThT) in a kinetic aggregation assay in the presence of Aβ40, an assay routinely used to monitor the formation of β-sheet rich amyloid fibrils.[110] The whole series was assessed using two concentrations of compounds, 25 μM and 10 μM (Table 2.1). Compounds **2-14** and **2-22-2-25** (bolded/italicized results) display a strong inhibitory effect in this assay, even at 10 μM concentrations.

Table 2.1 Screening results employing Edaravone derivatives in the ThT kinetic aggregation assay, monitoring the formation of β-sheet rich amyloid fibrils (at 25 μM and 10 μM). Compounds with bold/italicized results display a strong inhibitory effect.

ID	% inhib. $A\beta_{40}$ - 25 μM	% inhib. $A\beta_{40}$ - 10 μM	ID	% inhib. $A\beta_{40}$ - 25 μM	% inhib. $A\beta_{40}$ - 10 μM
2-1	17.18	-	**2-13**	30	23
2-2	22.7	-	**2-14**	***51***	***34***
2-3	30.9	-	**2-15**	47	30
2-4	16.27	21.95	**2-16**	54	38
2-5	missing	missing	**2-17**	insoluble	insoluble
2-6	pending	pending	**2-18**	53.35	35.67
2-7	26.3	-	**2-19**	20.2	-
2-8	7.45	11.09	**2-20**	insoluble	insoluble
2-9	26.2	-	**2-21**	pending	pending
2-10	30	24	**2-22**	***78.75***	***57***
2-11	54	31	**2-23**	***69.59***	***40.0***
2-12	26.42	23.08	**2-24**	***53.2***	***40.9***
-	-	-	**2-25**	***60***	***33***

With these data in hand, compounds were screened through a biochemical assay specifically designed to monitor the formation of smaller, neurotoxic-associated oligomers. Using biotinylated Aβ42 (bio-Aβ42) in an analogous ELISA based assay developed by Levine III,[111] the analogs were screened at a single concentration of 25 μM with % inhibition measured directly via absorbance readings (Figure 2.2). This was followed by re-testing at varying concentration for the most active compounds (**2-14**, **2-22**-**2-25**; Table 2.2) in an effort to determine IC_{50} values. It should be noted that, while 13 of the 20 compounds for which results were obtained afforded a positive % inhibition (preventing aggregation), the remaining compounds gave a negative response, implying they actually increased the formation of toxic oligomers (including Edaravone, **2-1**). Regardless of these findings, the desirable properties of compounds **2-14, 2-22** and **2-25** highlight the benefit of expanding the library of Edaravone derivatives (including modification of successful compounds) by use of hydrazine cross-coupling. Further catalyst research should enable a broader substrate scope to be achieved, which in turn may afford compounds displaying greater activity; this research will be conducted in partnership with the Treventis Corporation.

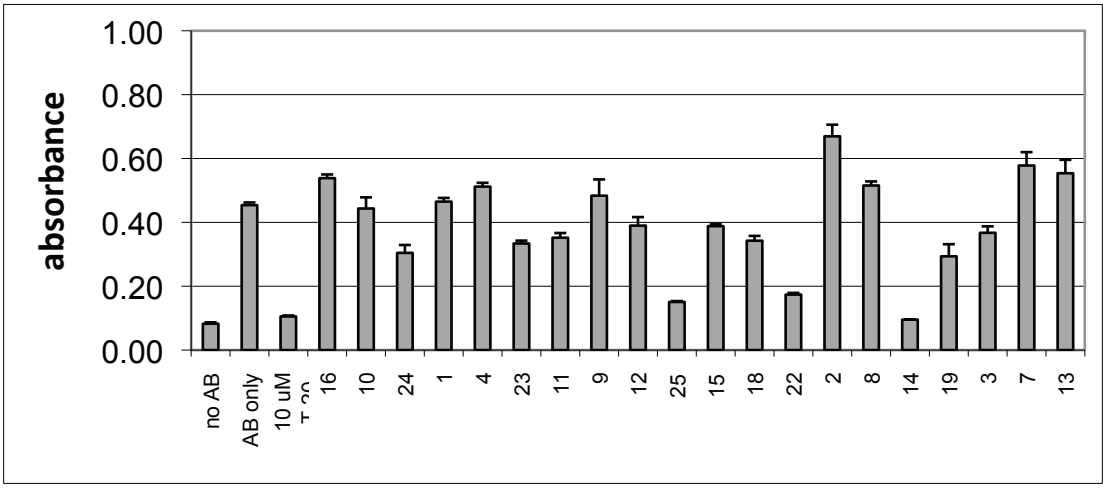

Figure 2.2 Effects of compounds [25 μM] on absorbance measurements related to oligomer formation in the Biotin-Aβ Oligo Assay (T-20 = Tween-20).

Table 2.2 Inhibition (%) on oligomer formation [25 μM] in the Biotin-Aβ Oligo Assay and IC_{50} values for compounds (**2-14**, **2-22**-**2-25**) displaying strong inhibition.

ID	% inhib. Biotin-Aβ42 - [25 μM]	IC_{50} values Biotin-Aβ42	ID	% inhib. $Aβ_{40}$ - 25 μM	IC_{50} values Biotin-Aβ42
2-1	-2	-	**2-13**	-20	-
2-2	-45	-	**2-14**	79	7.06
2-3	21	-	**2-15**	14	-
2-4	-13	-	**2-16**	-19	-
2-5	N/A	-	**2-17**	insoluble	-
2-6	N/A	-	**2-18**	26	-
2-7	7	-	**2-19**	37	-
2-8	-11	-	**2-20**	insoluble	-
2-9	-7	-	**2-21**	N/A	-
2-10	2	-	**2-22**	62	1.51
2-11	22	-	**2-23**	26	5.75
2-12	14	-	**2-24**	33	1.37
-	-	-	**2-25**	67	3.53

2.3. SUMMARY AND CONCLUSIONS

The results highlighted in this chapter demonstrate the utility of Pd-catalysts supported by DalPhos ligands developed by the Stradiotto group, specifically the ligand **1-4**, which has been exploited for the preparation of a diverse range of (hetero)aryl hydrazines. These compounds served as intermediates in the synthesis of functionalized N-aryl pyrazolones, heterocyclic compounds identified via *in silico* screening by our collaborative partners (Treventis Corporation) as a potent class of anti-aggregants that may prevent the formation of toxic Aβ oligomer species, and serve as candidates for the treatment of Alzheimer's Disease. A tandem protocol involving condensation of monoaryl hydrazines with ethylacetoacetate under acidic conditions was used to afford 25 examples of structurally diverse Edaravone derivatives in good yield. The use of (hetero)aryl (pseudo)halides substrates allowed substitution at the *N*-aryl position to incorporate fluoro, trifluoromethyl, methoxy, tolyl, naphthyl, pyridyl, amine, and ether groups. Despite the substrate scope tolerated, including the formation of aryl hydrazines that had not been achieved in the Stradiotto group's initial report on hydrazine arylation,[97] the utility of heteroaryl chlorides (e.g. thiophene, imidazole, quinoline, indole) in general proved to be challenging. Notwithstanding relatively large structural variation this class of substrates encompasses, the further development of Pd-DalPhos catalysts capable of tolerating additional functionality remains a focus of our current research efforts (Chapter 3). Lastly, biological testing of new Edaravone derivatives by means of a ThT kinetic aggregation assay and a Biotin-Aβ Oligo Assay allowed identification of several compounds highly active toward inhibition of Aβ–40 and biotin-Aβ42; their IC_{50} values were also determined. The future synthesis and testing of new Edaravone derivatives will be pursued in partnership with Treventis Corporation, with the Stradiotto group focusing on the development of synthetic methodologies that will advance BHA and related cross-coupling processes.

2.4. EXPERIMENTAL SECTION

2.4.1. General Considerations

Unless otherwise noted, all reactions were set up inside a dinitrogen-filled inert atmosphere glovebox and worked up in air using benchtop procedures. Toluene was deoxygenated by sparging with dinitrogen followed by passage through an mBraun

double column solvent purification system packed with copper-Q5 reactant. 1,4-Dioxane was purchased from Aldrich then dried over Na/benzophenone followed by distillation under an atmosphere of dinitrogen. Solvents used within the glovebox were stored over activated 4 Å molecular sieves. $[Pd(cinnamyl)Cl]_2$ was prepared according to a literature procedure.[112] Mor-DalPhos was prepared via our established method.[93] Aryl tosylates were prepared via literature methods.[64,113] All other chemicals were purchased from commercial sources in high purity and used as received. Flash column chromatography was performed on silica gel (SiliaFlash P60). Gas chromatography (GC) data were obtained on a Shimadzu GC-2014 equipped with a SGE BP-5 30 m, 0.25 mm I.D. column. All ^{1}H and $^{13}C\{^{1}H\}$ NMR spectral data were collected at 300 K on a Bruker AV-500 spectrometer operating at 500.1 and 125.8 MHz respectively, with chemical shifts reported in parts per million downfield of $SiMe_4$. NMR spectral data were acquired with the assistance of Dr. M. Lumsden (NMR-3, Dalhousie University) while mass spectrometric data were acquired by Mr. Xiao Feng (Mass Spectrometry Laboratory, Dalhousie University).

2.4.2. Experimental Section for Section 2.2

General catalytic and condensation protocols to prepare pyrazolones:[107]

In an inert atmosphere glovebox, $[Pd(cinnamyl)Cl]_2$ (typically 2.5 mol%) and Mor-DalPhos (typically 7.5 mol%) were added to a vial sealed with a cap containing a PTFE septum and stirred in toluene for 5 min, then NaOtBu (2.1 equiv.) was added along with the aryl chloride substrate (1 equiv., [ArCl] = 0.1 M) if it was a solid. After removing the vial from the glovebox the aryl chloride was added via a syringe if it was a liquid, along with hydrazine hydrate (2.0 equiv.). The solution was stirred at the desired temperature for 0.5-3 h. Generally, after a short period of time, solutions were observed to darken and considerable black precipitate was formed. After completion of the reaction was observed by TLC, the solution was allowed to cool and filtered through a short plug of neutral alumina, which was washed with CH_2Cl_2/MeOH (25:1). The resulting eluent solution was concentrated and charged with ethyl acetoacetate (1 equiv., [ethyl acetoacetate] = 0.125 M) and glacial acetic acid. The solution was heated at reflux for 0.5-3 h, and the reaction progress was monitored by use of TLC. After complete

consumption of the aryl hydrazine, the solution was cooled, diluted with EtOAc (40 mL) and washed with H_2O (60 mL) followed by 1:1 H_2O/brine (60 mL). The organic fractions were dried over Na_2SO_4, filtered and concentrated to afford crude product which was purified by column chromatography. Typical reaction scales were 0.4 -1.0 mmol. Aryl hydrazines were unstable at room temperature and were stored at -4 ^oC for no longer than 12 hours before reacting with ethyl acetoacetate.

Characterization of Reaction Products:

5-Methyl-2-phenyl-2,4-dihydropyrazol-3-one (2-1). Intermediate aryl hydrazine was prepared from chlorobenzene employing the standard catalytic protocol (temp. = 90 ^oC, reaction time (rt) = 1 h), however, 5 mol% $[Pd(cinnamyl)Cl]_2$ and 15 mol% Mor-DalPhos was used. Title compound **2-1** was isolated employing the standard condensation protocol (rt = 45 min) in 76 % yield as a off-white solid (73 mg, 0.36 mmol) after column chromatography (15:1 CH_2Cl_2:EtOAc). Following the same procedure, title compound **2-1** was alternatively prepared from phenyl tosylate in 77 % yield (67 mg, 0.39 mmol). ^1H NMR ($CDCl_3$): δ 7.86 (m, 2H), 7.39 (m, 2H), 7.14 (m, 1H), 3.43 (s, 2H), 2.20 (s, 3H). $^{13}C\{^1H\}$ NMR ($CDCl_3$): δ 170.7, 156.5, 138.1, 129.0, 125.2, 119.0, 43.3, 17.2. HRMS (ESI/$[M+H]^+$) calcd. for $C_{10}H_{10}N_2O$: 175.0866. Found: 175.0858. Spectral data are in good in agreement with previously reported ^1H and ^{13}C NMR spectral data for the title product.[114] The title compound could also be prepared on a larger scale (460 mg, 2.64 mmol, 53 % yield) employing the standard protocol.

5-Methyl-2-*o*-tolyl-2,4-dihydropyrazol-3-one (2-2). Intermediate aryl hydrazine was prepared from 2-chlorotoluene employing the standard catalytic protocol (temp. = 90 ^oC, rt = 1.5 h). Title compound **2-2** was isolated employing the standard condensation protocol (rt = 2.5 h) in 70% yield as a grey solid (66 mg, 0.36 mmol) after column chromatography (1:1 CH_2Cl_2:EtOAc). ^1H NMR ($CDCl_3$): δ 7.30-7.24 (m, 4H), 3.41 (s, 2H), 2.29 (s, 3H), 2.19 (s, 3H). $^{13}C\{^1H\}$ NMR ($CDCl_3$): δ 171.3, 156.2, 135.9, 135.2, 131.3, 128.6, 126.7,41.8, 18.5, 17.2. HRMS (ESI/$[M+H]^+$) calcd. for $C_{11}H_{13}N_2O$: 189.1022. Found: 189.1019. Spectral data are in good in agreement with previously reported ^1H and ^{13}C NMR spectral data for the title product.[115]

5-Methyl-2-*m*-tolyl-2,4-dihydropyrazol-3-one (2-3). Intermediate aryl hydrazine was prepared from chlorobenzene employing the standard catalytic protocol (temp. = 90 ^{o}C, rt = 1 h). Title compound **2-3** was isolated employing the standard condensation protocol (rt = 1.5 h) in 64% yield as a pale beige solid (60 mg, 0.32 mmol) after column chromatography (10:1 CH_2Cl_2:EtOAc). ^{1}H NMR ($CDCl_3$): δ 7.65 (m, 2H), 7.27 (t, *J* = 7.7 Hz, 1H), 7.00 (d, *J* = 7.3 Hz, 1H), 3.42 (s, 2H), 2.38 (s, 3H), 2.19 (s, 3H). ^{13}C{^{1}H} NMR ($CDCl_3$): δ 170.7, 156.4, 138.9, 138.0, 128.8, 126.1, 119.7, 116.3, 43.3, 21.7, 17.2. HRMS (ESI/$[M+H]^+$) calcd. for $C_{11}H_{13}N_2O$: 189.1022. Found: 189.1027. Spectral data are in good in agreement with previously reported ^{1}H and ^{13}C NMR spectral data for the title product.[115]

5-Methyl-2-*p*-tolyl-2,4-dihydropyrazol-3-one (2-4). Intermediate aryl hydrazine was prepared from chlorobenzene employing the standard catalytic protocol (temp. = 90 ^{o}C, rt = 1 h), however, 5 mol% $[Pd(cinnamyl)Cl]_2$ and 15 mol% Mor-DalPhos was used. Title compound **2-4** was isolated employing the standard condensation protocol (rt = 45 min) in 65% yield as an off-white solid (61 mg, 0.33 mmol) after column chromatography (10:1 CH_2Cl_2:EtOAc). ^{1}H NMR ($CDCl_3$): δ 7.71 (d, *J* = 7.6 Hz, 2H) 7.18 (d, *J* = 8.2 Hz, 2H), 3.41 (s, 2H), 2.34 (s, 3H), 2.19 (s, 3H). ^{13}C{^{1}H} NMR ($CDCl_3$): δ 170.6, 156.3, 135.7 134.9, 129.5, 119.1, 43.2, 21.1, 17.2. HRMS (ESI/$[M+H]^+$) calcd. for $C_{11}H_{13}N_2O$: 189.1022. Found: 189.1014. Spectral data are in good in agreement with previously reported ^{1}H and ^{13}C NMR spectral data for the title product.[116]

5-Methyl-2-naphthalen-1-yl-2,4-dihydropyrazol-3-one (2-5). Intermediate aryl hydrazine was prepared from chlorobenzene employing the standard catalytic protocol at (temp. = 65 ^{o}C, rt = 45 min). Title compound **2-5** was isolated employing the standard condensation protocol (rt = 45 min) in 68% yield as a beige solid (64 mg, 0.29 mmol) after column chromatography (7:3 CH_2Cl_2:EtOAc). ^{1}H NMR ($CDCl_3$): δ 7.90-7.84 (m, 3H), 7.55-7.50 (m, 4H), 3.49 (s, 2H), 2.20 (s, 3H). ^{13}C{^{1}H} NMR ($CDCl_3$): δ 172.3, 156.8, 134.7, 133.2, 129.4, 129.2, 128.5, 126.9, 126.5, 125.5, 124.6, 123.5, 42.1, 17.3. HRMS (ESI/$[M+Na]^+$) calcd. for $C_{14}H_{12}N_2NaO$: 247.0842. Found: 247.0844.

5-Methyl-2-naphthalen-2-yl-2,4-dihydropyrazol-3-one (2-6). Intermediate aryl hydrazine was prepared from 2-naphthyl tosylate employing the standard catalytic protocol at (temp. = 65 ^{o}C, rt = 45 min). Title compound **2-6** was isolated via the standard condensation protocol (rt = 0.5 h) in 65% yield as a beige solid (73 mg, 0.33 mmol) after column chromatography (10:1 CH_2Cl_2:EtOAc). ^{1}H NMR ($CDCl_3$): δ 8.33 (m, 1H), 8.07 (m, 1H), 7.87-7.81 (m, 2H), 7.49-7.42 (m, 2H), 3.48 (s, 2H), 2.24 (s, 3H). $^{13}C\{^{1}H\}$ NMR ($CDCl_3$): δ 170.8, 156.6, 135.8, 133.6, 131.1, 128.8, 128.1, 127.7, 126.6, 125.5, 118.6, 116.0, 43.4, 17.2. HRMS (ESI/$[M+H]^+$) calcd. for $C_{14}H_{13}N_2O$: 225.1022. Found: 225.1029.

2-(2-Ethylphenyl)-5-methyl-2,4-dihydropyrazol-3-one (2-7). Intermediate aryl hydrazine was prepared from 2-ethylphenyl tosylate employing the standard catalytic protocol (temp. = 65 ^{o}C, rt = 1 h). Title compound **2-7** was isolated employing the standard condensation protocol (rt = 0.5 h) in 74% yield as a yellow oil (75 mg, 0.37 mmol) after column chromatography (3:2 CH_2Cl_2:EtOAc). ^{1}H NMR ($CDCl_3$): δ 7.34-7.26 (m, 4H), 3.40 (s, 2H), 2.64 (q, J = 7.6 Hz, 2H), 2.17 (s, 3H), 1.20 (t, J = 7.6 Hz, 3H). $^{13}C\{^{1}H\}$ NMR ($CDCl_3$): δ 171.7, 156.3, 141.3, 135.2, 129.4, 129.1, 127.2, 126.7, 41.7, 24.6, 17.2, 14.4. HRMS (ESI/$[M+H]^+$) calcd. for $C_{12}H_{15}N_2O$: 203.1179. Found: 203.1180.

2-(2,5-Dimethylphenyl)-5-methyl-2,4-dihydropyrazol-3-one (2-8). Intermediate aryl hydrazine was prepared from 1-chloro-2,5-dimehtylbenzene employing the standard catalytic protocol (temp. = 90 ^{o}C, rt = 1 h), however, 5 mol% $[Pd(cinnamyl)Cl]_2$ and 15 mol% Mor-DalPhos was used. Title compound **2-8** was isolated employing the standard condensation protocol (rt = 1 h) in 72% yield as a pale beige solid (73 mg, 0.36 mmol) after column chromatography (10:1 CH_2Cl_2:EtOAc → 5:1 CH_2Cl_2:EtOAc). Following the same procedure, title compound **2-8** was alternatively prepared from 2,5-dimethylphenyl tosylate in 45% yield (45 mg, 0.23 mmol). ^{1}H NMR ($CDCl_3$): δ 7.16 (m, 1H), 7.10-7.06 (m, 2H), 3.39 (m, 2H), 2.32 (s, 3H), 2.22 (s, 3H), 2.17 (s, 3H). $^{13}C\{^{1}H\}$

NMR ($CDCl_3$): δ 171.4, 156.4, 136.5, 135.5, 132.0, 131.0, 129.5, 127.1, 41.8, 20.9, 18.0, 17.2. HRMS (ESI/$[M+H]^+$) calcd. for $C_{12}H_{15}N_2O$: 203.1179. Found: 203.1178.

2-(5-Fluoro-2-methylphenyl)-5-methyl-2,4-dihydropyrazol-3-one (2-9)

Intermediate aryl hydrazine was prepared from 2-chloro-4-fluorotoluene employing the standard catalytic protocol (temp. = 90 ^oC, rt = 0.5 h), however, 5 mol% $[Pd(cinnamyl)Cl]_2$ and 15 mol% Mor-DalPhos was used. Title compound **2-9** was isolated employing the standard condensation protocol (rt = 1 h) in 71% yield as a white solid (73 mg, 0.35 mmol) after column chromatography (9:1 CH_2Cl_2:EtOAc → 7:3 CH_2Cl_2:EtOAc). ^1H NMR ($CDCl_3$): δ 7.23-7.20 (m, 1H), 7.03 (td, J = 2.7, 8.3 Hz, 1H), 3.01 (s, 2H), 2.23 (s, 3H), 2.10 (s, 3H). $^{13}C\{^1H\}$ NMR δ ($CDCl_3$): 171.2, 160.9 (d, J_{CF} = 245 Hz), 156.9, 136.5 (d, J_{CF} = 10 Hz), 132.2 (d, J_{CF} = 8.6 Hz), 130.6 (d, J_{CF} = 3 Hz), 115.4 (d, J_{CF} = 21 Hz), 113.5 (d, J = 23 Hz), 41.8, 18.0, 17.2. HRMS (ESI/$[M+H]^+$) calcd. for $C_{11}H_{12}FN_2O$: 207.0928. Found: 207.0921.

2-(3-Fluoro-4-methylphenyl)-5-methyl-2,4-dihydropyrazol-3-one (2-10).

Intermediate aryl hydrazine was prepared from 4-chloro-2-fluorotoluene employing the standard catalytic protocol (temp. = 90 ^oC, rt = 1 h). Title compound **2-10** was isolated employing the standard condensation protocol (rt = 3 h) in 62% yield as a pale beige solid. (63 mg, 0.31 mmol) after column chromatography (15:1 → 10:1 CH_2Cl_2:EtOAc). ^1H NMR ($CDCl_3$): δ 7.61-7.55 (m, 2H), 7.16 (m, 1H), 3.41 (s, 2H), 2.25 (m, 3H), 2.18 (s, 3H). $^{13}C\{^1H\}$NMR ($CDCl_3$): δ 170.5, 161.1 (d, J_{CF} = 243 Hz), 156.6, 137.2, 131.4, 121.3 (d, J_{CF} = 17.4 Hz), 113.9, 106.0 (d, J_{CF} = 28 Hz), 43.3, 17.1, 14.3. HRMS (ESI/$[M+H]^+$) calcd. for $C_{11}H_{12}FN_2O$: 207.0928. Found: 207.0922.

5-Methyl-2-(4-trifluoromethyl)phenyl-2,4-dihydropyrazol-3-one (2-11).

Intermediate aryl hydrazine was prepared from 4-trifluoromethylchlorobenzene employing the standard catalytic protocol (temp. = 90 ^oC, rt = 1 h). Title compound **2-11** was isolated employing the standard condensation protocol (rt = 1.5 h) in 43% yield as a white solid (52 mg, 0.22 mmol) after column chromatography (10:1 CH_2Cl_2:EtOAc), and subsequent washing with hexanes. ^1H NMR ($CDCl_3$): δ 8.05 (d, J = 8.5 Hz, 2H), 7.63 (d,

J = 8.6 Hz, 2H), 3.47 (m, 2H), 2.22 (s, 3H). $^{13}C\{^1H\}$ NMR ($CDCl_3$): δ 170.9, 157.1, 140.9, 126.5 (m), 126.2 (d, J_{CF} = 4 Hz), 125.2 (d, J_{CF} = 272 Hz), 118.2, 43.3, 17.2. HRMS (ESI/$[M+H]^+$) calcd. for $C_{11}H_{10}F_3N_2O$: 243.0740. Found: 243.0745. Spectral data are in good in agreement with previously reported ^1H and ^{13}C NMR spectral data for the title product.[116]

2-(3-Fluoro-5-methoxy-phenyl)-5-methyl-2,4-dihydro-pyrazol-3-one (2-12). Intermediate aryl hydrazine was prepared from 1-chloro-3-fluoro-5-methoxybenzene employing the standard catalytic protocol (temp. = 90 ^oC, rt = 1 h). Title compound **2-12** was isolated employing the standard condensation protocol (rt = 3 h) in 75% yield as a pale beige solid solid (83 mg, 0.37 mmol) after column chromatography (20:1 CH_2Cl_2:EtOAc → 12:1 CH_2Cl_2:EtOAc). ^1H NMR ($CDCl_3$): δ 7.26-7.22 (m, 2H), 6.37 (d, J = 10 Hz, 1H), 3.75 (s, 3H), 3.35 (s, 2H), 2.11 (s, 3H). $^{13}C\{^1H\}$ NMR ($CDCl_3$): δ 170.6, 163.6 (d, J_{CF} = 243 Hz), 161.1 (d, J_{CF} = 13 Hz), 156.6, 139.8 (d, J_{CF} = 14 Hz), 99.6, 98.4 (d, J_{CF} = 9 Hz), 98.2 (d, J_{CF} = 7 Hz), 55.6, 43.3, 17.0. HRMS (ESI/$[M+H]^+$) calcd. for $C_{11}H_{12}FN_2O_2$: 223.0877. Found: 223.0874.

2-(3-Methoxy-phenyl)-5-methyl-2,4-dihydro-pyrazol-3-one (2-13). Intermediate aryl hydrazine was prepared from 3-methoxyphenyl tosylate employing the standard catalytic protocol (temp. = 90 ^oC, rt = 1 h). Title compound **2-13** was isolated employing the standard condensation protocol (rt = 3 h) 50% yield as an off-white solid (51 mg, 0.25 mmol) after column chromatography (20:1 CH_2Cl_2:MeOH). ^1H NMR ($CDCl_3$): δ 7.49-7.46 (m, 2H), 7.30-7.26 (m, 1H), 6.74-6.72 (m, 1H), 3.83 (s, 3H), 3.42 (s, 2H), 2.19 (s, 3H). $^{13}C\{^1H\}$ NMR ($CDCl_3$): δ 170.7, 160.1, 156.4, 139.3, 129.7, 111.2, 111.1, 104.5, 55.5, 43.3, 17.2. HRMS (ESI/$[M+H]^+$) calcd. for $C_{11}H_{13}N_2O_2$: 205.0972. Found: 205.0971.

2-(4-Diphenylamino-phenyl)-5-methyl-2,4-dihydro-pyrazol-3-one (2-14). Intermediate aryl hydrazine was prepared from (4-chloro-phenyl)-diphenyl-amine employing the standard catalytic protocol (temp. = 90 ^{o}C, rt = 1 h). Title compound **2-14** was isolated employing the standard condensation protocol (rt = 3 h) in 37% yield as a brown solid (60 mg, 0.18 mmol) after column chromatography (20:1 CH_2Cl_2:EtOAc). ^{1}H NMR ($CDCl_3$): δ 7.68 (m, 2H), 7.26-7.22 (m, 4H), 7.13-7.07 (m, 6H), 6.99 (t, *J* = 7.3 Hz, 2H), 3.42 (s, 2H), 2.19 (s, 3H). $^{13}C\{^{1}H\}$ NMR ($CDCl_3$): δ 170.5, 156.5, 147.8, 145.1, 133.0, 129.3, 124.7, 124.1, 122.8, 120.6, 43.1, 17.1. HRMS (ESI/$[M+H]^+$) calcd. for $C_{22}H_{20}N_3O$: 342.1601. Found: 342.1588.

5-Methyl-2-(3-pyrrolidin-1-yl-phenyl)-2,4-dihydro-pyrazol-3-one (2-15). Intermediate aryl hydrazine was prepared from 1-(3-chloro-phenyl)-pyrrolidine employing the standard catalytic protocol (temp. = 90 ^{o}C, rt = 1 h). Title compound **2-15** was isolated employing the standard condensation protocol (rt = 3 h) in 50% yield as a pale white solid (60 mg, 0.25 mmol) after column chromatography (12:1 CH_2Cl_2:EtOAc). ^{1}H NMR ($CDCl_3$): δ 7.21 (t, *J* = 8.1 Hz, 1H), 7.12 (m, 1H), 7.07 (t, *J* = 2.2 Hz, 1H), 6.39 (dd, *J* = 8.2, 1.8 Hz, 1H), 3.39 (s, 2H), 3.30 (m, 4H), 2.17 (s, 3H), 2.00-1.98 (m, 4H). $^{13}C\{^{1}H\}$ NMR ($CDCl_3$): δ 170.7, 156.0, 148.5, 139.0, 129.4, 108.8, 106.4, 102.5, 47.8, 43.3, 25.5, 17.1. HRMS (ESI/$[M+H]^+$) calcd. for $C_{14}H_{18}N_3O$: 244.1444. Found: 244.1447.

5-Methyl-2-(4-pyrrol-1-yl-phenyl)-2,4-dihydro-pyrazol-3-one (2-16). Intermediate aryl hydrazine was prepared from 4-(*N*-pyrrole)chlorobenzene employing the standard catalytic protocol (temp. = 90 ^{o}C, rt = 1 h). Title compound **2-16** was isolated employing the standard condensation protocol (rt = 3 h) in 86% yield as a pale white solid (109 mg, 0.43 mmol) after column chromatography (10:1 CH_2Cl_2:EtOAc). ^{1}H NMR ($CDCl_3$): δ 7.93 (m, 2H), 7.41 (m, 2H), 7.08 (t, *J* = 2.2 Hz, 2H), 6.35 (t, 2.2 Hz, 2H), 3.45 (s, 2H), 2.21 (s, 3H). $^{13}C\{^{1}H\}$ NMR ($CDCl_3$): δ 170.6, 156.7, 137.7, 135.8, 120.9, 120.0, 119.5, 110.5, 43.2, 17.2. HRMS (ESI/$[M+H]^+$) calcd. for $C_{14}H_{14}N_3O$: 240.1131. Found: 240.1120.

5-Methyl-2-(3-methylsulfanyl-phenyl)-2,4-dihydro-pyrazol-3-one (2-17). Intermediate aryl hydrazine was prepared from 3-chlorothioanisole employing the standard catalytic protocol (temp. = 110 ^{o}C, rt = 0.5 h), however, 5 mol% [Pd(cinnamyl)Cl]$_2$ and 15 mol% Mor-DalPhos was used. Title compound **2-17** was isolated employing the standard condensation protocol (rt = 3 h) in 60% yield as a beige solid (66 mg, 0.30 mmol) after column chromatography (CH_2Cl_2 → 10:1 CH_2Cl_2:EtOAc). ^{1}H NMR ($CDCl_3$): δ 7.80 (t, *J* = 1.9 Hz, 1H), 7.66 (ddd, *J* = 8.4, 1.9, 0.8 Hz, 1H), 7.29 (t, *J* = 8 Hz, 1H), 7.06 (m, 1H), 3.43 (s, 2H), 2.50 (s, 3H), 2.19 (s, 3H). ^{13}C{^{1}H} NMR ($CDCl_3$): δ 170.7, 156.5, 139.5, 138.7, 129.2, 123.0, 116.5, 115.4, 43.3, 17.2, 15.8. HRMS (ESI/[M+H]$^+$) calcd. for $C_{11}H_{13}N_2OS$: 221.0743. Found: 221.0748.

2-(3-Benzyloxymethyl-phenyl)-5-methyl-2,4-dihydro-pyrazol-3-one (2-18). Intermediate aryl hydrazine was prepared from distilled 3-benzyloxymethylchlorobenzene employing the standard catalytic protocol (temp. = 65 ^{o}C, rt = 1 h). Title compound **2-18** was isolated employing the standard condensation protocol (rt = 3 h) in 82% yield as a dark yellow oil (121 mg, 0.41 mmol) after column chromatography (10:1 CH_2Cl_2:EtOAc). ^{1}H NMR ($CDCl_3$): δ 7.88 (s, 1H), 7.83 (d, *J* = 8.2 Hz, 1H), 7.40-7.35 (m, 5H), 7.31-7.28 (m, 1H), 7.22 (d, *J* = 7.6 Hz, 1H), 4.58 (s, 2H), 4.57 (s, 2H), 3.41 (s, 2H), 2.17 (s, 3H). ^{13}C{^{1}H} NMR ($CDCl_3$): 176.2, 170.8, 156.5, 139.3, 138.3, 138.2, 129.1, 128.5, 128.0, 127.8, 124.5, 118.3, 72.3, 72.1, 43.3, 17.2. HRMS (ESI/[M+Na]$^+$) calcd. for $C_{18}H_{18}N_2NaO_2$: 317.1260. Found: 317.1253.

5-Methyl-2-pyridin-3-yl-2,4-dihydro-pyrazol-3-one (2-19). Intermediate aryl hydrazine was prepared from 3-chloropyridine employing the standard catalytic protocol (temp. = 65 ^{o}C, rt = 1.5 h). Title compound **2-19** was isolated employing the standard condensation protocol (rt = 1 h) in 61% yield as a pale yellow solid (53 mg, 0.30 mmol) after column chromatography (50:1 CH_2Cl_2:MeOH). ^{1}H NMR ($CDCl_3$): δ 9.13 (s, 1H), 8.40 (d, *J* = 4.2, 1H), 8.24 (d, *J* = 8.0 Hz, 1H), 7.30 (m, 1H), 3.43 (s, 2H), 2.20 (s, 3H). ^{13}C{^{1}H} NMR ($CDCl_3$): δ 171.0, 157.4, 145.7, 140.2, 135.0, 125.5, 123.5, 42.8, 17.2. HRMS (ESI/[M+H]$^+$) calcd. for $C_9H_{10}N_3O$: 176.0818. Found: 176.0811.

5-Methyl-2-(2-methyl-pyridin-3-yl)-2,4-dihydro-pyrazol-3-one (2-20). Intermediate aryl hydrazine was prepared from 2-methyl-3-pyridyl tosylate employing the standard catalytic protocol (temp. = 90 ^{o}C, rt = 1.5 h), however, 5 mol% [Pd(cinnamyl)Cl]$_2$ and 15 mol% Mor-DalPhos was used. Title compound **2-20** was isolated employing the standard condensation protocol (rt = 1 h) in 74% yield as an off-white solid (70 mg, 0.37 mmol) after column chromatography (20:1 CH_2Cl_2:MeOH). ^{1}H NMR ($CDCl_3$): δ 8.48 (m, 1H), 7.63 (m, 1H), 7.21 (m, 1H), 3.42 (s, 2H), 2.52 (s, 3H), 2.18 (s, 3H). ^{13}C{^{1}H} NMR ($CDCl_3$): δ 171.3, 157.1, 155.3, 148.7, 134.1, 132.2, 121.6, 41.8, 21.8, 17.2. HRMS (ESI/[M+H]$^{+}$) calcd. for $C_{10}H_{12}N_3O$: 190.0975. Found: 190.0983.

2-(2,6-Dimethoxy-pyrimidin-4-yl)-5-methyl-2,4-dihydro-pyrazol-3-one (2-21). Intermediate aryl hydrazine was prepared from 4-Chloro-2,6-dimethoxy-pyrimidine employing the standard catalytic protocol (temp. = 90 ^{o}C, rt = 1 h), however, 5 mol% [Pd(cinnamyl)Cl]$_2$ and 15 mol% Mor-DalPhos was used. Title compound **2-21** was isolated employing the standard condensation protocol (rt = 3 h) in 61% yield as a beige solid (60 mg, 0.25 mmol) after column chromatography (10:1 CH_2Cl_2:EtOAc → 5:1 CH_2Cl_2:EtOAc). ^{1}H NMR ($CDCl_3$): δ 11.98 (s, 1H), 6.71 (S, 1H), 5.39 (S, 1H), 3.99 (s, 3H), 2.21 (s, 3H). ^{13}C{^{1}H} NMR ($CDCl_3$): δ 173.2, 163.6, 161.1, 157.2, 153.5, 88.9, 85.6, 55.2, 54.7, 14.8. HRMS (ESI/[M+H]$^{+}$) calcd. for $C_{10}H_{12}N_4NaO_3$: 259.0802. Found: 259.0794.

2-Biphenyl-4-yl-5-methyl-2,4-dihydro-pyrazol-3-one (2-22). Intermediate aryl hydrazine was prepared from 4-chloro-biphenyl employing the standard catalytic protocol (temp. = 90 ^{o}C, rt = 1 h). Title compound **2-22** was isolated employing the standard condensation protocol (rt = 3 h) in 50% yield as a pale white solid solid (63 mg, 0.25 mmol) after column chromatography (12:1 CH_2Cl_2:EtOAc). ^{1}H NMR ($CDCl_3$): δ 7.95 (m, 2H), 7.64-7.59 (m, 4H), 7.44 (m, 2H), 7.34 (t, J = 7.4 Hz, 1H), 3.45 (s, 2H), 2.22 (s, 3H). ^{13}C{^{1}H} NMR ($CDCl_3$): δ 170.7, 156.6, 140.6, 137.9, 137.4, 128.9, 127.6, 127.3, 127.1, 119.2, 43.3, 17.2. HRMS (ESI/[M+H]$^{+}$) calcd. for $C_{16}H_{15}N_2O$: 251.1179. Found: 251.1178.

2-(4'-Methoxy-biphenyl-4-yl)-5-methyl-2,4-dihydro-pyrazol-3-one (2-23). Intermediate aryl hydrazine was prepared from 4-chloro-(4'- methoxybiphenyl) employing the standard catalytic protocol (temp. = 90 ^{o}C, rt = 0.5 h). Title compound **2-23** was isolated employing the standard condensation protocol (rt = 3 h) in 66% yield as a pale beige solid (91 mg, 0.33 mmol) after column chromatography (9:1 CH_2Cl_2:EtOAc). ^{1}H NMR ($CDCl_3$): δ 7.90 (m, 2H), 7.58 (m, 2H), 7.53 (m, 2H), 6.97 (m, 2H), 3.85 (s, 3H), 3.44 (s, 2H), 2.21 (s, 3H). ^{13}C{^{1}H} NMR ($CDCl_3$): 170.7, 159.2, 156.6, 137.6, 136.9, 133.2, 128.1, 127.1, 119.3, 114.4, 55.5, 43.3, 17.2. HRMS (ESI/$[M+H]^+$) calcd. for $C_{17}H_{17}N_2O_2$: 281.1285. Found: 281.1277. The title compound could also be prepared on a larger scale (49% yield, 680 mg, 2.43 mmol) employing the standard protocol.

5-Methyl-2-(4-pyridin-3-yl-phenyl)-2,4-dihydro-pyrazol-3-one (2-24). Intermediate aryl hydrazine was prepared from 4-(3'-pyridinyl)chlorobenzene employing the standard catalytic protocol (temp. = 65 ^{o}C, rt = 2 h). Title compound **2-24** was isolated employing the standard condensation protocol (rt = 3 h) in 55% yield as a light yellow solid (165 mg, 0.66 mmol) after column chromatography (1:1 CH_2Cl_2: EtOAc). ^{1}H NMR ($CDCl_3$): δ 8.85 (m, 1H), 8.57 (dd, J = 4.8, 1.6 Hz, 1H), 8.00 (m, 2H), 7.88 (m, 1H), 7.61 (m, 2H), 7.36 (m, 1H), 3.47 (m, 2H), 2.22 (s, 3H). ^{13}C{^{1}H} NMR ($CDCl_3$): δ 170.7, 156.8, 148.4, 148.2, 138.2, 136.1, 134.3, 127.6, 123.7, 119.3, 43.3, 17.2. HRMS (ESI/$[M+H]^+$) calcd. for $C_{15}H_{14}N_3O$: 252.1131. Found: 252.1134.

5-Methyl-2-[4-(2-phenyl-indol-1-yl)-phenyl]-2,4-dihydro-pyrazol-3-one (2-25). Intermediate aryl hydrazine was prepared from 1-(4-chlorophenyl)-2-phenyl-1*H*-indole[72i] chlorobenzene employing the standard catalytic protocol (temp. = 90 ^{o}C, rt = 1 h). Title compound **2-25** was isolated employing the standard condensation protocol (rt = 3 h) in 83% yield as a pale white solid (97 mg, 0.27 mmol) after column chromatography (20:1 CH_2Cl_2:EtOAc). ^{1}H NMR ($CDCl_3$): δ 7.96 (m, 2H), 7.72-7.65 (m, 1H), 7.33-7.15 (m, 10H), 6.80 (s, 1H), 3.46 (s, 2H), 2.21 (s, 3H). ^{13}C{^{1}H} NMR ($CDCl_3$): δ 170.7, 156.8, 140.9, 139.2, 137.0, 135.1, 132.5, 129.1, 128.5, 128.4, 127.5, 122.5, 120.8, 120.6, 119.4, 110.7, 103.8, 43.2, 17.2. HRMS (ESI/$[M+Na]^+$) calcd. for $C_{24}H_{19}N_3NaO$: 384.1420. Found: 384.1420.

The following protocol was used to analyze compounds in the Thioflavin T (ThT) aggregation Assay:

Preparation of $A\beta_{40}$ stock solutions:

$A\beta_{40}$ (1.0 mg) was pre-treated in a 1.5 mL microfuge tube with HFIP (1 mL) and sonicated for 20 min to disassemble any pre-formed Aβ aggregates. The HFIP was removed with a stream of argon and the Aβ dissolved in Tris base (5.8 mL, 20 mM, pH ~10). The pH was adjusted to 7.4 with concentrated HCl (~ 10 μL) and the solution filtered using a syringe filter (0.2 μm) before being used.

Procedure for ThT Aβ aggregation assay:

The kinetic ThT assay for Aβ aggregation is similar to that reported by Gervais *et al*.[110] Briefly, pre-treated Aβ40 (40 μM in 20 mM Tris, pH 7.4), was diluted with an equal volume of 8 μM ThT in Tris (20 mM, pH 7.4, 300 mM NaCl). Aliquots of Aβ/ThT (200 μL) were added to wells of a black polystyrene 96-well plate, followed by 2μL of a compound in DMSO (variable concentration), or DMSO alone (controls). Incubations were performed in triplicate and were taken to contain 20 μM Aβ, various concentration of compound in 20 mM Tris, pH 7.4, 150 mM NaCl, 1% DMSO. Plates were covered with clear polystyrene lids and incubated at 37 ^{o}C in a Tecan Genios microplate reader. Fluorescence readings (λ_{ex} = 450 nm, λ_{em} = 480 nm) were taken every 15 minutes, after first shaking at high intensity for 15 s and allowing to settle for 10 s before each reading. Active compounds attenuated the increase in fluorescence over time that occurred in controls. Compounds **2-1**-**2-25** (excluding **2-5**-**2-6**, and **2-21**; **2-17** and **2-20** were found to be insoluble) were tested for their inhibitory aggregation effect at two concentrations, 25μM and 10 μM.

Procedure for N-biotinyl-Aβ42 (bio-Ab42) Oligomer Assembly Assay:

The degree of Aβ oligomer formation was quantified using N-biotinyl-Aβ42 (bio-

Aβ42) Oligomer Assembly Assay (for detailed experimental procedure please refer to two recent reports by Levine III *et al*).[111] Bio-Aβ42, treated with hexafluoroisopropanol (HFIP) and trifluoroacetic acid (TFA) to disassemble pre-formed aggregates, is re-suspended in DMSO 1 h before use. The bio-Aβ42 was added to 96-well polypropylene plates containing test compound or vehicle control and the reaction started by the addition of Oligo Formation Buffer (OFB). After stopping the reaction with Tween-20 (polyoxyethylene sorbitan monolaurate; a wetting agent utilized to quench the reaction and prevent monomer re-association without destroying oligomers formed over the course of the assay), samples of the reaction mixture were added to a 96-well polystyrene plate pre-coated with NeutrAvidin, where the oligomeric form will bind to the plate in this assay without interference from non-biotin containing compounds.[111a] Following washes and the addition of Streptavidin-HRP and substrate, the colour was allowed to develop for 5-10 min and the absorbance read at 450 nM.

Compounds **2-1**-**2-25** (excluding **2-5**-**2-6**, and **2-21**; **2-17** and **2-20** were found to be insoluble) were tested for their inhibitory effect on oligomer formation at 25μM. Several compounds (**2-14** and **2-22**-**2-25**) showing strong inhibition at 25μM were retested at several concentrations in order to obtain an IC_{50} value.

CHAPTER 3. RATIONAL STRUCTURAL DIVERSIFICATION OF THE DALPHOS LIGAND FAMILY

3.1. INTRODUCTION AND CHAPTER OVERVIEW

Advances in transition metal catalysis are rooted in the development of new, highly reactive metal complexes that can mediate chemical transformations of what are otherwise relatively inert molecules (e.g, alkanes, alkenes, amines). Ancillary ligands that are capable of supporting electronically and coordinatively unsaturated metal centers have been key to this endeavor; such unsaturated metal centers are typically highly reactive in that they feature empty coordination sites capable of substrate binding. The development of new classes of ancillary ligands, as discussed in Chapter 1, has contributed greatly to the success of the palladium-catalyzed amination of (hetero)aryl (pseudo)halides. To this end, BHA has emerged as a synthetic methodology for the construction of complex organic structures in widespread applications.[1]

Tertiary monodentate/bidentate (bis)phosphines[32] and NHCs[3a] have successfully been employed in combination with carefully chosen Pd-precursors, allowing for an advancement of the scope and efficiency of BHA. Studies whereby new task-specific ligands are applied to address reaction challenges (e.g. ammonia arylation; Chapter 1, Section 1.5.2), have allowed researchers to establish general trends in catalyst behavior, fuelling the development of advanced catalyst systems. Although these trends rely on a variety of factors, such as the steric and electronic profile of the catalyst and substrates employed, ancillary ligands offer a great degree of control over reactivity. While the goal of cross-coupling any N-H containing nucleophile with any (hetero)aryl electrophiles (i.e., catalyst universality) remains unaccomplished, many research groups have significantly advanced the scope of BHA through ligand design.[33b]

The Buchwald group has developed the most successful family of structurally related ligands for BHA; these task-specific monodentate dialkylbiaryl phosphines may be used to generate highly active catalysts for accomplishing some of the most challenging aminations.[32,33c] Similarly, the Hartwig group has developed several generations of active catalysts, in most cases by exploiting known ligands, for which they have established structure-activity relationships. This is perhaps best exemplified by studies on analogs of the most successful (for the coupling of primary amines) JosiPhos ligand.[35] Inspired by

the Stradiotto group's recent success in developing a class of k^2-*P,N* ligands, a conceptual middle ground between ligands employed by the Buchwald and Hartwig groups (Section 1.4), I have investigated the rational structural diversification of our most effective ligand, Mor-Dalphos (**1-4**). Analogues of **1-4** may not only ascribe new and/or improved reactivity in challenges such as ammonia[93] and hydrazine[97] monoarylation, they may exhibit unexpected reactivity when screened in other challenging cross-coupling reactions (e.g. monoarylation of acetone).

The success of **1-4** owes to a combination of an electron rich, bulky and rigid P(1-Ad)$_2$ moiety and a potentially hemilabile morpholino group capable of supporting low-coordinate Pd-complexes;[33b,117] modification of these groups even subtly results in significantly altered catalyst performance.[89] To complement work ongoing in the group where the substitution pattern at phosphorus and nitrogen are being explored, I was focusing on substitution on and within the ligand arene backbone. In particular, I chose to examine the influence of substitution *para* to phosphorus or nitrogen, which should reveal electronic pertubations, rather than sterically promoted effects. Notably, the Buchwald group has shown that methoxy substitution on the upper biaryl ring of BrettPhos may promote reductive elimination.[32] In light of these considerations, it was proposed that the electronic profile of phosphorus and nitrogen may be modified via substitution of the 4- and 5-, positions of the phenylene-backbone with electron-donating or electron-withdrawing groups of varying strength (Figure 3.1).

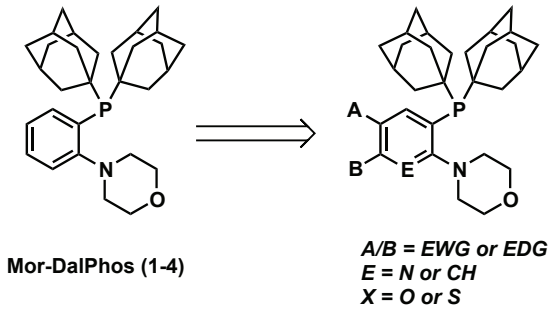

Figure 3.1 Proposed structural diversification of the Mor-DalPhos ligand **1-4**.

Predicting qualitatively the effect that structural diversification of **1-4** may impart upon Pd-catalysts, I have taken into consideration *meta* and *para* substituent constants for substituted benzene derivatives, σ_m and σ_p (Hammett parameters).[118] For example, halogens such as fluorine may inductively withdraw electron-density in the *meta* position,

alkyl groups such as methyl may be electron-donating in both the *para* and *meta* position, and methoxy groups may donate electron density to the *para* position while withdrawing electron density from the *meta* position. The observed effects arise from a combination of inductive and mesomeric resonance processes. Pertinent comments and discussion are provided in Section 3.3 of this chapter, on a case-by-case basis.

The simple synthesis of eight air-stable, affordable variants of **1-4,** from commercially available iodobromo(hetero)aryl (or closely related) precursors is disclosed herein. In one example, a procedure adapted from literature protocols is used to afford economically on gram-scale, a reagent sold for $84,000/g. Considering that Buchwald and Hartwig have both used the synthesis and characterization of coordination complexes to verify ligand interactions with Pd, similar studies have been conducted herein; these coordination complexes may represent pre-catalysts in the general catalytic cycle for BHA reactions involving DalPhos ligands. To determine the identity of species formed in precatalyst mixtures of seven of the eight DalPhos ligands synthesized, their coordination to Pd has been probed via NMR spectroscopy and X-ray crystallography techniques (Figure 3.2). For example, in an effort to understand how binding of the morpholino unit of **1-4** effects catalyst activity and lifetime, oxygen has been substituted with sulfur, giving rise to a surprising κ^3-*P,N,S* binding mode when combined with Pd. Ligand **1-4** has similarly been shown to stabilize low-coordinate catalytic intermediates upon exposure to halide abstracting agents (e.g. AgOTf).[117]

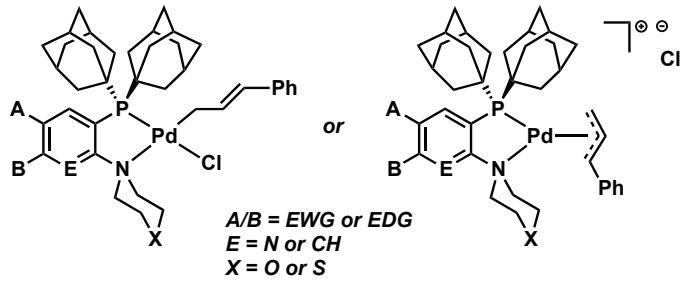

Figure 3.2 Palladium-ligand complexes; potential pre-catalysts in C-N cross-coupling.

New ligands have been screened in a series of C-X (X = N, C, O) cross-coupling reactions, allowing a direct measure of comparison to the activity observed for **1-4**, as well as an inroad to the identification of reaction limitations these task-specific ligands may address (i.e. improvements on **1-4**). Preliminary screening results highlight a ligand

featuring a pyridine-backbone as an excellent candidate for the monoarylation of acetone. Notwithstanding the broad scope of **1-4** for the cross-coupling of (hetero)aryl (pseudo)halides with primary and secondary alkyl and aryl amines, this ligand falls short with respect to weakly nucleophilic N-H containing substrates, including imidazole, indole, pyrazole, triazole and hydroxylamine. In this context, our newly developed screening process may allow for the future identification of DalPhos variants that overcome these challenges.

3.2. SYNTHESIS OF NEW DALPHOS ANCILLARY LIGANDS

The Stradiotto group has developed successful methodologies for the simple synthesis of air-stable, affordable DalPhos ligands; with few exceptions these ligands are prepared via similar synthetic routes.[93] Typically, iodobromobenzene precursors are coupled with amine substrates using BHA procedures to afford *N*-(2-bromo)aryl compounds and subsequently cross-coupled with a secondary phosphine (Chapter 1, Section 1.5.1).[119] While the analogues of **1-4** have been prepared in a similar manner, in several cases aryl fluoride and aryl chloride precursors bearing strongly electron-withdrawing groups may be *N*-substituted via S_NAr methods. Given the observed reactivity benefits imparted upon Pd-catalysts featuring DalPhos ligands bearing the sterically bulky, rigid, electron-rich phosphine moiety, [P(1-Ad)$_2$], this privileged phosphine group (along with morpholino substitution) has been maintained. The robust and air-stable nature of such phosphine ligands bypasses the requirement for oxygen and moisture sensitive (and often pyrophoric) reagents utilized for the preparation of other bulky alkylphosphine ligands.[89]

Prior to the preparation of *N*-(2-bromo)aryl intermediates, a examination of reagents offered by commercial chemical suppliers was conducted, specifically with respect to compounds bearing electron-donating and electron-withdrawing group substitution at the 4- and 5-position of the phenylene-backbone (Figure 3.3). These positions place substituents *para* to nitrogen and phosphorus in the respective ligands. Iodobromobenzene (**3-1**), utilized in the preparation of many DalPhos variants, was chosen as a precursor to a target dinuclear P_2N_2 ligand, as well as a variation of **1-4** with sulfur replacing oxygen in the morpholino fragment (*vide infra*). Reagents **3-2**-**3-9** were identified as starting points for the synthesis of ligands encompassing substitution with

fluorine in both the 4-, and 5-position, methyl substitution at the 5-position, and nitrile and nitro groups at the 4-position. Prior to the synthesis of ligands presented herein, the Stradiotto group had not reported a heteroaryl DalPhos ligand, with only phenylene-backbone variants having been explored. Commercially available **3-5** and **3-6** were chosen for the preparation of pyridyl-structural isomers of **1-4**, giving the potential for an unexpected binding mode with Pd as a result of the presence of a lone-pair on nitrogen in close proximity to the metal center. The precursor **3-7**, bearing two strongly electron-donating groups was also identified as commercially available, however, in order to maintain the cost-efficient synthetic protocols established for our ligand family, a cheaper synthetic methodology was established.

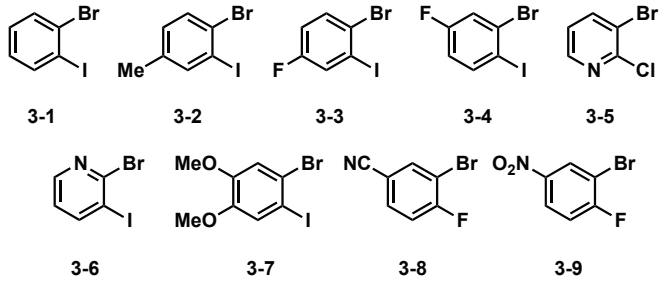

Figure 3.3 Iodo-, chloro- and fluoro-bromo(hetero)aryl ancillary ligand precursors.

A two-step method for the preparation of **3-7** from veratrole was reported in 2006 by Fürstner *et al*. Unfortunately this route required the use of hazardous and toxic main-group reagents (Br_2 and HgO).[120] Also, the desired product as reported is contaminated by a dibromide species resulting from consecutive double bromination in the second synthetic step. In an effort to selectively mono-iodinate and thereby ease product purification, further investigation of the literature resulted in identification of a mild and regioselective method for the iodination of electron-rich aromatics with *N*-iodosuccinimide (NIS) and catalytic trifluoroacetic acid (TFA).[121] In this report, a variety of aromatic compounds substituted with methoxy groups are regioselectively iodinated in excellent yield at room temperature; however, no examples of deactivated methoxy aromatic derivatives were reported. Given the propensity for the reported system to mono-iodinate *para*-to methoxy functionality, it was predicted that the compound 4-bromoveratrole may potentially undergo a selective mono-iodination and bypass the need for bromination at a later stage. Indeed, the desired product was accessed in gram-

quantity (99% yield), albeit at elevated temperature (65 ^{o}C) for 24 h to ensure full consumption of ArBr starting material (Scheme 3.1).

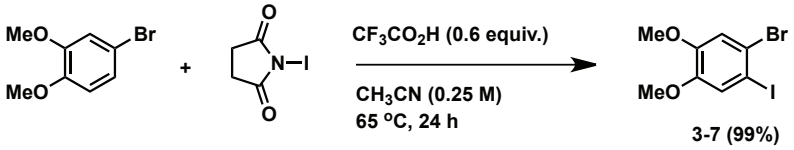

Scheme 3.1 Regioselective iodination of 4-bromoveratrole with *N*-iodosuccinimide; isolated yield denoted in parentheses.

With compounds **3-1-3-9** in hand, I employed simple processes for their conversion to *N*-(2-bromo)aryl intermediates **3-10**-**3-19** (Scheme 3.2). Employing a combination of Pd_2dba_3 (1 mol%) and *rac*-BINAP (3 mol%) afforded the aryl bromide compounds **3-10**, **3-11** and **3-16** in good isolated yields of 80, 78, and 79%, respectively. An adapted version of this protocol was developed to allow the preparation of **3-19** from 1 equiv. **3-1** and 0.5 equiv. piperazine via double C-N cross-coupling, albeit in lower yield (45%); increased Pd_2dba_3 (3 mol%) and *rac*-BINAP (9 mol%) loadings were required to effectively promote this transformation. Attempts to use Pd_2dba_3/*rac*-BINAP for the preparation of intermediates **3-12, 3-13,** and **3-15** were unsuccessful, resulting in either lower yield of the desired product, or conversion to several products as shown by GC analysis. In screening alternative ligands capable of enabling such couplings, a mixture of Pd_2dba_3 (3-5 mol%) and the wide bite-angle bisphosphine XantPhos (9-15 mol%) proved effective, affording products **3-12** (5 mol% Pd), **3-13** (5 mol% Pd) and **3-15** (3 mol% Pd) in 71, 74 and 68%, respectively.

Given that 2-iodo-3-bromopyridine is not commercially available, an alternative synthetic procedure employing nucleophilic aromatic substitution (S_NAr) on 2-chloro-3-bromopyridine (**3-5**) was utilized. The availability of **3-5**, and the preference for pyridine to undergo an S_NAr process at the 2-position of this reagent,[29] allowed the isolation of **3-14** in 81% yield. Substitution was carried out with morpholine in the presence of K_2CO_3 at 130 ^{o}C. Intermediates **3-17** and **3-18** were prepared in 32% and 95% via similar routes (differing only with respect to aprotic solvent choice) from their respective aryl fluoride reagents (**3-8** and **3-9**).

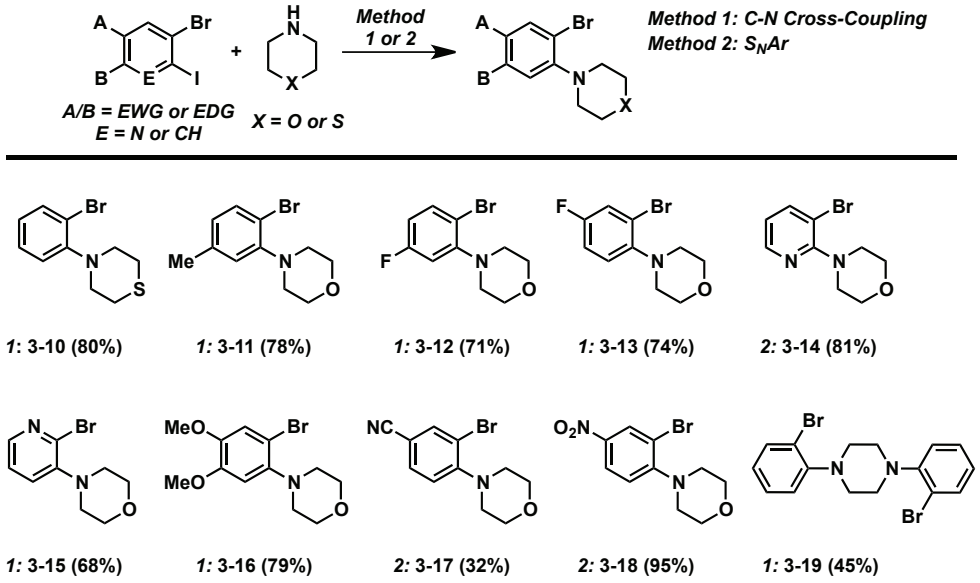

Scheme 3.2 Synthesis of N-(2-bromo)aryl intermediates **3-10**-**3-19**. Synthetic method (italicized): *1*: C-N cross-coupling; *2*: S_NAr. Isolated yield (%) in parentheses.

With a diverse set of (hetero)arylbromide intermediates featuring EWG and EDG substitution, ligands **3-20**-**3-29** were synthesized via installation of the bulky di(1-adamantyl)phosphino [$P(1\text{-}Ad)_2$] fragment (representative spectra for ligand **3-25** are provided in Appendix I). Employing a combination of $Pd(OAc)_2$ (2.5-5 mol%) and D*i*PPF (Pd:L ~1:1.1), this system tolerates a broad scope of electron-rich and sterically-hindered ArBr substrates.[119] Pleasingly, this synthetic procedure allowed **3-20**-**3-27** to be prepared in 73-98% isolated yield (Figure 3.4). This method however, was not suitable for ligands **3-28** and **3-29**. In each case, monitoring reaction progress via ^{31}P NMR spectroscopy indicated that decomposition of starting material occurred to generate a complex product mixture. Considering the potential sensitivity of the nitro moiety of **3-28** to undergo a reductive process in the presence of Pd/L, a series of alternative base and solvent combinations were explored; unfortunately no combinations were observed to afford a single major product when monitoring reaction progress via ^{31}P NMR spectroscopic analysis. A combination of $Ni(OAc)\cdot 4H_2O$ and NEt_3[122] was explored as an alternative to Pd-catalyzed cross-coupling, although $HP(1\text{-}Ad)_2$ remained primarily unconsumed after heating for 24 h. Further attempts at preparing this ligand were abandoned. Similarly, the attempted synthesis of ligand **3-29** via double P-C cross-

coupling was unsuccessful. It is currently unclear what is causing decomposition (observed by ^{1}H and ^{31P} NMR spectroscopy) of the Ar_2Br_2 reagent. As filtration and purification of the product mixture was inhibited by insolubility in both CH_2Cl_2 and $CHCl_3$, further attempts at isolating this product were abandoned.

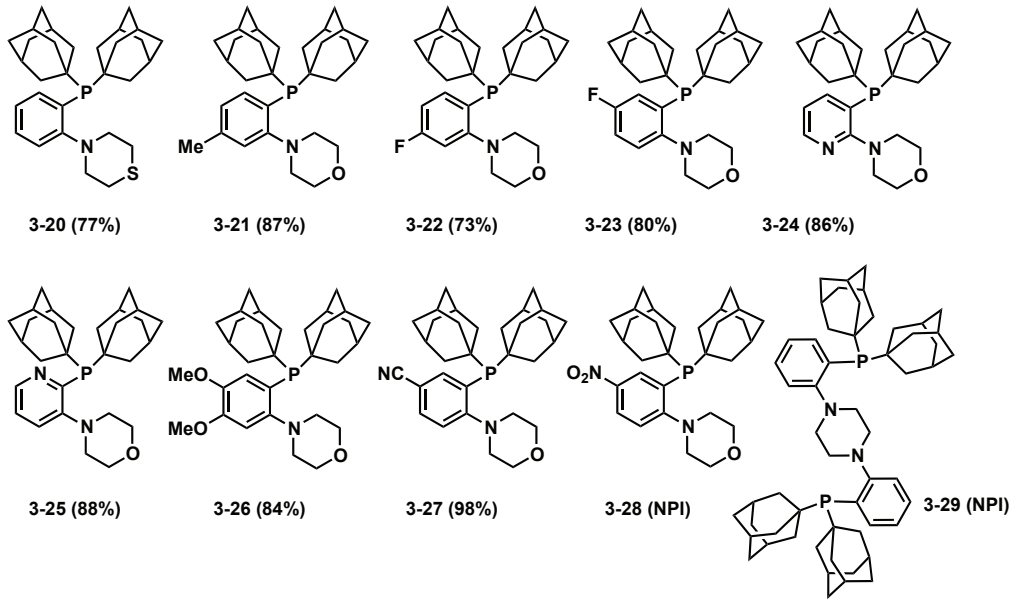

Figure 3.4 Structurally diversified analogues of DalPhos ligand **1-4**; isolated yields denoted in parentheses; NPI (no product isolated).

Lastly, single-crystal X-ray diffraction data were collected and solved (in collaboration with Dr. Craig Wheaton) for ligands **3-20**, **3-22**, and **3-24**-**3-26**; their ORTEP diagrams [123] are presented collectively in Figure 3.5. An examination of the P-N bond distance provides an approximation of their respective bite-angles. Given their varying substitution, it was proposed that this distance may vary, particularly for ligands **3-24** and **3-25** where the pyridyl-nitrogen may effect the electron density at phosphorus and nitrogen mesomerically. The P-N distances obtained in all cases, (Table 3.1; **1-4**, Stradiotto group unpublished results) while statistically different, are not so divergent as to have a profound effect in terms of Pd-binding. This is likely a result of the inflexible, planar nature of their (hetero)aryl ligand backbone.

Table 3.1 P-N interatomic distances (Å) for **1-4**, **3-20**, **3-22** and **3-24**-**3-26**.

1-4	**3-20**	**3-22**	**3-24**	**3-25**	**3-26**
2.969(1)	3.007(2)	2.985(1)	3.071(2)	2.979(1)	3.022(1)

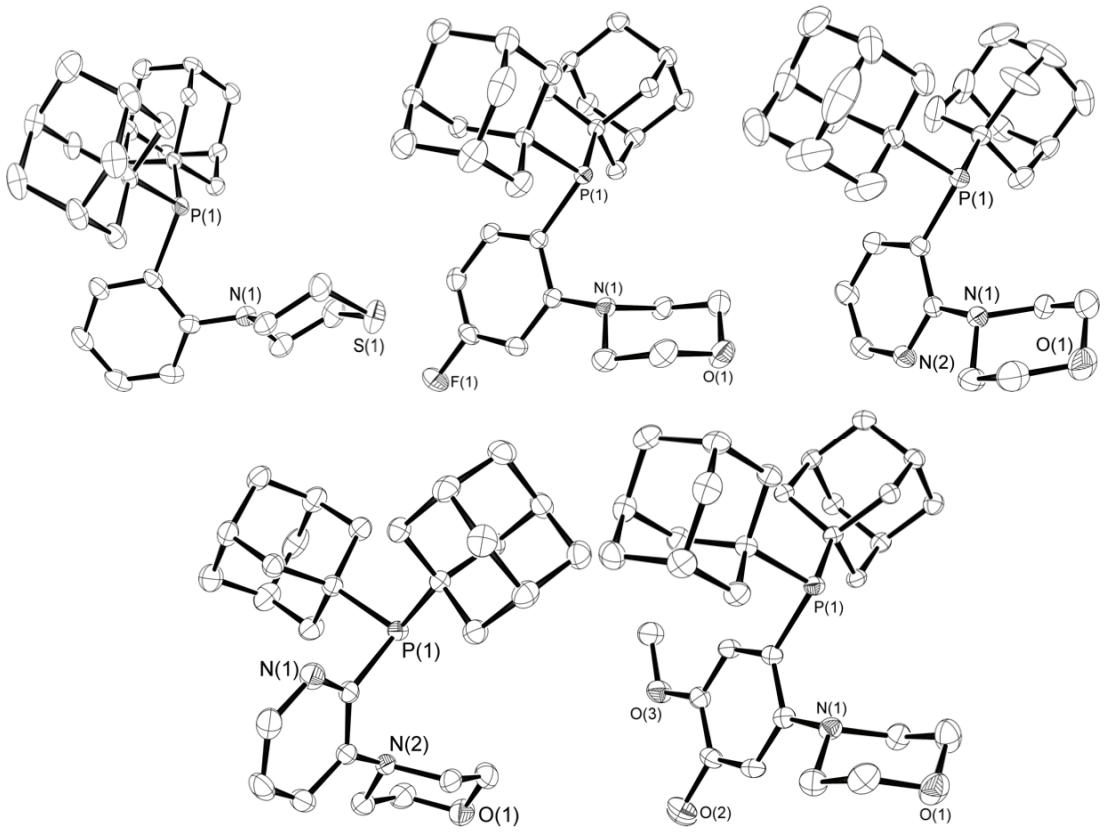

Figure 3.5 ORTEP diagrams for DalPhos ligands **3-20**, **3-22**, **3-24**, **3-25**, **3-26** (*from top left to bottom right),* depicted with 50% displacement ellipsoids; selected H-atoms have been omitted for clarity.

3.3. SYNTHESIS OF PUTATIVE PRE-CATALYST COMPLEXES

The development of catalysts that address various C-N cross coupling reactions has been made possible via mechanistic studies on the interaction of Pd and carefully designed supporting ancillary ligands. An array of reports highlight reactivity benefits attained through use of pre-formed Pd-ligand complexes in BHA reactions.[3a,b,35,67b,69a,81]

In this regard, the Buchwald group has synthesized and characterized coordination complexes featuring monodentate dialkylbiarylphosphine ligands, identifying their interaction with Pd as a strong and weak interaction. Similarly, Hartwig and co-workers have prepared and examined pre-catalyst complexes featuring the bisphosphine JosiPhos. Following the Stradiotto group's development of the ligand **1-4**, coordination complexes bearing this ligand were prepared in an effort to study (by use of NMR spectroscopy and X-ray crystallography) proposed intermediates in the catalytic cycle for ammonia arylation. These studies ultimately culminated in the development of an improved, effective precatalyst [(κ^2-*P,N*-**1-4**)Pd(Ph)Cl] (**3-30**) for the BHA of (hetero)aryl (pseudo)halides with ammonia at room temperature (Scheme 3.3).[117]

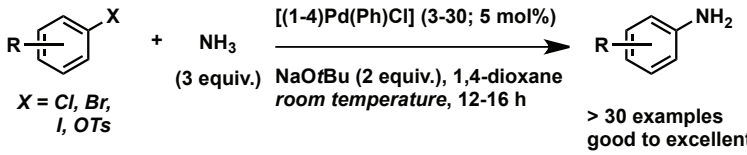

Scheme 3.3 [(κ^2-*P,N*-**1-4**)Pd(Ph)Cl] (**3-30**), an efficient precatalyst for the monoarylation of ammonia at room temperature.

Originally the [Pd(cinnamyl)Cl]$_2$/**1-4** mixture was employed successfully at temperatures above 50 ^{o}C for the preparation of electron-rich, electron-poor, and heterocyclic products of ammonia monoarylation.[93] Unfortunately, pre-catalyst mixtures of Pd and **1-4** featuring η^1- and η^3-cinnamyl coordination (**3-31** and **3-32**, respectively) were ineffective toward room temperature monoarylation (Figure 3.6). Considering **3-30** was later found to promote this transformation for a small number of aryl chlorides, catalyst activation may represent a potential inhibitory factor in BHA reactions. A better understanding of these findings has been made possible via investigation of Pd-species that are formed initially from the component(s) of the precatalyst mixture, specifically stoichiometric reactivity studies providing insight toward Pd-ligand binding and resultant catalyst formation with [Pd(cinnamyl)Cl]$_2$/**1-4** mixtures. To this end, Alsabeh *et al.* examined Pd(0) and Pd(II) sources toward formation of coordination complexes in an attempt to measure the amount of presumed **1-4**/Pd(0) species generated at room temperature.[117] The use of NMR spectroscopy and single-crystal X-ray diffraction assisted in the identification of key complexes, such as the κ^2-P,N square-planar complex

3-30. These data will serve as a valuable model for comparison, as the study of new DalPhos ligand (**3-20**-**3-26**) coordination complexes may similarly allow the development of improved, more efficient catalyst systems.

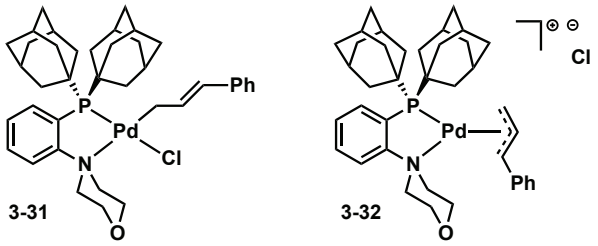

Figure 3.6 Solid-state structures of **3-31** and **3-32**, featuring η^1- and η^3-cinnamyl coordination, respectively. Single crystals for X-ray diffraction analysis were grown from the same precatalyst mixture of $[Pd(cinnamyl)Cl]_2$/**1-4**.

3.3.1. Synthesis of Pd-Precatalysts Supported by New DalPhos Ligands

DalPhos ligands **3-20**-**3-26** (structurally analogous to **1-4**) were combined with $[Pd(cinnamyl)Cl]_2$ in a 2:1 ratio in CH_2Cl_2 at room temperature, to afford complexes featuring solution phase η^1-, and solid state η^1- or η^3-cinnamyl coordination. In each case, these complexes have been comprehensively characterized by 2D-NMR spectroscopy, and in several cases, via single-crystal X-ray diffraction.

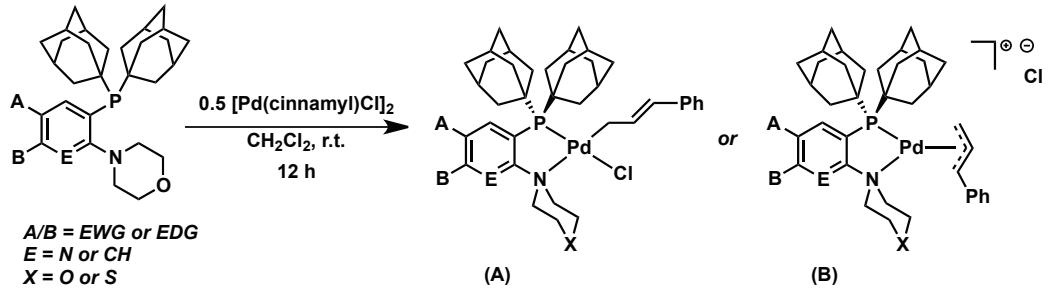

Scheme 3.4 Synthesis of Pd/(**3-20**-**3-27**) complexes featuring examples of η^1- and η^3-cinnamyl coordination. (A) Identified for solution and solid-state structures; (B) identified only in the solid-state.

I began my studies by examining precatalyst formation with ligand **3-21**, given the strong likelihood of this ligand to exhibit both electronic and structurally related interactions (to that of **1-4**) with the Pd(cinnamyl)Cl fragment. Stirring **3-21** with 0.5 equiv. $[Pd(cinnamyl)Cl]_2$ at room temperature in CH_2Cl_2 for 12 hours resulted in the formation (as detected via ^{31}P NMR spectroscopy) of a single new species (Figure 3.7).

Isolated as an analytically pure yellow solid in 87% yield, solution NMR spectroscopy was used to verify the product as the [(κ^2-*P,N*-**3-21**)Pd(η^1-cinnamyl)Cl] complex (**3-33;** representative spectra are provided in Appendix I). The η^1-cinnamyl structural assignment was made based on the presence of two alkenyl signals at 6.68 and 6.32 ppm, and a Pd-CH_2 benzylic resonance at 3.55 ppm. As predicted, data for the structure proposed are in good agreement with the previously reported assignment of the solution structure for **3-31**.[117] Single crystals suitable for X-ray diffraction analysis were grown via vapor diffusion of Et_2O to a saturated solution of **3-33** in CH_2Cl_2. Upon analysis, the solid-state structure was revealed to be [(κ^2-*P,N*-**3-21**)Pd(η^3-cinnamyl)]Cl complex (**3-34**), a cationic species featuring an outer-sphere chloride counteranion (Figure 3.7). The observation of differing solution and solid state structural isomers **3-33** and **3-34** is not particularly surprising given the crystal growth of **3-31** and **3-32**, from the same solution; both of these isomers likely comprise the product precatalyst mixture.

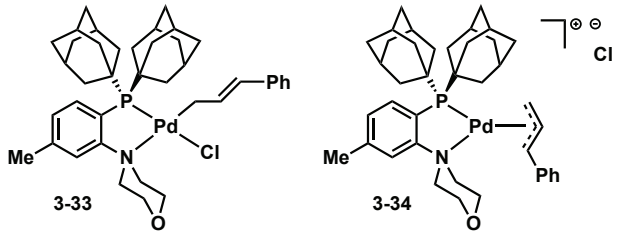

Figure 3.7 Solution-phase (left) and solid-state (right) determined structures of [(κ^2-*P,N*-**3-21**)Pd(η^1-cinnamyl)Cl] (**3-33**) and [(κ^2-*P,N*-**3-21**)Pd(η^3-cinnamyl)]Cl (**3-34**).

Analysis of selected metrical parameters for **3-34** confirm an unsymmetrically bound η^3-cinnamyl group (Figure 3.8), with the Pd-C(31) (2.0838(19) Å), Pd-(C32) (2.2677(18) Å, Pd-C(33) (2.6121(19) Å) bond lengths increasing upon moving from Pd-CH_2 closer to the cinnamyl phenyl. These values agree with those obtained for **3-32** (for a side-by-side comparison of key metrical parameters for **3-32** and **3-34** see Table 3.2). While the Pd-P bond lengths for **3-32** and **3-34** (2.2666(4) and 2.2614(4) Å, respectively) are statistically different (±3 esd's), they do not differ to an extent that implicates Me-substitution *para*- to phosphorus as having a significant effect on complex structure. In this regard, the increased electron density at phosphorus (methyl groups have a para subsituent constant, σ_p, of -0.170 indicating a mild electron-releasing ability) that results from this substitution, has to a small extent resulted in a decreased Pd-P bond length, as

predicted. Despite the structural similarity between **3-32** and **3-34**, an electronic contribution may be attributed to methyl-substitution, and would likely manifest in reaction chemistry featuring this ligand (preliminary screening discussed in Section 3.3.3).

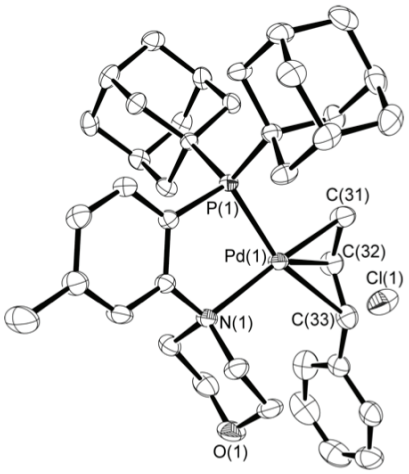

Figure 3.8 ORTEP diagram for **3-34**, depicted with 50% displacement ellipsoids; selected H-atoms have been omitted for clarity.

Synthesis of precatalyst mixtures from [Pd(cinnamyl)Cl]$_2$ and ligands (**3-20**, **3-22**-**3-26**) was carried out in a manner analogous to that of **3-33**. Notably, upon introducing fluorine substitution *para* to phosphorus, analysis of solution NMR spectral data indicated characteristics similar to that of **3-33**; formation of the square-planar [(κ^2-*P,N*-**3-22**)Pd(η^1-cinnamyl)Cl] complex (**3-35**) with chlorine *trans* to phosphorus was identified. Interestingly, the morpholino resonances in the ^{1}H NMR spectrum are considerably broadened, lacking the sharp line shape that was observed for **3-33**. This likely implies a more dynamic interaction between Pd and morpholine, and may impart unexpected reactivity preferences in catalysis. Also dissimilar to the η^3-structure of **3-34**, is the solid-state structure of **3-35**, presenting η^1-cinammyl binding (Figure 3.9). This binding mode was identified via the C(31)-C(32) (1.482(2) Å), C(32)-C(33) (1.337(2) Å), and C(33)-C(34) (1.468(2) Å) bond lengths, consistent with single, double and single bonds. Considering the ligand **1-4** displays an η^1-cinammyl binding mode in solution, and both η^1 and η^3-coordination in the solid state, the growth of single-crystals of only

the structural isomer **3-35**, does not rule out the presence of an η^3-structural isomer in solution.

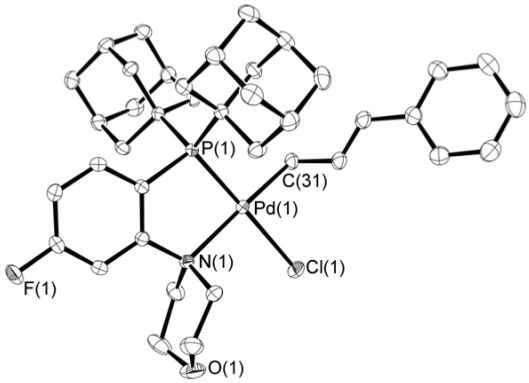

Figure 3.9 ORTEP diagram for **3-35**, depicted with 50% displacement ellipsoids; selected H-atoms have been omitted for clarity.

Table 3.2 Selected interatomic distances (Å) for **3-31**, **3-32**, **3-34**, and **3-35.**

Metrical Parameters	**η^{3}-3-32**[112]	**η^{3}-3-34**[b]	**η^{1}- 3-31**[112]	**η^{1}-3-35**
Pd-P	2.2666(4)	2.2614(4)	2.2357(9)	2.2338(4)
Pd-N	2.2625(14)	2.2559(14)	2.261(3)	2.2652(12)
Pd-C(31)	2.0951(17)	2.0838(19)	2.074(3)	2.0823(15)
Pd-C(32)	2.2432(17)	2.2677(18)	---	---
Pd-C(33)	2.5100(18)	2.6121(19)	---	---
P-C(1)	1.8375(17)	1.8259(17)	1.840(4)	1.8302(15)
Pd-Cl	---	---	2.3952(9)	2.4050(4)
N-C(2)	1.479(2)	1.477(2)	1.464(4)	1.4650(18)
C(31)-C(32)	1.418(3)	1.420(3)	1.466(5)	1.482(2)
C(32)-C(33)	1.374(3)	1.352(3)	1.336(5)	1.337(2)
C(33)-C(34)	1.470(3)	1.467(3)	1.465(5)	1.468(2)

Inspired by this finding, a comparison was made between the metrical parameters of **3-35** and **3-31** (Table 3.2). Despite the prediction that substitution with an EWG in a

position *para* to phosphorus may lead to an increase in the Pd-P bond length (decreased electron-density at phosphorus via inductive effects), a significant effect on structure was not found. The Pd-N bond length is also nearly identical to that of the **3-31** which does not feature substitution; this was surprising given that fluorine has an even greater, more positive *meta* substituent constant (σ_m +0.34 vs. σ_p +0.06)[113b], and in light of the observed divergent behavior of the morpholino group of **3-35**. In this regard, these values suggest **3-23** may impart a significant effect on the Pd-P bond length as phosphorus is in a position *meta* to fluorine; a solid-state structure of this ligand bound to Pd has however yet to be obtained. In summary, these conclusions are similar to those made upon comparing **3-32** and **3-34**; substitution imparts minimal impact on complex structure.

Despite the aforementioned findings that suggest phenylene-backbone substitution with mildly electron-donating and withdrawing groups in a position *para* to phosphorus imparts minimal effect on pre-catalyst formation and structure, further examination of complexes supported by new DalPhos ligands was conducted. This includes the preparation of the complexes [(κ^2-*P,N*-**3-23**)Pd(η^1-cinnamyl)Cl] (**3-36**) and [(κ^2-*P,N*-**3-26**)Pd(η^1-cinnamyl)Cl] (**3-37**), isolated as analytically pure yellow and orange solids in 84 and 91% yields, respectively (Figure 3.10). Similarity to **3-33** (methyl *para* to phosphorus) and **3-35** (fluorine *para* to phosphorus), the single solution state structure determined for these complexes is consistent with η^1-cinnamyl coordination and square-planar geometry at Pd with chlorine *trans* to phosphorus. Neither ligand-complex presents an observable dynamic interaction between morpholine and Pd, like that observed in **3-35**. Given the minimal structural significance (on metrical parameters) imparted by methyl and fluorine substitution of the ligand backbone on complexes **3-34** and **3-35**, no attempt was made to isolate single-crystals of **3-36** or **3-37** for X-ray diffraction characterization. However, these ligands have been utilized in a series of preliminary catalytic screening reactions (Section 3.3.3) in an effort to correlate the effect of structural diversification of **1-4**, to observed reactivity in challenging cross-coupling reactions.

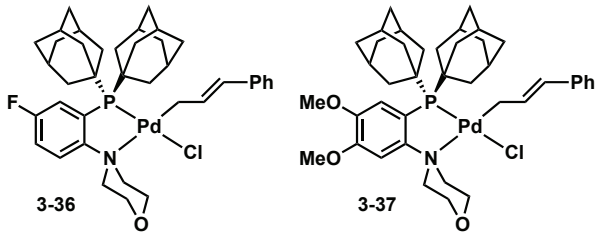

Figure 3.10 Solution NMR spectroscopy determined structures of [(κ^2-*P,N*-**3-23**)Pd(η^1-cinnamyl)Cl] (**3-36**) and [(κ^2-*P,N*-**3-26**)Pd(η^1-cinnamyl)Cl] (**3-37**).

3.3.2. Synthesis of Pd-Precatalysts Supported by DalPhos Ligands BPyridine-Backbone or Thiomorpholine Motifs

The synthesis of DalPhos variants featuring phenylene-backbone substitution with electron-withdrawing and electron-donating groups were initially predicted to subtly alter the electronic environment at phosphorus and nitrogen through inductive and/or mesomeric effects, without jeopardizing the structural features ([P(1-Ad)$_2$] and morpholine fragments) considered to be responsible for the unprecedented reactivity **1-4** imparts upon Pd. Indeed, an examination of the solid state structures of **3-34** and **3-35** which feature EDG and EWG substitution *para* to phosphorus, reveals structures that do not exhibit structural parameters differing significantly from those of **3-32** and **3-31**, respectively. In consideration of these findings, directly replacing the phenylene-backbone with a pyridine-backbone was proposed to impart a greater effect on complex structure when combined with Pd. Whereas a single example of phenylene-backbone substitution was reported by Lundgren and Stradiotto during their search for a ligand capable of addressing ammonia monoarylation (methoxy substitution *ortho* to phosphorus in **1-3**),[93] no examples of a heteroaryl-bridged DalPhos ligand have been previously reported.

Pyridine-bridged P,N ligands **3-24** and **3-25** were combined with 0.5 [Pd(cinnamyl)Cl]$_2$ in an analogous fashion to the aforementioned synthetic procedures. Conversion to a single product (detected via ^{31}P NMR spectroscopy) was observed for the former, and isolated as an analytically pure yellow solid in 89% yield. Characterization by solution NMR spectroscopy identified this product as the [(κ^2-*P,N*-**3-24**)Pd(η^1-cinnamyl)Cl] complex (**3-38,** Scheme 3.5), displaying a strikingly dynamic interaction between Pd and morpholine (resonances nearly indistinguishable from the baseline). Perhaps more interestingly, the latter afforded two products (^{31}P{^{1}H} NMR

chemical shifts, 68.7 and 46.5 ppm) in a *ca*. 2.3:1.0 ratio. While solid-state structural data have yet to be obtained for this mixture, an attempt at characterization has been made on the basis of solution NMR spectroscopy (both 2D and saturation transfer) experiments. Given the ^{31}P NMR chemical shifts and the potential for coordination of the lone-pair on the prydinyl-nitrogen to Pd, the complexes [(κ^2-*P,N*$_{mor}$-**3-25**)Pd(η^1-cinnamyl)Cl] (**3-39**) and [(κ^2-*P,N*$_{pyr}$-**3-25**)Pd(η^1-cinnamyl)Cl] (**3-40**) have been proposed (Scheme 3.5). To determine if these complexes are in equilibrium, ^{31}P NMR spectroscopy saturation transfer experiments were conducted (Figure 3.11).[124] Intensity suppression was noted for both resonances in the absence of observable intermediates, indicating slow conversion between **3-39**/**3-40**. Unlike **3-31**-**3-38**, decomposition for this mixture occurs in $CDCl_3$; studies were however successfully carried out in CD_2Cl_2. **3-39** has been tentatively proposed as the major isomer based on similarity between the chemical shift of this isomer (68.7 ppm) and that of **3-31**-**3-38** (*ca*. 63-75 ppm) which display similar κ^2-*P,N*$_{mor}$-Pd binding.

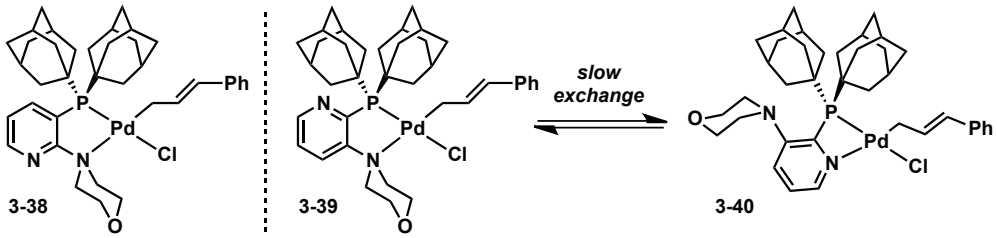

Scheme 3.5 Proposed structure of **3-38** and structural isomers **3-39** and **3-40**, in slow-exchange on the NMR timescale (indicated via saturation transfer experiments).

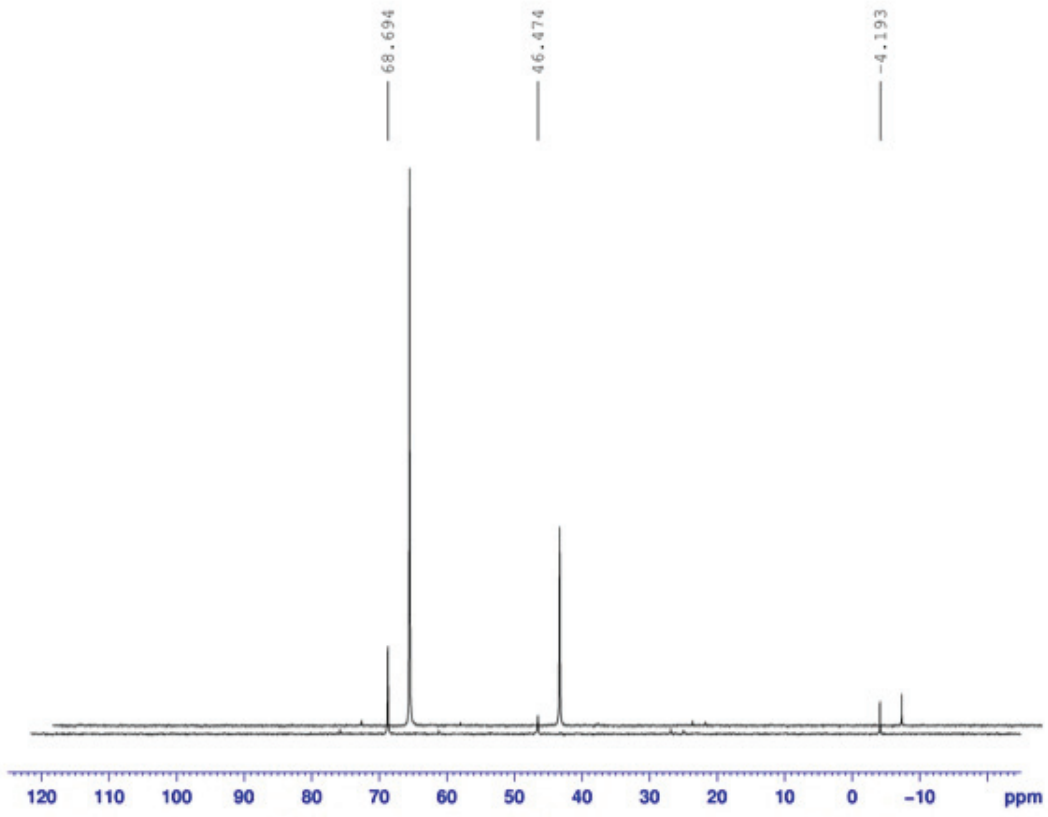

Figure 3.11 Overlapping saturation transfer spectra: low power CW irradiation (0.32 μW) was applied to P(1-Ad)2, δ $^{31}P\{^{1}H\}$ = 46.5, over a 10 s interval (*foremost spectrum*). Diminished intensity implies a slow exchange between **3-39** and **3-40**.

The final structural analog of **1-4** was prepared by replacement of the morpholino fragment with thiomorpholine. It was envisioned that this ligand would provide an understanding of the role of this fragment on stabilizing intermediates within the catalytic cycle, given that the Stradiotto group has reported on the reactivity of [(κ^2-*P,N*-**1-4**)Pd(Ph)Cl] complex (**3-30**) under halide abstraction conditions, whereby the oxygen donor of **1-4** binds to the open coordination site forming the distorted square planar complex, [(κ^3-*P,N,O*-**1-24)**Pd(Ph)]OTf (**3-41**).[117] This structure confirms the ability of **1-4** to impart stabilization in response to reduced coordination number, a characteristic that may prove beneficial or detrimental during catalysis. Similarly, halide abstraction from **3-31** forces formation of the complex [(κ^2-*P,N,*-**1-4)**Pd(η^3-cinnamyl)]OTf (**3-42**), where the

ligand does not coordinate through the oxygen of **1-4** likely due to the ability of the cinnamyl group to adopt a η^3-binding mode (Figure 3.12).

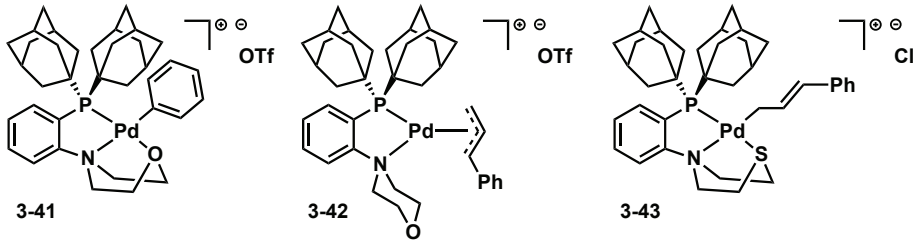

Figure 3.12 [(κ^3-*P,N,O*-**1-24)**Pd(Ph)]OTf (**3-41**), [(κ^2-*P,N,*-**1-4)**Pd(η^3-cinnamyl)]OTf (**3-42**), and [(κ^3-*P,N,S*-**3-20)**Pd(η^1-cinnamyl)]Cl (**3-43**) complexes.

In light of these two findings, it was proposed that upon replacing oxygen with a softer (larger, less electronegative and more polarizable) sulfur donor atom, this stabilization effect may be enhanced, leading to an impact on reactivity in catalysis. Strikingly, the cationic complex [(κ^3-*P,N,S*-**3-20)**Pd(η^1-cinnamyl)]Cl (**3-43**) was immediately formed without addition of a halide abstracting agent (Figure 3.12). This complex was characterized via solution NMR spectroscopy and single-crystal X-ray diffraction studies following isolation as an analytically pure yellow solid in 85% yield (Figure 3.13). Key metrical parameters (Table 3.3) indicate all four Pd-ligand interactions of **3-43** to be longer than those in **3-41**; this includes the Pd-S 2.3836(6) Å bond length compared to Pd-O 2.227(2) Å. The bite-angle of **3-20** (87.33(5)^o) is also slightly larger than that of **3-21** (84.46(3)^o and **3-22** (85.27(4)^o).

Table 3.3 Selected interatomic distances (Å) for **3-41**[a] and **3-43**[b]

Metrical Parameters	Pd-P	Pd-N	P-C(1)	N-C(2)	Pd-S	Pd-O
3-41[112]	2.2207(8)	2.116(2)	1.859(3)	1.463(4)	---	2.227(2)
3-43	2.2468(5)	2.1541(17)	1.8445(19)	1.464(3)	2.3836(6)	---

[a] Pd-C_{Ph} 2.001(3), [b] Pd-$C_{cinnamyl}$ 2.069(2)

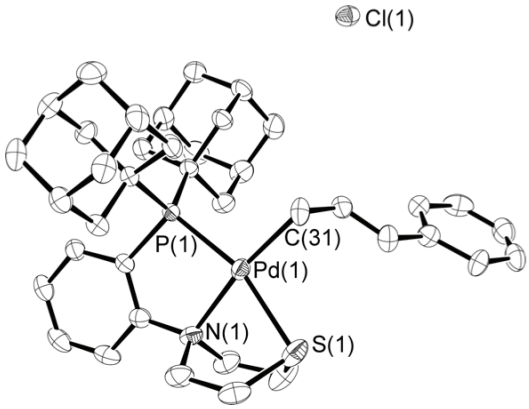

Figure 3.13 ORTEP diagram for **3-43**, depicted with 50% displacement ellipsoids; selected H-atoms have been omitted for clarity.

3.3.3. Preliminary Screening of Ligands 3-20-3-27 in Challenging C-X (X = N, C, O) Cross-Coupling Reactions

With a detailed understanding of the binding preference of ligands **3-20-3-26** established, their screening in a series of challenging C-X (X = N, C, O) cross-coupling reactions was conducted. Results from the screening of ligand **3-27** have also been obtained, however precatalyst studies are currently outstanding. The screening protocols were developed and carried out by Stradiotto post-doctoral researcher Dr. Sarah Crawford, in a manner that provides a look at the overall utility of each new ligand under standardized conditions. This includes evaluating any outstanding challenges the new ligands may be capable of addressing and any reactions for which the new ligands may offer a greater yield compared to **1-4**. Furthermore, considering the rational diversification of the structure of **1-4** in all cases (except **3-20**) maintained the phosphorus and nitrogen components of **1-4** considered to impart high activity upon Pd-catalysts, in cases where advanced activity is observed, qualitative conclusions may be drawn between electronic/structural environment imparted by the ligand and activity.

To ensure consistent results, **1-4** was screened alongside the newly prepared ligands in every test reaction. The first set of reactions tested was designed to examine the scope of C-N cross-coupling reactions each ligand may allow (Figure 3.14; GC conversions/isolated yield and reaction conditions detailed in experimental Section 3.5.4). These include the cross-coupling of chlorobenzene with the primary aryl and alkyl amines, aniline and octylamine. Also, coupling with the secondary alkyl amine, morpholine, and weakly nucleophilic indole was tested; the latter represents a

shortcoming for Pd/**1-4** catalysts. Finally, **3-20**-**3-27** were employed toward the monoarylation of ammonia.

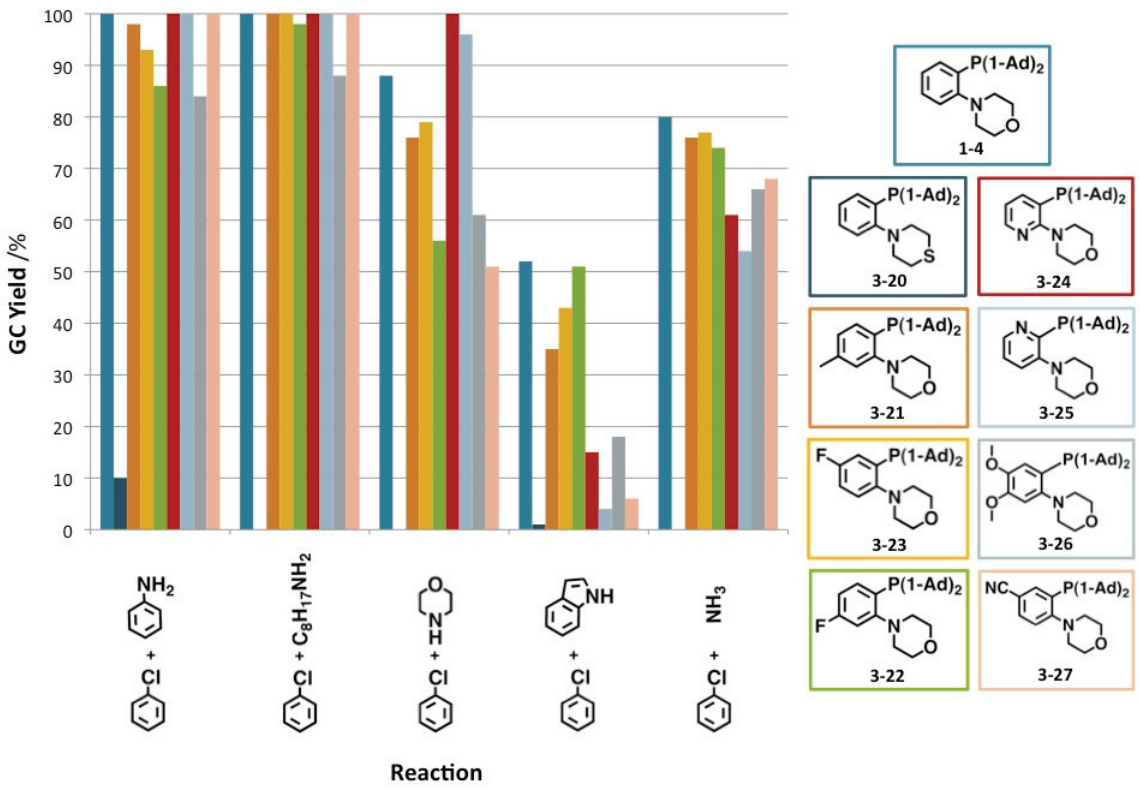

Figure 3.14 Ligands **1-4** and **3-20**-**3-27** in catalytic C-N bond forming reactions; calibrated GC yield of cross-coupled product after 18 h.

Qualitative observations from the C-N cross-coupling reactions indicated poor performance for ligand **3-20** in all reactions. This is not surprising given the κ^3-cationic structure this ligand uniquely forms with Pd in the precatalyst mixture. These observations indirectly suggest that κ^3-*P,N,O* binding in **1-4** inhibits rather than promotes catalysis. Ligands **3-21**-**3-27** all performed well with aniline and octylamine (typically 90-100%), with ligand **3-26** providing a slightly reduced yield of desired product in both cases, despite complete conversion of chlorobenzene. The cross-coupling of morpholine appears to benefit from the pyridine-backbone featured in both **3-24** and **3-25**, with yields of desired product for **3-24** exceeding that of **1-4** by 12% (100% yield and conversion). Indeed, **3-24** displays 100% yield of desired product, in all three aforementioned reactions. While no ligands perform exceptionally well toward the cross-coupling of

indole (**3-22** is on par with **1-4**), the use of pyridine-bridged ligands or substitution with strongly electron-donating or withdrawing groups (methoxy/nitrile) leads to decreased yield. Furthermore, comparing **3-23** and **3-27**, both featuring EWGs *meta* to phosphorus, the yield decreases as the strength of the EWG increases (fluoro σ_m = 0.34, nitrile σ_m = 0.48). Lastly, toward the monoarylation of ammonia, **3-21**-**3-27** performed well against **1-4**, with limited diarylation in most cases (Figure 3.15).

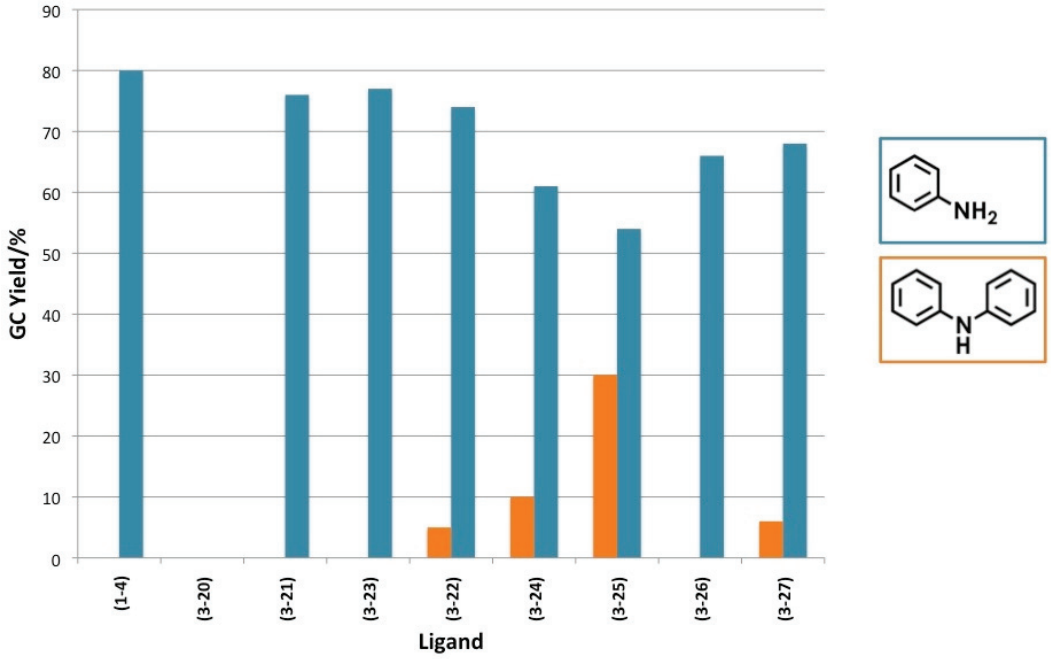

Figure 3.15 Ligands **1-4** and **3-20**-**3-27** employed in the reaction of chlorobenzene and ammonia; calibrated GC yield of aniline and diphenylamine and ammonia after 18 h.

Lastly, the newly synthesized ligands were screened in C-C and C-O cross-coupling reactions in a manner analogous to the aforementioned C-N reactions. The results depicted in Figure 3.16 highlight the broad utility of DalPhos ligands in acetone arylation, and the absence of any reactivity toward the hydroxylation or methoxylation of aryl sterically hindered aryl chlorides employing the readily available reagents $CsOH{\cdot}H_2O$ and MeOH. Surprisingly the ligand **3-20**, with minimal reactivity in C-N and C-O cross-coupling, likely due to the lack of an open coordination site resulting from the favorable interaction between Pd and S, generated 60% isolated yield of the desired C-C coupling acetone α-arylation product (71% conversion of chlorobenzene). Furthermore, **3-24** and **3-25** each perform exceptionally well in this reaction, with **3-25** affording the

desired product in 100% isolated yield. While it is not possible at this time to draw firm conclusions as to the enhanced reactivity associated with pyridine-bridged ligands, the apparent isomerization between **3-39** and **3-40** in solution may serve to promote this transformation. Analysis of X-ray data for Pd complexes featuring **3-38**-**3-40** would further assist in this process.

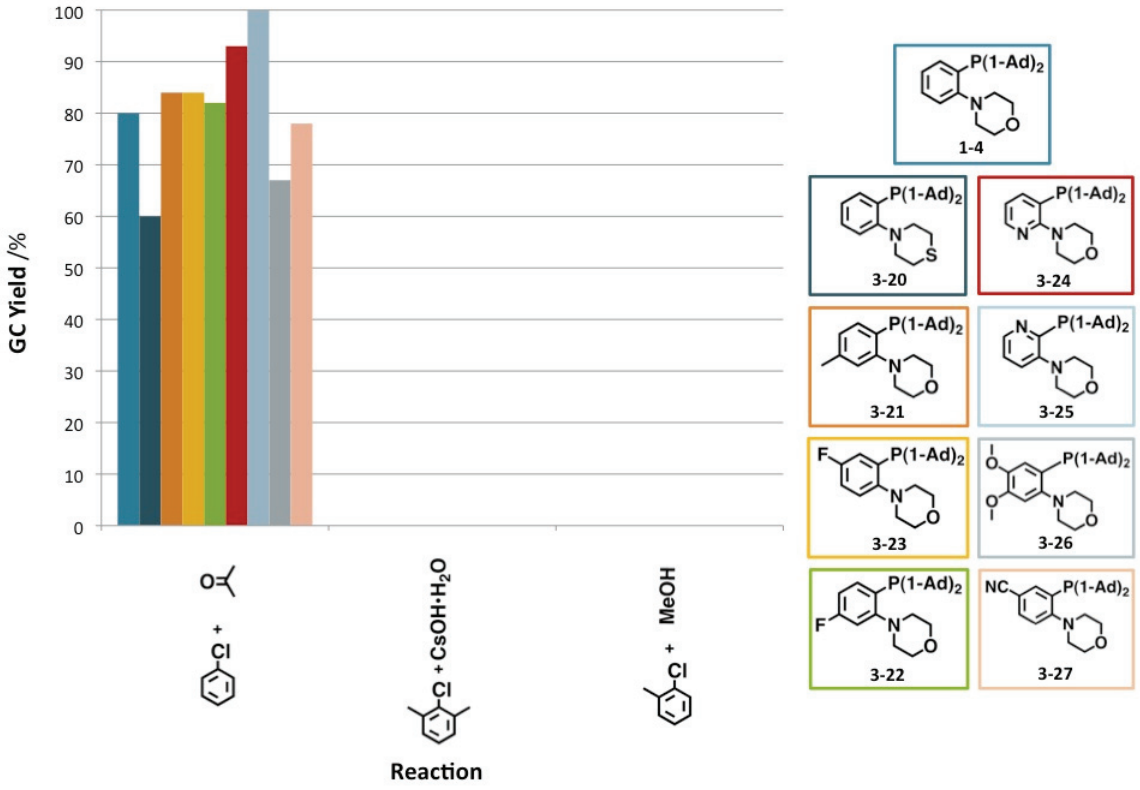

Figure 3.16 Ligands **1-4** and **3-20**-**3-27** employed in C-C and C-O cross-coupling reactions; calibrated GC yield of cross-coupled product after 18 h.

3.4. SUMMARY AND CONCLUSIONS

The results highlighted in this chapter provide a preliminary look at the formation of precatalyst mixtures formed upon combination of Pd and newly synthesized structural analogues of **1-4**. These complexes likely represent key intermediates in the formation of active catalysts for BHA and other related cross-coupling reactions. While most ancillary ligand precursors were obtained from commercial sources, a simple synthetic methodology allowing the preparation of an otherwise expensive ligand precursor (**3-7**)

was disclosed. Previously reported C-N cross-coupling reactions, or standard nucleophilic substitution reactions, were followed by Pd-catalyzed P-C cross-coupling to afford the target ligands in good to excellent yield. The ligand set prepared incorporates a series electron-donating and electron-withdrawing groups of varying strength (determined via consideration of relevant Hammett parameters). Substitution targeted the phenylene-backbone of **1-4** in positions *para* to phosphorus or nitrogen without altering these fragments, as these are known to impart desirable electronic and structural characteristics upon palladium. For the first time, two structural isomers of DalPhos ligands have been prepared where the phenylene-backbone has been replaced with pyridine. While the aforementioned examples are restricted to backbone-substitution, an example is also disclosed whereby the morpholino group is replaced with a thiomorpholino group.

Ligands **3-20**-**3-26** were combined with $[Pd(cinnamyl)Cl]_2$ in a 2:1 ratio, and the respective coordination complexes were isolated in excellent yield. In most cases, a single [κ^2-*P,N*-Pd(η^1-cinnamyl)Cl] complex was identified in solution by use of NMR spectroscopic methods. In the case of **3-20**, a cationic κ^3-*P,N,S*- binding mode was found, while in the case of **3-25**, two structural isomers in slow exchange on the NMR time-scale were confirmed via ^{31}P NMR spectroscopy saturation transfer experiments. These isomers are proposed to differ via coordination to palladium through the morpholino or pyridine nitrogen lone pairs. X-Ray diffraction studies to further examine these complexes would be beneficial, particularly to examine the effect these coordination modes have on bite-angle.

Considering the variable Hammett parameters of the substituents on the phenylene backbone of **3-21**-**3-23** and **3-26**-**3-27**, it was predicted that through either inductive or mesomeric effects, these ligands may interact with Pd in a manner differing from that of **1-4**. However, key metrical parameters were found to be similar for Pd-complexes bearing unsubstituted **1-4** (η^1 and η^3) as well as the methyl and fluorine substituted ligands **3-21** and **3-22**. The incorporation of a thiomorpholine unit did, however, lead to the aforementioned κ^3-binding mode, with all Pd-ligand bonds being longer than those in the κ^3-Pd complex featuring ligand **1-4**, reported recently by the Stradiotto group.

Screening of ligands **3-20**-**3-27** (against **1-4**) in challenging C-N, C-C, and C-O cross-coupling reactions revealed that these ligands perform well, and in some cases equally as well as **1-4**. The ligand **3-20** demonstrated no activity in most cases except acetone arylation (limited yield); the possibility that the displayed reactivity is attributable to a blocked coordination site by sulfur remains to be confirmed. Lastly, the unique isomerization displayed by **3-25** when bound to Pd, may be responsible for the superior performance of this ligand in the arylation of acetone. Further studies must be conducted to confirm or reject these hypotheses.

3.5. EXPERIMENTAL SECTION

3.5.1. General Considerations

Unless noted, reactions were set up inside a dinitrogen-filled inert atmosphere glovebox and worked up in air using benchtop procedures. Benzene, hexanes, pentane and toluene were deoxygenated by sparging with dinitrogen followed by passage through an mBraun double column solvent purification system packed with alumina and copper-Q5 reactant; dichloromethane was purified over two alumina-packed columns. THF was dried over Na/benzophenone, distilled, and stored over 4 Å molecular sieves. Di(1-adamantyl)phosphine[125] and $[Pd(Cinnamyl)Cl]_2$[112] were prepared according to literature procedures; all other chemicals were obtained from commercial sources in high purity and used as received. $CDCl_3$ (Sigma-Aldrich) and C_6D_6 (Cambridge Isotopes) used for NMR spectroscopic analysis were degassed by using at least three repeated freeze-pump-thaw cycles and stored over 4 Å molecular sieves for 24 h prior to use. Column chromatography was carried out using Silicycle SiliaFlash 60 with particle size 40-63 μm (230-400 mesh). Gas chromatography (GC) data were obtained on a Shimadzu GC-2014 equipped with a SGE BP-5 30 m, 0.25 mm I.D. column. Unless otherwise noted, ^{1}H, ^{13}C, and ^{31}P NMR spectral data were collected at 300 K on a Bruker AV-500 spectrometer operating at 500.1, 125.8, and 202.5 MHz (respectively) with chemical shifts reported in parts per million downfield of $SiMe_4$ (for ^{1}H and ^{13}C) or 85% H_3PO_4 in D_2O (for ^{31}P). Structural elucidation was enabled through analysis of $^{1}H-^{1}H$ COSY, $^{1}H-^{13}C$ HSQC, $^{1}H-^{13}C$ HMBC, DEPTQ-135 and saturation transfer data; NMR spectral data were acquired with the technical assistance of Dr. Michael Lumsden (NMR-3, Dalhousie University), while mass spectrometric data were acquired by Mr. Xiao Feng (Mass

Spectrometry Laboratory, Dalhousie University). Single-crystal X-ray diffraction data were collected by Dr. Robert McDonald and Dr. Michael Ferguson (X-Ray Crystallography laboratory, University of Alberta). Elemental analysis data have yet to be obtained. Chemical shifts of common trace ^{1}H NMR impurities (ppm): H_2O: 1.56, DMSO: 2.50, Dioxane: 3.71, CH_2Cl_2: 5.30, $CHCl_3$: 7.26.

3.5.2. Experimental Section for Section 3.2

Representative Catalytic Protocol A:[60a]

In an inert atmosphere glovebox, Pd_2dba_3 (1 mol %) and *rac*-BINAP (3 mol %) were added to a vial sealed with a cap containing a PTFE septum and stirred in toluene ([ArI] = 0.50 M) for 5 min after which NaO*t*Bu (1.3 equiv.) and 18-Crown-6 (1.3 equiv.) were added along with the aryl iodide substrate (1 equiv.) if it was a solid. After removing the vial from the glovebox the aryl iodide was added if it was a liquid, along with the corresponding morpholine variant (1.2 equiv.). The solution was then stirred vigorously overnight at room temperature and reaction progress was monitored by use of GC methods. After complete consumption of the aryl iodide was observed (16-24 h), the reaction mixture was diluted with EtOAc (40 mL) and washed with 1:1 water/brine (3 x 50 mL). The organic layer was dried over sodium sulfate, filtered and concentrated to afford crude product which was further purified by column chromatography.

Representative Catalytic Protocol B:

In an inert atmosphere glovebox, Pd_2dba_3 (3-5 mol %) and Xantphos (Pd:L 1:3) were added to a vial sealed with a cap containing a PTFE septum and stirred in toluene ([ArI] = 0.40 M) for 5 min after which NaO*t*Bu (1.1-2.5 equiv.) was added along with the aryl iodide substrate (1 equiv.) if it was a solid. After removing the vial from the glovebox the aryl iodide was added if it was a liquid, along with morpholine (1.1 equiv.). The vial was then placed in a temperature-controlled heating block set at 110 °C and the solution was stirred vigorously. Reaction progress was monitored by use of GC methods and after complete consumption of the aryl iodide was observed (12-24 h), the reaction mixture was allowed to cool and then filtered through a short plug of silica on celite, which was

washed with CH_2Cl_2/MeOH (50:1). The resulting eluent solution was concentrated to afford crude product which was further purified by column chromatography.

Representative Catalytic Protocol C:[119]

In an inert atmosphere glovebox, $Pd(OAc)_2$ (2.5-5 mol%) and D*i*PPF (1,1'-bis(diisopropylphosphino)ferrocene; Pd:L ~1:1.1) were combined in toluene ([ArBr] = 0.50 M) and stirred for 10 minutes. This solution was then added to a vial containing di(1-adamantyl)phosphine (1.00 equiv.) and NaO*t*Bu (1.2 equiv.) followed by the addition of the aryl halide (1.05 equiv.); the vial was then capped and removed from the glovebox. The resulting mixture was heated at 110 °C until complete consumption of the phosphine was achieved, as judged via ^{31}P NMR spectroscopy (typically 16-24 h). The solution was then cooled and filtered through a plug of silica on celite, which in turn was washed with CH_2Cl_2. The resulting eluent solution was concentrated to afford products that were furthered purified by washing with cold pentane (3 x 5-10 mL). All ligands were worked up in air and were found to be stable when handled on the benchtop.

1-Bromo-2-iodo-4,5-dimethoxybenzene (3-7). A solution of N-iodosuccinimide (1.35 g, 6.0 mmol) in acetonitrile ([ArBr] = 0.25 M) was treated dropwise with trifluoroacetic acid (138 μL, 1.8 mmol); after stirring for 5 minutes, 4-bromoveratrole (432 mL, 3.0 mmol) was added to the resulting deep yellow mixture. The vial was then placed in a temperature-controlled heating block set at 65 °C, and the solution was stirred vigorously. Reaction progress was monitored by GC methods; following full consumption of the ArBr (24 h) the resulting orange solution was cooled to room temperature and poured into water (50 mL) and extracted with EtOAc (3 x 30 mL). The combined organic extracts were washed with aq. sat. $NaHCO_3$ (25 mL), aq. $Na_2S_2O_3$ (10%, 3 x 20 mL) and brine (20 mL), before being dried over sodium sulfate, filtered and concentrated. The title compound was isolated in 99 % yield as an off-white solid (1.02 g, 3.0 mmol) following column chromatography (20:1 hex/EtOAc). ^1H NMR ($CDCl_3$): δ 7.21 (s, 1H), 7.06 (s, 1H), 3.84 (s, 3H), 3.83 (s, 3H). $^{13}C\{^1H\}$ NMR ($CDCl_3$): δ 150.0, 148.8, 122.1, 120.3, 115.4, 89.0, 56.4, 56.3. HRMS (ESI/[M+H]+) calcd. for

$C_8H_8BrINaO_2$: 364.8645. Found: 364.8649. Spectral data are in good agreement with previously reported ^1H and ^{13}C NMR spectral data for the title product.[120]

4-(2-Bromophenyl)thiomorpholine (3-10). Prepared from iodobromobenzene and thiomorpholine via representative catalytic protocol A, the title compound was isolated in 80% yield as a white solid (829 mg, 3.20 mmol) after column chromatography (100:1 Hexane:EtOAc). ^1H NMR ($CDCl_3$): δ 7.56 (dd, J = 8.0, 1.5 Hz, 1H), 7.27 (td, J = 7.7, 1.5 Hz, 1H), 7.04 (dd, J = 8.0, 1.5 Hz, 1H), 6.93(m, 1H), 3.25 (m, 4H), 2.84 (4H, m). $^{13}C\{^1H\}$ NMR ($CDCl_3$): δ 151.8, 138.9, 128.43, 124.8, 121.9, 120.7, 54.5, 28.4. HRMS (ESI/[M+H]+) calcd. for $C_{10}H_{13}BrNS$: 257.9947. Found: 257.9938.

4-(2-Bromo-5-methylphenyl)morpholine (3-11). Prepared from 1-bromo-2-iodo-4-methyl-benzene and morpholine via representative catalytic protocol A, the title compound was isolated in 78% yield as a yellow oil (1.40 g, 5.47 mmol) after column chromatography (25:1 Hexane:EtOAc). ^1H NMR ($CDCl_3$): δ 7.43 (d, J = 8.0 Hz, 1H), 6.85 (d, J = 2.0 Hz, 1H), 6.75 (dd, J = 8.3, 1.5 Hz, 1H), 3.88 (t, J = 4.5 Hz, 4H), 3.03 (t, J = 4.5 Hz, 4H), 2.30 (s, 3H). $^{13}C\{^1H\}$ NMR ($CDCl_3$): δ 150.1, 138.5, 133.7, 125.5, 121.8, 116.5, 67.4, 52.3, 21.3. HRMS (ESI/[M+H]+) calcd. for $C_{11}H_{15}BrNO$: 256.0332. Found: 256.0319.

4-(2-Bromo-5-fluorophenyl)morpholine (3-12). Prepared from 1-bromo-4-fluoro-2-iodo-benzene via representative catalytic protocol B employing 5 mol% Pd and 2.5 equiv. NaO*t*Bu. The title compound was isolated in 71% yield as a pale yellow oil (139 mg, 0.53 mmol) after column chromatography (50:1 Hexane:EtOAc). Limited exposure is necessary to prevent loss of product under reduced pressure. ^1H NMR ($CDCl_3$): δ 7.50 (m, 1H 6.77 (m, 1H), 6.67 (m, 1H), 3.90-3.85 (m, 4H), 3.07-3.02 (m, 4H). $^{13}C\{^1H\}$ NMR ($CDCl_3$): δ 162.7 (d, J_{CF} = 247.3 Hz, C_{quat}), 152.0 (d, J_{CF} = 8.2 Hz), 134.6 (d, J_{CF} = 9.1 Hz), 113.6 (d, J_{CF} = 3.2 Hz), 111.4 (d, J_{CF} = 22.5 Hz), 108.6 (d, J_{CF} = 23.8 Hz), 67.2, 52.01. HRMS (ESI/[M+H]+) calcd. for $C_{10}H_{12}BrFNO$: 260.0081. Found: 260.0073.

4-(2-Bromo-4-fluorophenyl)morpholine (3-13). Prepared from 2-bromo-4-fluoro-1-iodo-benzene via representative catalytic protocol B employing 5 mol% Pd and 2.5 equiv. NaO*t*Bu. The title compound was isolated in 74% yield as a yellow oil (518 mg, 2.00 mmol) after column chromatography (25:1 → 15:1 Hexane:EtOAc). Limited exposure is necessary to prevent loss of product under reduced pressure. ^{1}H NMR ($CDCl_3$): δ 7.33 (m, 1H) 7.06-6.96 (m, 2H), 3.92-3.81 (m, 4H), 3.03-2.93 (m, 4H). $^{13}C\{^{1}H\}$ NMR ($CDCl_3$): δ 246.4 (d, J_{CF} = 246.4, C_{quat}),146.9, 121.6 (d, J_{CF} = 8.5 Hz), 121.0 (d, J_{CF} = 25.1 Hz), 120.4 (d, J_{CF} = 9.5Hz), 115.0 (d, J_{CF} = 21.6 Hz), 67.3, 52.5. HRMS (ESI/[M+H]+) calcd. for $C_{10}H_{12}BrFNO$: 260.0081. Found: 260.0076.

4-(3-Bromopyridin-2-yl)morpholine (3-14). 3-bromo-2-chloropyridine (866 mg, 4.5 mmol), morpholine (779 μL, 9.0 mmol) and K_2CO_3 (1.49 g, 10.8 mmol) were weighed into a vial to which DMF ([ArCl] = 0.30 M) was added. The reaction mixture was stirred vigorously overnight at 130 ^{o}C and progress was monitored by GC methods. Following full consumption of the heteroaryl chloride (30 h) the resulting bright yellow solution was cooled to room temperature and poured into saturated NH_4Cl_{aq} (50 mL) and Et_2O (50 mL). The DMF-water phase was extracted with Et_2O (3 x 20 mL) and the combined organic phases were dried over sodium sulfate, filtered and concentrated; the crude product was afforded as a yellow oil. The title compound was isolated in 81% yield as white crystals (882 mg, 3.63 mmol) after column chromatography (3:1 Hexane:EtOAc). ^{1}H NMR ($CDCl_3$): δ 8.24 (dd, *J* = 4.8, 1.4 Hz, 1H), 7.79 (dd, *J* = 7.7, 1.4 Hz, 1H), 6.80 (dd, *J* = 7.7 Hz, 4.8 Hz, 1H), 3.87-3.85 (m, 4H), 3.35-3.33 (m, 4H). $^{13}C\{^{1}H\}$ NMR ($CDCl_3$): δ 159.4, 146.7, 142.5, 118.9, 113.0, 67.1, 50.1. HRMS (ESI/[M+H]+) calcd. for $C_9H_{12}BrN_2O$: 243.0128. Found: 243.0116. Spectral data are in good agreement with previously reported ^{1}H and ^{13}C NMR spectral data for the title product.[126]

4-(2-Bromopyridin-3-yl)morpholine (3-15). Prepared from 2-Bromo-3-iodo-pyridine via representative catalytic protocol B employing 3 mol% Pd and 1.1 equiv. NaO*t*Bu (increasing base equivalency led to undesired C-O cross-coupling at the bromide of **L6'**). The title compound was isolated in 68% yield as a yellow oil (496 mg, 2.04

mmol) after column chromatography (10:1 Hexane:EtOAc). *Note*: column chromatography was carried out using Brockman III alumina as opposed to Silicycle SiliaFlash 60. ^{1}H NMR ($CDCl_3$): δ 8.07 (m, 1H) 7.30 (m, 1H), 7.23 (m, 1H), 3.90-3.87 (m, 4H), 3.09-3.05 (m, 4H). $^{13}C\{^{1}H\}$ NMR ($CDCl_3$): δ 147.6, 144.0, 140.2, 128.4, 123.4, 67.1, 51.8. HRMS (ESI/[M+H]+) calcd. for $C_9H_{11}BrN_2NaO$: 264.9947. Found: 264.9940.

4-(2-Bromo-4,5-dimethoxyphenyl)morpholine (3-16). Prepared from 1-Bromo-2-iodo-4,5-dimethoxy-benzene (**3-7**) and morpholine via representative catalytic protocol A, the title compound was isolated in 79% yield as an off-white solid (308 mg, 1.02 mmol) after column chromatography (5:1 Hexane:EtOAc). ^{1}H NMR ($CDCl_3$): δ 7.05 (s, 1H), 6.65 (s, 1H), 3.87-3.85 (m, 7H), 3.84 (s, 3H). $^{13}C\{^{1}H\}$ NMR ($CDCl_3$): δ 149.0, 146.0, 143.7, 116.5, 110.0, 105.1, 67.4, 56.4, 56.3, 52.5. HRMS (ESI/[M+H]+) calcd. for $C_{12}H_{16}BrNNaO_3$: 324.0206. Found: 324.0109.

3-Bromo-4-morpholinobenzonitrile (3-17). 3-Bromo-4-fluoro-benzonitrile (1.00 g, 5.0 mmol), morpholine (865 μL, 10.0 mmol) and K_2CO_3 (2.00 g, 14.5 mmol) were weighed into a vial to which DMSO ([ArF] = 0.50 M) was added. The reaction mixture was stirred vigorously overnight at 150 ^{o}C and progress was monitored by GC methods. Following full consumption of the ArF (24 h) the resulting yellow solution was cooled to room temperature and poured into EtOAc (30 mL) and washed with water (6 x 50 mL). The organic phase was dried over sodium sulfate, filtered and concentrated. The title compound was isolated in 32% yield as white crystals (425 mg, 1.59 mmol) after column chromatography (5:1 Hexane:EtOAc). ^{1}H NMR ($CDCl_3$): δ 7.83 (d, J = 1.9 Hz, 1H), 7.57 (dd, J = 8.4, 1.9 Hz, 1H), 7.04 (d, J = 8.4 Hz, 1H), 3.88 (app. t, J = 4.6 Hz, 4H), 3.13 (app. t, J = 4.6 Hz, 4H). $^{13}C\{^{1}H\}$ NMR ($CDCl_3$): δ 154.5, 137.6, 132.6, 120.8, 118.9, 117.9, 107.3, 66.9, 51.6. HRMS (ESI/[M+H]+) calcd. for $C_{11}H_{11}BrN_2NaO$: 288.9947. Found: 288.9935.

4-(2-Bromo-4-nitrophenyl)morpholine (3-18). A solution of 2-Bromo-1-fluoro-4-nitrobenzene (2.61 g, 11.9 mmol) in acetonitrile ([ArF] = 0.5 M) was treated with morpholine (2.05 mL, 23.8 mmol) and the mixture was heated under reflux for 6h.

Following full consumption of the ArF the resulting yellow solution was cooled to room temperature and poured into water (50 mL) and extracted with EtOAc (3 x 25 mL). The organic extracts were dried over sodium sulfate, filtered and concentrated. The title compound was isolated in 95% yield as yellow crystals (3.25 g, 11.32 mmol), without the need for purification by column chromatography. ^{1}H NMR operating at 300.1 MHz ($CDCl_3$): δ 8.44 (d, *J* = 2.6 Hz, 1H), 8.15 (dd, *J* = 8.2, 2.6 Hz, 1H), 7.05 (d, *J* = 8.9 Hz, 1H), 3.89 (m, 4H), 3.19 (m, 4H). ^{13}C{^{1}H} NMR operating at 75.7 MHz ($CDCl_3$): δ 156.1, 143.0, 130.0, 124.2, 119.8, 117.9, 66.9, 51.6.

1,4-bis(2-bromophenyl)piperazine (3-19). In an inert atmosphere glovebox, Pd_2dba_3 (3 mol %) and *rac*-BINAP (9 mol %) were added to a vial sealed with a cap containing a PTFE septum and stirred in THF ([ArI] = 0.50 M) for 5 min after which NaO*t*Bu (3.0 equiv.), 18-Crown-6 (3.0 equiv.) and iodobromobenzene (2.3 equiv., 590 μL, 4.6 mmol) were added along with piperazine (1.0 equiv., 175 mg, 2.0 mmol). The vial was then stirred vigorously overnight at reflux; reaction progress was monitored by use of GC methods. After complete consumption of the amine was observed (24 h), the reaction mixture was cooled to room temperature and poured into water (50 mL) extracted with EtOAc (3 x 25 mL). The organic extracts were dried over sodium sulfate, filtered and concentrated. The title compound was isolated in 45% yield as a white solid (365 mg, 0.92 mmol), after column chromatography (100:1 Hexane:EtOAc). ^{1}H NMR ($CDCl_3$): δ 7.59 (m, 2H), 7.35-7.27 (m, 2H), 7.18-7.12 (m, 2H), 6.94 (m, 2H), 3.25 (br s., 8H). ^{13}C{^{1}H} NMR ($CDCl_3$): δ. 150.8, 134.0, 128.5, 124.6, 121.3, 120.1, 52.1. HRMS (APCI/[M+H]+) calcd. for $C_{16}H_{17}Br_2N_2$: 394.9753. Found: 394.9745.

3-20. Prepared by the coupling of $(1\text{-Ad})_2PH$ and 4-(2-bromo-phenyl)-thiomorpholine (**3-10**) via representative catalytic protocol C employing 2.5 mol% Pd and 2.75 mol% ligand in 77% yield as a beige solid (667 mg, 1.39 mmol). ^{1}H NMR ($CDCl_3$): δ 7.70 (d, *J* = 7.6 Hz, 1H) 7.29 (m, 1H), 7.06-7.01 (m, 2H), 3.26-3.20 (m, 4H), 2.81 (t, *J* = 4.4 Hz, 4H), 1.99-1.89 (m, 18H), 1.69 (s, 12H) . ^{13}C{^{1}H} NMR ($CDCl_3$): δ 161.0 (d, J_{CP} = 20.9Hz, C_{quat}), 137.5, 131.9 (d, J_{CP} = 26.6 Hz, $_{Cquat}$), 129.5, 122.4, 121.1, 55.6, 42.1 (d, J_{CP} = 13.3Hz), 37.2, 37.0 (d, J_{CP} = 27.5 Hz), 29.1(d, J_{CP} = 8.3 Hz), 28.0.

$^{31}P\{^{1}H\}$ NMR ($CDCl_3$): δ 20.4. HRMS (ESI/[M+H]+) calcd. for $C_{30}H_{43}NPS$: 480.2848. Found: 480.2842. A suitable crystal for single-crystal X-ray diffraction was afforded via slow evaporation of a concentrated benzene/hexanes solution of **3-20** at ambient temperature.

3-21. Prepared by the coupling of $(1\text{-Ad})_2PH$ and 4-(2-bromo-5-methyl-phenyl)-morpholine (**3-11**) via representative catalytic protocol C employing 2.5 mol% Pd and 2.75 mol% ligand in 87% yield as a white solid (920 mg, 1.93 mmol). ^{1}H NMR ($CDCl_3$): δ 7.59 (d, J = 8.0 Hz, 1H) 6.86 (app. d, J = 6.0 Hz, 2H), 3.83 (t, J = 4.5 Hz, 4H), 3.03 (t, J = 4.3 Hz, 4H), 2.34 (s, 3H), 1.98-1.86 (m, 18H), 1.67 (s, 12H). $^{13}C\{^{1}H\}$ NMR ($CDCl_3$): δ 159.6 (d, J_{CP} = 21.0 Hz, C_{quat}), 139.5, 137.5, 127.5 (d, J_{CP} = 25.9 Hz, $_{Cquat}$), 123.2, 120.9 (d, J_{CP} = 3.4Hz), 67.4, 53.6 (d, J_{CP} = 5.6 Hz), 42.1 (d, J_{CP} = 13.3 Hz), 37.2, 36.9 (d, J_{CP} = 26.7 Hz), 29.1 (d, J_{CP} = 8.4 Hz), 21.6. $^{31}P\{^{1}H\}$ NMR ($CDCl_3$): δ 19.3. HRMS (ESI/[M+H]+) calcd. for $C_{31}H_{45}NOP$: 478.3233. Found: 478.3233.

3-22. Prepared by the coupling of $(1\text{-Ad})_2PH$ and 4-(2-bromo-5-fluoro-phenyl)-morpholine (**3-12**) via representative catalytic protocol C employing 5 mol% Pd and 5.5 mol% ligand in 73% yield as a white solid (350 mg, 0.73 mmol). ^{1}H NMR (C_6D_6): δ 7.59 (m, 1H), 6.72-6.67 (m, 2H), 3.77 (t, J = 4.5 Hz, 4H), 2.86 (t, J = 4.3 Hz, 4H), 2.06-1.97 (m, 12H), 1.88 (s, 6H), 1.65 (s, 12H). $^{13}C\{^{1}H\}$ NMR ($CDCl_3$): δ 163.8 (d, J_{CF} = 248.7 Hz, C_{quat}), 161.8 (m), 138.8 (app. d, J = 6.1 Hz), 126.1 (m), 109.1 (d, J = 19.8 Hz), 107.4 (m), 67.2, 53.5, 42.0, 37.1, 29.0. $^{31}P\{^{1}H\}$ NMR operating at 121.5 MHz ($CDCl_3$): δ 19.2. HRMS (ESI/[M+H]+) calcd. for $C_{30}H_{42}FNOP$: 482.2983. Found: 482.2977. A suitable crystal for single-crystal X-ray diffraction was afforded via slow evaporation of a concentrated benzene/hexanes solution of **3-22** at ambient temperature.

3-23. Prepared by the coupling of $(1\text{-Ad})_2PH$ and 4-(2-bromo-4-fluoro-phenyl)-morpholine (**3-13**) via representative catalytic protocol C employing 2.5 mol% Pd and 2.75 mol% ligand in 80% yield as a white solid (709 mg, 1.47 mmol). ^{1}H NMR operating at 300.1 MHz ($CDCl_3$): δ 7.42 (dd, J = 9.7, 1.5 Hz, 1H), 7.07-6.94 (m, 2H), 3.85-3.77 (m, 4H), 3.00-2.93 (m, 4H), 2.00-1.85 (m, 18H) 1.68 (s, 12H). $^{13}C\{^{1}H\}$ NMR ($CDCl_3$): δ

157.7 (d, J_{CF} = 245.8 Hz, C_{quat}), 155.7 (d, J = 19.0 Hz), 134.3 (m), 123.4 (app. d, J = 20.1 Hz), 121.3 (m), 116.0 (d, J = 21.8 Hz), 67.3, 53.7 (d, J_{CP} = 4.8 Hz), 41.9 (d, J_{CP} = 12.5 Hz). 37.1, 28.9. $^{31}P\{^{1}H\}$ NMR operating at 121.5 MHz ($CDCl_3$): δ 20.4. HRMS (ESI/[M+H]+) calcd. for $C_{30}H_{42}FNOP$: 482.2983. Found: 482.2977.

3-24. Prepared by the coupling of $(1\text{-Ad})_2PH$ and 4-(3-Bromo-pyridin-2-yl)-morpholine (**3-14**) via representative catalytic protocol C employing 2.5 mol% Pd and 2.75 mol% ligand in 86% yield as a beige solid (628 mg, 1.35 mmol). ^{1}H NMR ($CDCl_3$): δ 8.25 (m, 1H), 7.92 (m, 1H), 6.89 (m, 1H), 3.83-3.81 (m, 4H), 3.37-3.35 (m, 4H), 1.97-1.82 (m, 18H), 1.71-1.60 (m, 12H). $^{13}C\{^{1}H\}$ NMR ($CDCl_3$): δ 168.5, 148.1, 146.5, 122.8, 116.8, 67.2, 51.9 (d, J_{CP} = 9.2 Hz), 42.0 (d, J_{CP} = 13.0 Hz), 37.4 (app. d, J_{CP} = 27.1 Hz), 37.0, 29.0 (d, J_{CP} = 8.5 Hz). $^{31}P\{^{1}H\}$ NMR ($CDCl_3$): δ 20.9. HRMS (ESI/[M+H]+) calcd. for $C_{29}H_{42}N_2OP$: 465.3029. Found: 465.3023. A suitable crystal for single-crystal X-ray diffraction was afforded via slow evaporation of a concentrated dichloromethane solution of **3-24** at ambient temperature.

3-25. Prepared by the coupling of $(1\text{-Ad})_2PH$ and 4-(2-Bromo-pyridin-3-yl)-morpholine (**3-15**) via representative catalytic protocol C employing 2.5 mol% Pd and 3.75 mol% ligand in 88% yield as a pale beige solid (727 mg, 1.57 mmol). ^{1}H NMR ($CDCl_3$): δ 8.44 (m, 1H), 7.24 (m, 1H), 7.11 (m, 1H), 3.84 (t, J = 4.5 Hz, 4H), 3.06 (t, J = 4.3 Hz, 4H), 2.10-2.02 (m, 6H), 1.96-1.83 (m, 12H), 1.67 (s, 12H). $^{13}C\{^{1}H\}$ NMR ($CDCl_3$): δ 159.7 (d, J_{CP} = 24.9 Hz), 155.7 (d, J_{CP} = 24.9 Hz), 143.8, 125.7 (d, J_{CP} = 3.4 Hz), 122.5, 67.3, 53.0 (d, J_{CP} = 6.1 Hz), 41.7 (d, J_{CP} = 12.0 Hz), 38.1 (d, J_{CP} = 23.8 Hz), 37.3, 29.1, (d, J_{CP} = 8.3 Hz). $^{31}P\{^{1}H\}$ NMR operating at 121.5 MHz ($CDCl_3$): δ 24.8. HRMS (ESI/[M+H]+) calcd. for $C_{29}H_{42}N_2OP$: 465.3029. Found: 465.3022. A suitable crystal for single-crystal X-ray diffraction was afforded via slow evaporation of a concentrated pentane solution of **3-25** at ambient temperature.

3-26. Prepared by the coupling of $(1\text{-Ad})_2PH$ and 4 4-(2-Bromo-4,5-dimethoxy-phenyl)-morpholine (**3-16**) via representative catalytic protocol C employing 2.5 mol% Pd and 3.75 mol% ligand in 84% yield as a white solid (330 mg, 0.63 mmol). ^{1}H NMR

($CDCl_3$): δ 7.24 (s, 1H), 6.67 (d, J_{CP} = 4.2 Hz, 1H), 3.89 (m, 6H), 3.82 (app. t, J = 4.5 Hz, 4H), 2.96 (app. t, J = 4.5 Hz, 4H), 1.98-1.85 (m, 18H), 1.67 (s, 12H). $^{13}C\{^1H\}$ NMR ($CDCl_3$): δ 154.0 (d, J_{CP} = 21.8 Hz), 149.7, 143.8, 122.2 (d, J_{CP} = 25.8 Hz), 120.0, 104.1 (d, J_{CP} = 3.6 Hz), 67.4, 56.4, 55.7, 53.8 (app. d, J_{CP} = 3.7 Hz), 42.1 (d, J_{CP} = 13.4 Hz), 37.2, 36.9 (d, J_{CP} = 26.9 Hz), 29.0 (d, J_{CP} = 8.4 Hz). $^{31}P\{^1H\}$ NMR operating at 121.5 MHz ($CDCl_3$): δ 19.5. HRMS (ESI/[M+H]+) calcd. for $C_{32}H_{47}NO_3P$: 524.3288. Found: 524.3269. A suitable crystal for single-crystal X-ray diffraction was afforded via slow evaporation of a concentrated dichloromethane/diethyl ether solution of **3-26** at ambient temperature.

3-27. Prepared by the coupling of $(1\text{-Ad})_2PH$ and 3-Bromo-4-morpholin-4-yl-benzonitrile (**3-17**) via representative catalytic protocol C employing 2.5 mol% Pd and 3.75 mol% ligand in 98% yield as a beige solid (600 mg, 1.23 mmol). ^1H NMR operating at 300.1 MHz ($CDCl_3$): δ 7.93 (m, J = 2.0 Hz, 1H), 7.56 (dd, J = 8.4, 2.0 Hz, 1H), 7.00 (dd, J = 8.4, 4.1 Hz, 1H), 3.85-3.82 (m, 4H), 3.17-3.14 (m, 4H), 1.90 (s, 18H), 1.68 (s, 12H). $^{13}C\{^1H\}$ NMR ($CDCl_3$): δ $^{13}C\{^1H\}$ NMR ($CDCl_3$): δ 163.5 (d, J_{CP} = 19.3 Hz), 141.4, 133.6, 132.0 (d, J_{CP} = 35.2 Hz), 119.9, 104.8, 66.9, 53.1 (d, J_{CP} = 8.1 Hz), 42.0 (d, J_{CP} = 13.1 Hz), 37.4 (d, J_{CP} = 27.4 Hz) , 37.0, 28.9 (d, J_{CP} = 8.5 Hz). $^{31}P\{^1H\}$ NMR ($CDCl_3$): δ 21.2. HRMS data has yet to be obtained for this compound.

3.5.3. Experimental Section for Section 3.3

Representative Procedure for the Synthesis of Palladium Complexes:

To a magnetically stirred solution of $[Pd(cinnamyl)Cl]_2$ (1 equiv.) in CH_2Cl_2 ([**L1**] = 0.15 M) was added **3-20** (2.0 equiv.) resulting in a transparent orange solution. The mixture was stirred magnetically for 12 h at ambient temperature, causing a color change from orange to bright yellow (unlike **3-21**-**3-26** which afforded red solutions); ^{31}P NMR spectroscopic analysis of the reaction mixture confirmed the consumption of **3-20** and the quantitative formation of a new product (**3-43**). The solvent and other volatiles were removed *in vacuo* and the residual solid was washed with pentane (3 x 2 mL) and then Et_2O (2 x 2 mL). Subsequent removal of the solvents *in vacuo* afforded (**3-43**) as an analytically pure yellow solid (131 mg, 0.18 mmol, 85 %). ^1H NMR ($CDCl_3$): δ 8.24 (br

s, 1H; ArH), 7.75-7.60 (m, 2H; ArH), 7.45 (br s, 1H; ArH), 7.35-7.21 (m, 5H; cin Ph), 7.17 (m, 1H; ArH), 6.70-6.54 (m, 2H; alkenyl H), 4.59-4.43 (m, 2H; morph CH_2), 4.04-3.86 (m, 2H; morph CH_2), 3.34-2.95 (m, 6H; morph CH_2/Pd-CH_2), 2.24 (br s, 6H; 1-Ad CH_2), 2.10-1.89 (m, 12H; 1-Ad CH/CH_2), 1.82-1.56 (br s, 12H; 1-Ad CH_2). $^{13}C\{^1H\}$ NMR ($CDCl_3$): δ 155.9 (d, J_{CP} = 11.0 Hz; aryl C_{quat}), 138.6 (s; cin Ph C_{quat}), 135.4 (s; Ar CH), 134.3 (s; alkenyl CH), 133.8 (s; Ar CH), 129.0 (s; cin Ph CH), 128.7 (s; Ar CH); 128.5 (s; Ar C_{quat}), 127.6 (s; Ar CH), 127.5 (s; alkenyl CH), 126.7 (s; cin Ph CH), 125.3 (s; cin Ph CH), 57.1 (s; morph CH_2), 43.3 (d, J_{CP} = 12.4 Hz; 1-Ad C_{quat}), 40.7 (s; 1-Ad CH_2), 36.2 (s; 1-Ad CH_2), 33.0 (s; morph CH_2), 28.5 (d, J_{CP} = 9.1 Hz; 1-Ad CH), 16.6 (s; Pd-CH_2). $^{31}P\{^1H\}$ NMR ($CDCl_3$): δ 67.8. Crystals suitable for single-crystal X-ray diffraction analysis were obtained via vapor diffusion of diethyl ether into a solution of **3-43** in dichloromethane.

3-33/3-34. Prepared by the treatment of a solution of [Pd(cinnamyl)Cl]$_2$ in CH_2Cl_2 with **3-21** according to the representative procedure (*vide supra*). The title compound was isolated in 87% yield as an analytically pure yellow solid (121 mg, 0.16 mmol). ^1H NMR ($CDCl_3$): δ 7.71-7.68 (m, 3H; ArH/cin Ph), 7.60 (m, 1H; ArH), 7.39-7.33 (m, 3H; cin Ph), 7.23 (m, 1H; ArH), 6.68 (dd, J = 14.5, 9.2 Hz, 1H; alkenyl H), 6.32 (m, 1H; alkenyl H), 3.80-3.76 (m, 2H; morph CH_2), 3.71-3.64 (m, 2H; morph CH_2), 3.55 (d, J = 9.2 Hz, 2H; Pd-CH_2), 3.48-3.41 (m, 2H; morph CH_2), 3.17-3.08 (m, 2H; morph CH_2), 2.41 (s, 3H; Ar-CH_3), 2.29-2.16 (m, 6H; 1-Ad CH_2), 2.07-1.85 (m, 12H; 1-Ad CH/CH_2), 1.74-1.56 (m, 12H; 1-Ad CH_2). $^{13}C\{^1H\}$ NMR ($CDCl_3$): δ 160.3 (d, J_{CP} = 14.8 Hz; aryl C_{quat}), 143.9 (s; aryl C_{quat}), 136.6 (s; Ph C_{quat}), 135.2 (s; Ph CH), 129.5 (s; Ph CH), 128.8 (s; aryl CH), 128.7 (m; aryl CH), 127.9 (s; Ph CH), 126.8 (d, J_{CP} = 7.9 Hz; aryl CH), 123.6 (d, J_{CP} = 31.1 Hz; aryl C_{quat}), 122.0 (d, J_{CP} = 17.9 Hz ; alkenyl CH), 113.2 (s; alkenyl CH), 65.0 (s; morph CH_2), 58.5 (s; morph CH_2), 42.9 (d, J_{CP} = 12.8 Hz; 1-Ad C_{quat}), 41.3 (s; 1-Ad CH_2), 36.2 (m; Pd-CH_2/1-Ad CH_2), 28.7 (d, J_{CP} = 9.3 Hz; 1-Ad CH), 21.7 (s; aryl-CH_3). $^{31}P\{^1H\}$ NMR ($CDCl_3$): δ 75.3. Crystals suitable of **3-34** for single-crystal X-ray diffraction analysis were obtained via slow diffusion of Et_2O into a solution of **3-33** in dichloromethane.

3-35. Prepared by the treatment of a solution of $[Pd(cinnamyl)Cl]_2$ in CH_2Cl_2 with **3-22** according to the representative procedure (*vide supra*). The title compound was isolated in 87% yield as an analytically pure yellow solid (121 mg, 0.16 mmol). ^1H NMR ($CDCl_3$): δ 7.83 (m, 1H; ArH), 7.72-7.65 (m, 2H; cin Ph), 7.56 (m, 1H; ArH), 7.37-7.30 (m, 3H; cin Ph), 7.17 (m, 1H; ArH), 6.89 (dd, J = 14.6, 8.7 Hz, 1H; alkenyl H), 6.41 (m, 1H; alkenyl H), 3.92-3.55 (m, 8H; Pd-CH_2/morph CH_2), 3.07-2.91 (m, 2H; morph CH_2), 2.31-2.17 (m, 6H; 1-Ad CH_2), 2.06-1.86 (m, 12H; 1-Ad CH/CH_2), 1.76-1.59 (m, 12H; 1-Ad CH_2). $^{13}C\{^1H\}$ NMR ($CDCl_3$): δ 166.1 (s; aryl CH), 164.1 (s; aryl CH), 162.6 (m; aryl CH), 137.1 (s; cin Ph C_{quat}), 136.7 (d; J_{CP} = 8.6 Hz aryl C_{quat}), 129.3 (s; cin Ph), 128.4 (s; cin Ph CH), 127.7 (s; cin Ph CH), 123.4 (m; alkenyl CH), 115.9 (s; alkenyl CH), 115.1 (m; aryl CH), 114.0 (m; aryl CH), 64.8 (s; morph CH_2), 58.2 (s; morph CH_2), 43.0 (d, J_{CP} = 11.9 Hz; 1-Ad C_{quat}), 41.3 (s; 1-Ad CH_2), 36.2 (s; 1-Ad CH_2), 34.2 (s; Pd-CH_2) 28.7 (d, J_{CP} = 9.3 Hz; 1-Ad CH). $^{31}P\{^1H\}$ NMR ($CDCl_3$): δ 71.6. Crystals suitable of **3-35** for single-crystal X-ray diffraction analysis were obtained via slow diffusion of Et_2O into a solution of the title compound in dichloromethane.

3-36. Prepared by the treatment of a solution of $[Pd(cinnamyl)Cl]_2$ in CH_2Cl_2 with **3-23** according to the representative procedure (*vide supra*). The title compound was isolated in 84% yield as an analytically pure yellow solid (129 mg, 0.17 mmol). ^1H NMR ($CDCl_3$): δ 7.87 (m, 1H; ArH), 7.75-7.67 (m, 2H; cin Ph), 7.48 (m, 1H; ArH), 7.38-7.29 (m, 4H; cin Ph/ArH), 6.90 (dd, J = 14.6, 8.9 Hz, 1H; alkenyl H), 6.40 (m, 1H; alkenyl H), 3.88-3.80 (m, 2H; morph CH_2), 3.70-3.54 (m, 6H; Pd-CH_2/morph CH_2), 3.07-3.00 (m, 2H; morph CH_2), 2.32-2.21 (m, 6H; 1-Ad CH_2), 2.06-2.01 (br s, 6H; 1-Ad CH), 1.99-1.91 (m, 6H; 1-Ad CH_2), 1.77-1.64 (m, 12H; 1-Ad CH_2). $^{13}C\{^1H\}$ NMR ($CDCl_3$): δ 160.9 (s; aryl CH), 158.9 (s; aryl CH), 156.3 (m; aryl CH), 137.1 (s; cin Ph C_{quat}), 129.3 (s; cin Ph), 128.5 (s; cin Ph CH), 127.7 (m; cin Ph CH/aryl CH), 123.8 (m; alkenyl CH), 121.2 (m; aryl CH), 120.0 (m; aryl CH), 115.3 (s; alkenyl CH), 115.1 (m; alkenyl H), 64.9 (s; morph CH_2), 58.5 (s; morph CH_2), 43.1 (d, J_{CP} = 11.0 Hz; 1-Ad C_{quat}), 41.3 (s; 1-Ad CH_2), 36.2 (s; 1-Ad CH_2), 34.8 (s; Pd-CH_2) 28.7 (d, J_{CP} = 9.3 Hz; 1-Ad CH). $^{31}P\{^1H\}$ NMR ($CDCl_3$): δ 74.2.

3-37. Prepared by the treatment of a solution of $[Pd(cinnamyl)Cl]_2$ in CH_2Cl_2 with **3-26** according to the representative procedure (*vide supra*). The title compound was isolated in 91% yield as an analytically pure orange solid (136 mg, 0.17 mmol). ^{1}H NMR ($CDCl_3$): δ 7.62 (d, J_{CP} = 7.6 Hz, 2H; cin Ph CH), 7.30-7.22 (m, 3H; cin Ph), 7.17 (m, 1H; ArH), 7.05 (m, 1H; ArH), 6.62 (dd, J = 14.4, 9.1 Hz, 1H; alkenyl H), 6.24 (m, 1H; alkenyl H), 3.84-3.78 (m, 6H; OCH_3), 3.71-3.65 (m, 2H; morph CH_2), 3.60-3.53 (m, 2H; morph CH_2), 3.48-3.39 (m, 4H; Pd-CH_2, morph CH_2), 3.06-2.95 (m, 2H; morph CH_2), 2.19-2.09 (m, 6H; 1-Ad CH_2), 1.96-1.82 (m, 12H; 1-Ad CH/CH_2), 1.65-1.55 (m, 12H; 1-Ad CH_2). $^{13}C\{^1H\}$ NMR ($CDCl_3$): δ 154.5 (d, J_{CP} = 15.1 Hz; aryl C_{quat}), 152.4 (s; aryl C_{quat}), 147.4 (d, J_{CP} = 5.0 Hz; aryl C_{quat}), 136.7 (s; cin Ph C_{quat}), 129.4 (s; cin Ph CH), 128.7 (s; cin Ph CH), 127.8 (s; cin Ph CH), 121.6 (d, J_{CP} = 17.7 Hz; alkenyl CH), 117.4 (d, J_{CP} = 32.1 Hz; aryl C_{quat}), 115.6 (s; aryl CH), 113.9 (s; alkenyl CH), 108.1 (d, J_{CP} = 9.1 Hz ; aryl CH), 64.9 (s; morph CH_2), 58.4 (s; morph CH_2), 56.5 (s; OCH_3), 56.2 (s; OCH_3), 42.9 (d, J_{CP} = 12.7 Hz; 1-Ad C_{quat}), 41.4 (s; 1-Ad CH_2), 36.2 (m; Pd-CH_2/1-Ad CH_2), 28.7 (d, J_{CP} = 9.2 Hz; 1-Ad CH). $^{31}P\{^1H\}$ NMR ($CDCl_3$): δ 74.7.

3-38. Prepared by the treatment of a solution of $[Pd(cinnamyl)Cl]_2$ in CH_2Cl_2 with **3-24** according to the representative procedure (*vide supra*). The title compound was isolated in 90% yield as an analytically pure yellow solid (141 mg, 0.20 mmol). ^{1}H NMR ($CDCl_3$): δ 8.66 (m, 1H; ArH), 8.24 (m, 1H; ArH), 7.61-7.56 (m, 2H; cin Ph), 7.54 (m, 1H; ArH), 7.40-7.34 (m, 2H; cin Ph), 7.30 (m, 1H; cin Ph), 6.50 (m, 1H; alkenyl H), 6.19 (dd, J = 14.2, 7.5 Hz, 1H; alkenyl H), 4.22-2.78 (m, 10H; morph CH_2/Pd-CH_2), 2.19-2.09 (m, 6H; 1-Ad CH_2), 1.99 (br s, 6H; 1-Ad CH), 1.92-1.81 (m, 6H; 1-Ad CH_2), 1.66 (br s, 12H; 1-Ad CH_2). $^{13}C\{^1H\}$ NMR ($CDCl_3$): δ 170.0 (d, J_{CP} = 17.2 Hz; aryl C_{quat}), 151.4 (s; aryl CH), 145.5 (s; aryl CH) 135.8 (s; cin Ph C_{quat}), 129.5 (s; cin Ph CH), 128.5 (s; cin Ph CH), 127.7 (s; cin Ph CH), 122.6 (s; aryl CH), 119.9 (d, J_{CP} = 27.5 Hz; aryl C_{quat}), 118.2 (br s; alkenyl CH), 114.3 (br s; alkenyl CH), 63.3 (s; morph CH_2), 56.7 (s; morph CH_2), 42.5 (d, J_{CP} = 12.3 Hz; 1-Ad C_{quat}), 41.3 (s; 1-Ad CH_2), 37.4 (br s; Pd-CH_2), 28.5 (d, J_{CP} = 9.4 Hz; 1-Ad CH). $^{31}P\{^1H\}$ NMR ($CDCl_3$): δ 63.2.

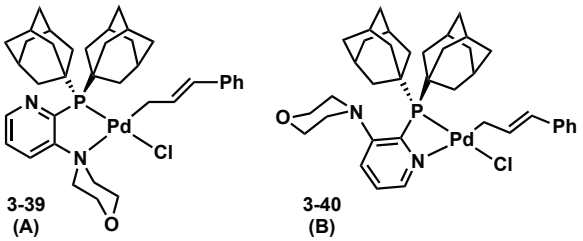

3-39 (A) /3-40 (B) *(to aid in the assignment of resonances, these compounds have been given a single letter label)*. Prepared by the treatment of a solution of $[Pd(cinnamyl)Cl]_2$ in CH_2Cl_2 with **3-25,** according to the representative procedure (*vide supra*), in 90% yield as an analytically pure yellow solid (140 mg, 0.19 mmol). The title compound was isolated as a mixture of isomers (*vide infra*) with a 2.3:1 ratio on the basis of ^1H and $^{31}P\{^1H\}$ NMR integrations. ^1H NMR ($CDCl_3$): δ 8.78 (d, J = 3.8 Hz, 1H; ArH_A), 8.40 (d, J = 4.0 Hz, 1H; ArH_B), 8.32 (m, 1H; ArH_A), 8.07 (d, J = 8.0 Hz, 1H; ArH_B), 7.58-7.52 (m, 2H; cin Ph_A), 7.51-7.46 (m, 1H; ArH_A), 7.43-7.36 (m, 2H; cin Ph_B), 7.35-7.19 (m, 6H; cin 3H Ph_A/3H Ph_B), 7.17-7.09 (m, 1H; ArH_B), 6.80 (m, 1H; alkenyl H_B), 6.72 (m, 1H; alkenyl H_A), 6.57 (m, 1H; alkenyl H_A), 6.35 (m, 1H; alkenyl H_B), 3.86-3.76 (m, 8H; 4H morph CH_{2A}/4H morph CH_{2B}), 3.65-3.38 (m, 6H; 4H morph CH_{2A}/2H Pd-CH_{2A}), 3.09 (d, J = 8.6 Hz, 2H; Pd-CH_{2B}), 3.01-2.93 (m, 4H; morph CH_{2B}), 2.50-2.38 (m, 12H; 6H 1-Ad CH_{2A}/6H 1-Ad CH_{2B}), 2.05-1.92 (m, 24H; 6 1-Ad CH_{2A}/6H 1-Ad CH_{2B}, 6H 1-Ad CH_A/6H 1-Ad CH_B), 1.77-1.,65 (12H 1-Ad CH_{2A}/12H 1-Ad CH_{2B}). $^{13}C\{^1H\}$ NMR ($CDCl_3$): δ 155.7 (s; aryl C_{quat}), 155.5 (s; aryl C_{quat}), 154.5 (s; aryl C_{quat}), 154.1 (s; aryl C_{quat}), 149.2 (d, J_{CP} = 8.5 Hz; aryl CH_A), 146.4 (d, J_{CP} = 12.7 Hz; aryl CH_B), 139.8 (s; cin Ph C_{quatB}), 138.3 (s; cin Ph C_{quatA}), 136.4 (s; aryl CH_B), 135.3 (s; alkenyl CH_B), 134.6 (d, J_{CP} = 6.4 Hz; aryl CH_A), 129.3 (s; cin Ph CH_A), 129.0 (s; cin Ph CH_B), 127.7 (s; cin Ph CH_B), 127.5 (s; cin Ph CH_B), 127.0 (s; cin Ph CH_A), 126.1 (s; aryl CH_B), 125.7 (s; cin Ph CH_A), 125.2 (s; aryl CH_A), 124.8 (s; alkenyl CH_A), 123.0 (d, J_{CP} = 11.0 Hz; alkenyl CH_A), 119.4 (m; alkenyl CH_B), 66.6 (s; morph CH_{2B}), 64.0 (s; morph CH_{2A}), 56.9 (s; morph CH_{2A}), 55.9 (s; morph CH_{2B}), 44.1 (d, J_{CP} = 13.4 Hz; 1-Ad C_{quatA}), 41.9 (m; 1-Ad C_{quatB}), 41.5 (s; 1-Ad CH_{2B}), 41.2 (s; 1-Ad CH_{2A}), 36.7 (s; 1-Ad CH_{2A}), 36.5 (s; 1-Ad CH_{2B}), 29.2 (d, J_{CP} = 9.3 Hz; 1-Ad CH_A), 28.9 (d, J_{CP} = 9.5 Hz; 1-Ad CH_B), 26.4 (s; Pd-CH_{2A}), 18.6 (s; Pd-$CH2_B$) .$^{31}P\{^1H\}$ NMR operating at 121.5 MHz (CD_2Cl_2): δ 68.7, 46.5.

3.5.4. GC Conversions and Isolated Yields For Screening Results in Section 3.4

Table 3.4 GC yield of cross-coupled products employing ligands **1-4** and **3-20**-**3-27**.

Reaction	**GC Yield of Cross-Coupled Product /%**								
	1-4	**3-20**	**3-21**	**3-23**	**3-22**	**3-24**	**3-25**	**3-26**	**3-27**
Chlorobenzene + Aniline[a]	100	10	98	93	86	100	100	84	100
Chlorobenzene + Octylamine[a]	100	0	100	100	98	100	100	88	100
Chlorobenzene + Morpholine[a]	88	0	76	79	56	100	96	61	51
Chlorobenzene + Indole[b]	52	1	35	43	51	15	4	18	6
Chlorobenzene + Ammonia *Aniline (Diphenylamine)* [c]	80(0)	0(0)	76(0)	77(0)	74(5)	61(10)	54(30)	66(0)	68(6)
Chlorobenzene + Acetone[d]	80	60	84	84	82	93	100	67	78
Chloro-*m*-xylene + Hydroxide[e]	0	0	0	0	0	0	0	0	0
2-Chlorotoluene + Methanol[f]	0	0	0	0	0	0	0	0	0

Reaction Conditions: All reactions conducted on 0.25 mmol scale employing $[Pd(cinnamyl)Cl]_2$ (1 mol%) and **3-20**-**3-27** (4 mol%); calibrated GC yield of cross-coupled product determined after 18 h. [a] Employing 1.2 equiv. amine, 1.4 equiv. NaO*t*Bu in toluene [ArCl] = 0.50 M, at 110 ^{o}C. [b] 1.0 equiv. indole, 1.4 equiv. NaO*t*Bu in toluene [ArCl] = 0.50 M, at 110 ^{o}C. [c] 3.0 equiv. ammonia, 2.0 equiv. NaO*t*Bu in 1,4-dioxane [ArCl] = 0.10 M at 90 ^{o}C. [d] excess (> 20 equiv.) acetone, 2.0 equiv. Cs_2CO_3 in toluene [ArCl] = 0.25 M, at 110 ^{o}C. [e] 3.0 equiv. $CsOH{\cdot}H_2O$ in THF [ArCl] = 0.50 M, at 65 ^{o}C. [f] 1.5 equiv. Cs_2CO_3 in MeOH:toluene (1:1) [ArCl] = 0.25 M, at 65 ^{o}C.

Table 3.5 GC consumption of aryl chloride in cross-coupling reactions employing ligands **1-4** and **3-20**-**3-27**.

Reaction	**GC Consumption of Aryl Chloride /%**								
	1-4	**3-20**	**3-21**	**3-23**	**3-22**	**3-24**	**3-25**	**3-26**	**3-27**
Chlorobenzene + Aniline	100	21	100	100	100	100	100	100	100
Chlorobenzene + Octylamine	100	10	100	100	100	100	100	100	100
Chlorobenzene + Morpholine	100	7	100	100	100	100	100	100	100
Chlorobenzene + Indole	56	10	42	55	64	26	27	58	23
Chlorobenzene + Ammonia	100	11	100	100	100	94	100	100	100
Chlorobenzene + Acetone	93	71	95	94	95	94	96	94	96
Chloro-*m*-xylene + Hydroxide	1	0	0	0	0	6	18	1	0
2-Chlorotoluene + Methanol	38	0	24	38	38	64	86	58	39

CHAPTER 4. CONCLUSIONS

4.1. CHAPTER 2: CONCLUSIONS AND FUTURE WORK

In Chapter 2 of this thesis, Stradiotto group protocols for the application of DalPhos ligands in the Pd-catalyzed cross-coupling of (hetero)aryl (pseudo)halides and N-H containing nucleophiles (Buchwald-Hartwig amination) were discussed. Considering the utility of Pd/Mor-DalPhos (**1-4**) catalysts for the monoarylation of challenging small-molecule substrates (e.g. ammonia, hydrazine, acetone),[94] this catalyst system was adopted in an effort to prepare a diverse array of functionalized *N*-aryl pyrazolones (including the free-radical scavenger Edaravone, *N*-aryl = Ph).[102] These compounds were identified via *in silico* screening, by Stradiotto group collaborators Dr. Mark Reed (Treventis Corporation) and Dr. Donald Weaver (Dalhousie), as a potent class of anti-aggregants for the inhibition of toxic Aβ oligomer formation associated with Alzheimer's Disease.

The synthesis of a small library of 25 structurally diverse Edaravone derivatives was accomplished by employing hydrazine monoarylation to form the requisite hydrazine intermediates, followed by condensation with ethylacetoacetate under acidic conditions. This modular synthetic approach afforded hydrazine synthons directly from (hetero)aryl (pseudo)halides and the convenient hydrazine monohydrate, allowing substitution at the *N*-aryl position to encompass fluoro, trifluoromethyl, methoxy, tolyl, napthhyl, pyridyl, amine, and ether groups. Following these diversification efforts, the library of compounds was subjected to screening in ThT kinetic aggregation and Biotin-Aβ Oligo assays. An analysis of the data collected revealed several compounds (**2-14** and **2-22**-**2-25**) that are high activity toward inhibiting the misfolding process proposed to be responsible for Alzheimer's Disease.

The development of highly active catalysts for hydrazine monoarylation could allow an expanded substrate scope, increasing the possibility of identifying compounds displaying greater activity. Notwithstanding the substrate scope described in Chapter 2, which expands on that initially reported,[97] the coupling of several classes of (hetero)aryl (pseudo)halides proved to be challenging (**2-26**-**2-55**). These compounds encompass thiophene, imidazole, pyrimidine and quinoline scaffolds, pendant NH-functionality,

ortho-substitution, and in some case strongly electron-poor, or –rich substitution. In an effort to accommodate the coupling of these challenging substrates, the development of increasingly robust catalyst systems capable of withstanding decomposition by the strongly reducing nature of hydrazine, with respect to unwanted hydrodehalogenation of the (hetero)aryl (pseudo)halide reagent, as well as formation of catalytically inactive palladium black, should be pursued. To this end, the strategic design of new DalPhos variants (discussed in Section 4.2) could increase the efficiency of this process both in terms of yield and substrate scope.

(Hetero)aryl mesylate substrates have been, to a limited extent, investigated for their use in BHA.[33b,65b] These coupling partners are easily prepared from commercially available phenols, and offer increased atom-economy relative to commonly employed tosylate and triflate sulfonates. Given the successful application of (hetero)aryl tosylates in this chemistry, extending our methodology to incorporate (hetero)aryl mesylate substrates would be advantageous. At this time, systems that promote the coupling of these substrates with less-challenging amines suffer from serious scope limitations (one report exploits primary anilines,[67a] another is limited to primary aryl amines and secondary amines[65a]); coupling with challenging small-molecule substrates such as ammonia and hydrazine, remains entirely unaddressed.[33b,65b]

4.2. CHAPTER 3: CONCLUSIONS AND FUTURE WORK

Several research groups have demonstrated the effect of strategic ancillary ligand design studies on furthering the development of highly active catalysts, particularly those ligated by tertiary monodentate/bidentate (bis)phosphines and N-heterocyclic carbenes variants that may modified sterically and electronically.[3a,24c,33c,35] To this end, mechanistic studies examining palladium-ligand interactions provide a means by which to assess ligand binding-mode and observed reactivity. The results discussed in Chapter 3 of this thesis covered the rational diversification of the Stradiotto group's successful DalPhos ligand (**1-4**). Considering that the success of **1-4** likely owes to a combination of a sterically encumbering, electron rich $P(1\text{-}Ad)_2$ moiety and a potentially hemilabile morpholino group capable of supporting low-coordinate catalytic intermediates, the ligand framework of **1-4** was structurally diversified without altering these positions (in

all but one case). The strategic modification at phosphorus and nitrogen is concurrently being explored by other Stradiotto group members.

Pd-Catalyzed C-N and P-C cross-coupling strategies previously found to be successful toward the preparation of DalPhos ligands were used to prepare eight new ligands from iodobromo(hetero)aryl starting materials. In several cases this synthetic procedure was not suitable, in which case nucleophilic aromatic substitution of deactivated (hetero)aryl fluoride or chloride substrates sufficed. The new ligand set features electron-withdrawing (fluoro, nitrile, nitro) and electron-donating (methoxy and methyl) group substitution on the phenylene-backbone, two structural isomers whereby the backbone of **1-4** has been replaced with pyridine, and a ligand with a thiomorpholino group; all prepared in good to excellent isolated yield (73-98%).

To gain a better understanding of the effect precatalyst formation imparts on catalyst performance, new DalPhos structural analogues were combined with [Pd(cinnamyl)Cl}$_2$ and their precatalyst mixtures isolated and characterized by means of 2D-solution NMR spectroscopy and X-ray crystallography. In most cases, a single [κ^2-*P,N*-Pd(η^1-cinnamyl)Cl] complex was observed in solution, with both η^1- and η^3-cinnamyl binding observed in the solid state. Future work could involve halide abstraction from these complexes in an effort to prepare complexes similar to **3-42**, in turn a comparison of metrical parameters to that of **3-42** could be performed to determine if any complexes bearing new ligand variants adopt a K^3-*P,N,O* binding mode under such circumstances. Notably, ligand **3-20** gave rise to a cationic κ^3-*P,N,S*-binding mode (as indicated by the solid-state structure), without forcing conditions.

Upon replacing the arene-backbone of **1-4** with pyridine, the pre-catalyst complex was found to display strikingly unique behavior in solution as indicated by ^{31}P NMR spectroscopic analysis. Saturation transfer experiments confirmed that the two species observed by ^{31}P NMR spectroscopy are in slow-exchange on the NMR time-scale. Given the Stradiotto group's recent examination of the coordination chemistry of **1-4**, and pre-catalyst mixtures for use in BHA, a comparison of structure and bonding between complexes bearing new ligand variants and complexes bearing **1-4**, were presented. Analysis of solid-state data revealed that substitution with electron-donating or withdrawing groups does not impart a significant impact on structure; no predictions

could be made regarding electronic perturbations, further studies were required. In the case of complexes **3-39** and **3-40**, it is believed that the pyridine backbone may bind to Pd through phosphorus as well as the lone-pair of the pyridine-nitrogen. An attempt to isolate single-crystals suitable for X-ray diffraction analysis may allow identification of these species. The growth of two isomers displaying unique binding modes may be possible considering that crystallization of both η^1- and η^3-cinnamyl complexes from the same Pd/**1-4** pre-catalyst mixture occurs, and these isomers are likely in equilibrium in solution. Furthermore, variable temperature NMR spectroscopy experiments may be explored in an effort to aid structural assignment.

Given that phenylene-backbone substitution imparts a minimal effect on pre-catalyst structure, where as incorporation of pyridine leads to unique binding characteristics, the synthesis of other P,N-heteroaryl-bridged ligands may be advantageous (thiophene, furan, pyrimidine or quinoline) and are currently being explored by our group. For example, the starting material 3-bromo-2-iodoquinoline could be exploited to afford a ligand similar to **3-38**; the extended ring system may also impart an effect on complex performance and stability. Ideally, new Dalphos variants will encompass the already broad substrate scope enabled by **1-4**, and extend the tolerated scope to include weakly acidic N-H substrates which currently pose a challenge (e.g., hydroxylamine, imidazole, indole, sulfonamides, etc).

The ability of **3-30** to promote the BHA of (hetero)aryl (pseudo)halides with ammonia at room temperature, not possible employing pre-catalyst mixtures featuring **3-31**/**3-32**, suggests that catalyst activation may be an inhibitory factor. The preparation of complexes of the type [(κ^2-*P,N*-(**3-20**-**3-27**)Pd(Ph)R] (R = Cl or NH_2) may not only allow for a structural/reactivity profile comparison to those bearing **1-4**, but also the identification of pre-catalysts that may afford milder conditions, broader substrate scope and improved functional group tolerance (Figures 4.1 and 4.2). With these putative catalytic intermediates in hand, exposure of the phenyl chloride oxidative addition pre-catalysts (Figure 4.1) to halide abstracting agents such as AgOTf, should provide complexes displaying similar or divergent behavior to [(κ^3-*P,N,O*-**1-24)**Pd(Ph)]OTf complex **3-41**. These complexes may subsequently be treated with ammonia in attempt to generate species similar to those depicted in Figure 4.2. Treatment of a cationic ammine

complex, bearing the ligand **1-4**, with $NaN(TMS)_2$ has been found to lead to pre-catalyst decomposition. New ligand variants may afford divergent reactivity, allowing preparation of the proposed amide complex (for further studies on the reductive elimination from such species). The unique behavior of pre-catalysts featuring ligands **3-20** and **3-25**, may also be better explained with these data in hand.

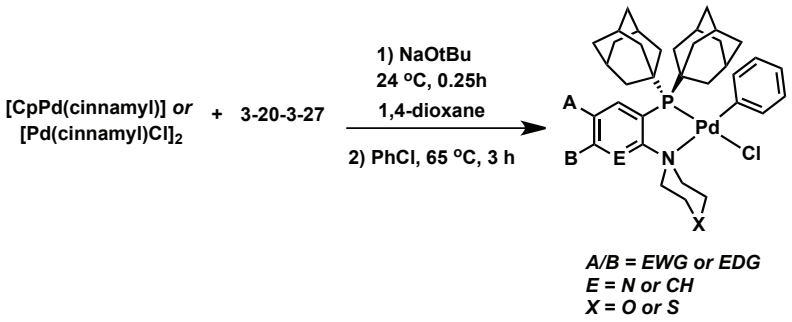

Figure 4.1 Preparation of phenyl chloride oxidative addition complexes bearing new DalPhos variants **3-20**-**3-27**; putative catalytic intermediates in the cycle for BHA.

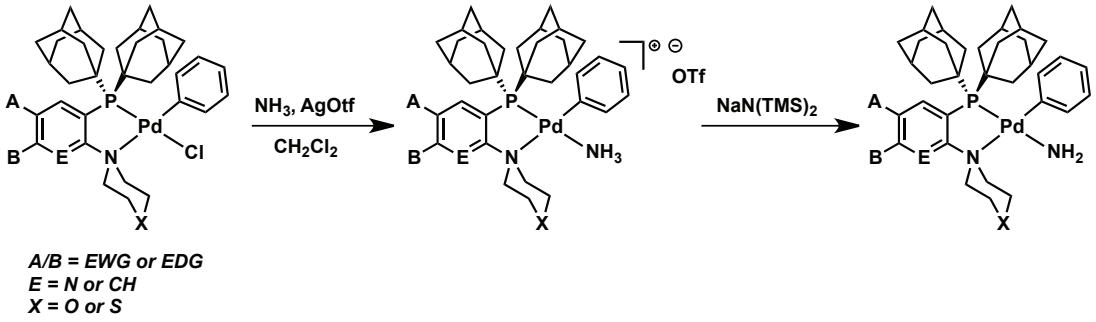

Figure 4.2 Exploring the reactivity of oxidative addition products under catalytically relevant conditions.

The screening of ligands **3-20**-**3-27** in challenging C-N, C-C, and C-O cross-coupling reactions has provided a preliminary look at the general efficiency of these ligands relative to **1-4**. It would be worthwhile to expand this set of C-X cross-coupling reactions where X = C, N, O, S, F, etc, to determine the span of their scope in Pd-catalyzed cross-coupling. Similarly, ligands that perform exceedingly well in particular reactions, should be followed up on; for example, ligands **3-24** and **3-25** which were highly efficient for the α-arylation of acetone. In order to determine if the success of these ligands extends to a variety of other carbonyl containing compounds, further testing must be performed. The limited reactivity of Pd/**3-20** catalysts in all reactions tested,

given the κ^3-*P,N,S* binding mode, was not overly surprising. This ligand highlights the extreme sensitivity of catalyst activity to changes at phosphorus and nitrogen and suggests that P(1-Ad)$_2$ and morpholino groups of **1-4** should be maintained while attempting to further optimize the electronic profile of these positions via backbone substitution. However, the Stradiotto group is concurrently working toward modification of these positions, along with their screening in the cross-coupling reactions disclosed in Chapter 3. Hypothetically, combining phosphorus, nitrogen and backbone fragments of ligands that independently display improved reactivity compared to **1-4**, may allow the preparation of a ligand that is capable of addressing a wide range of challenges (i.e., universality) not capable of being addressed by **1-4** alone.

APPENDIX I

Representative Spectra for Ligand 3-25:

^{1}H NMR spectrum of 3-25 ($CDCl_3$, 500.1 MHz, 300 K)

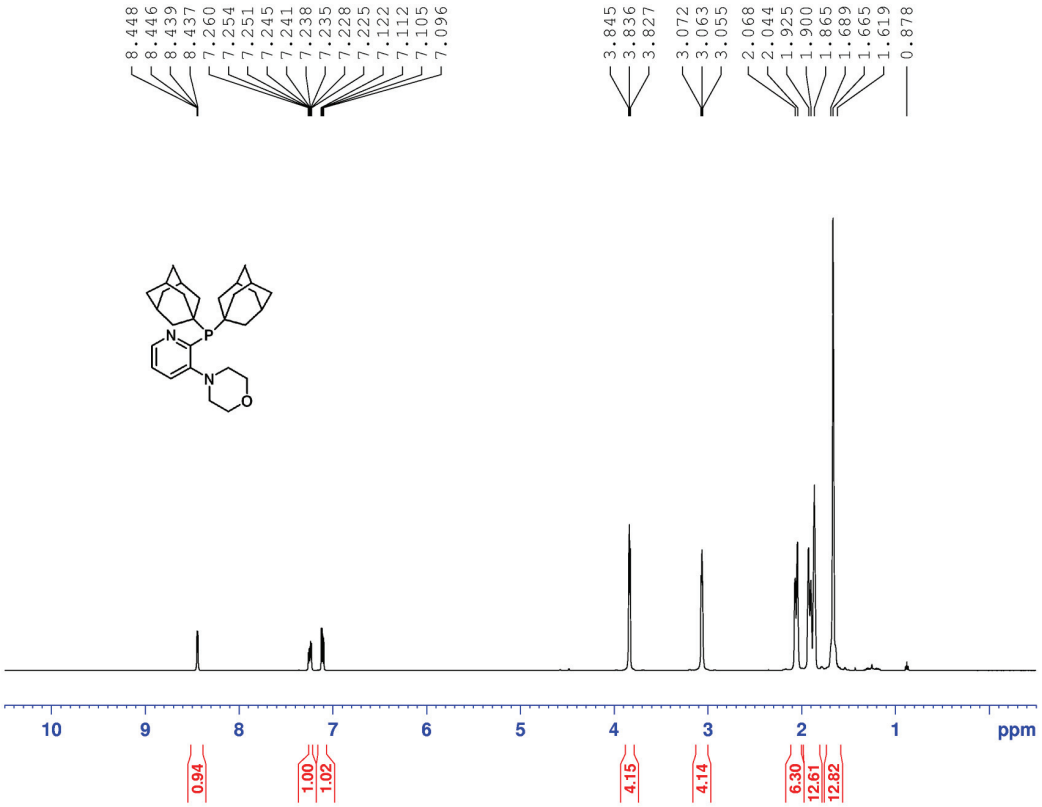

$^{13}C\{^{1}H\}$ spectrum of 3-25 ($CDCl_3$, 125.7 MHz, 300 K)

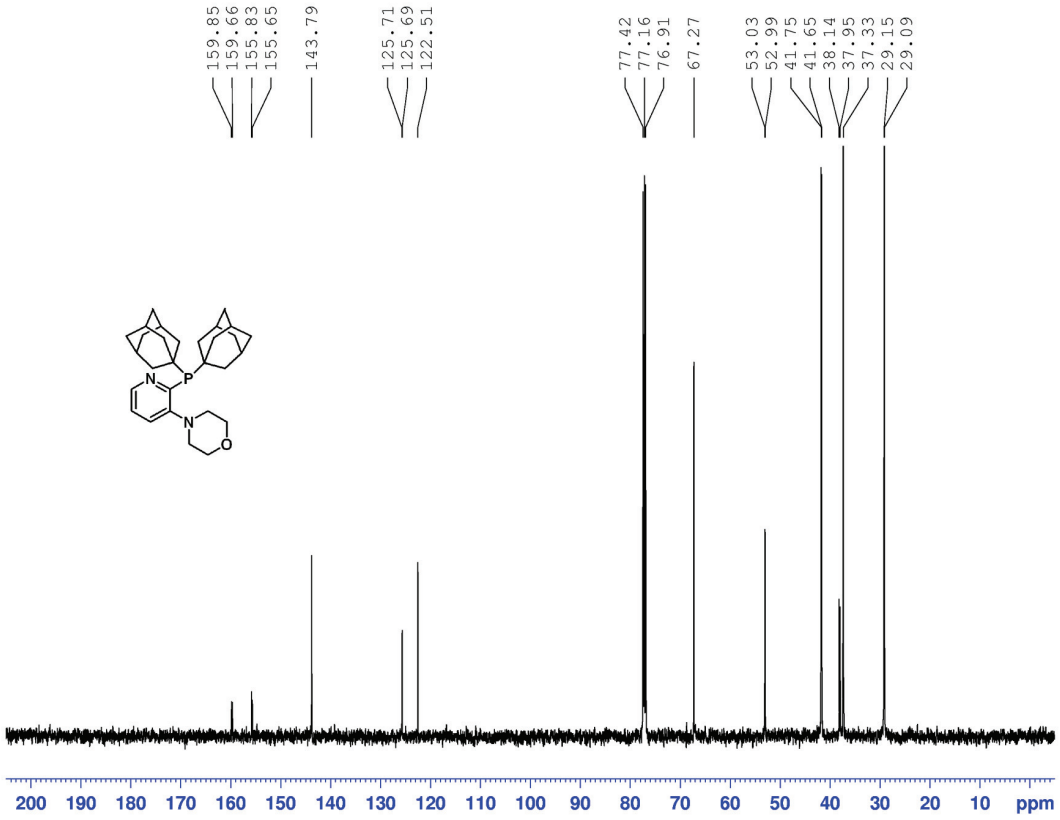

$^{31}P\{^{1}H\}$ NMR spectrum of 3-25 ($CDCl_3$, 121.5 MHz, 300 K)

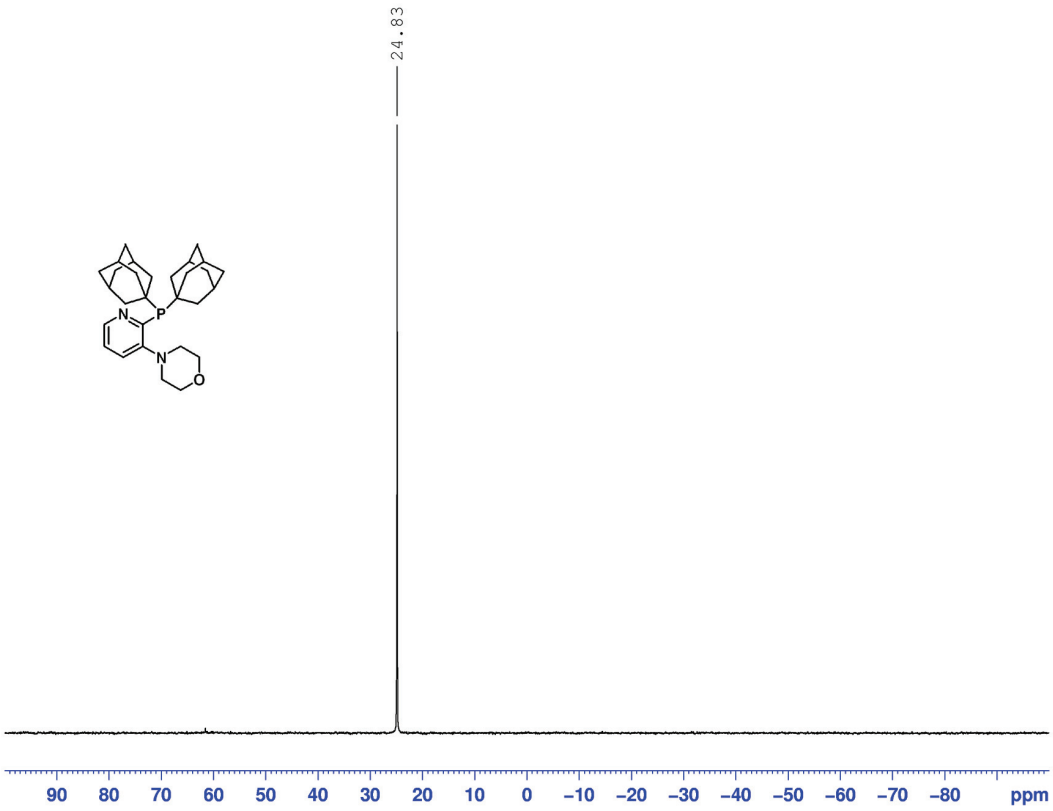

Representative Spectra for Complex 3-33:

^{1}H NMR spectrum of 3-33 ($CDCl_3$, 500.1 MHz, 300 K)

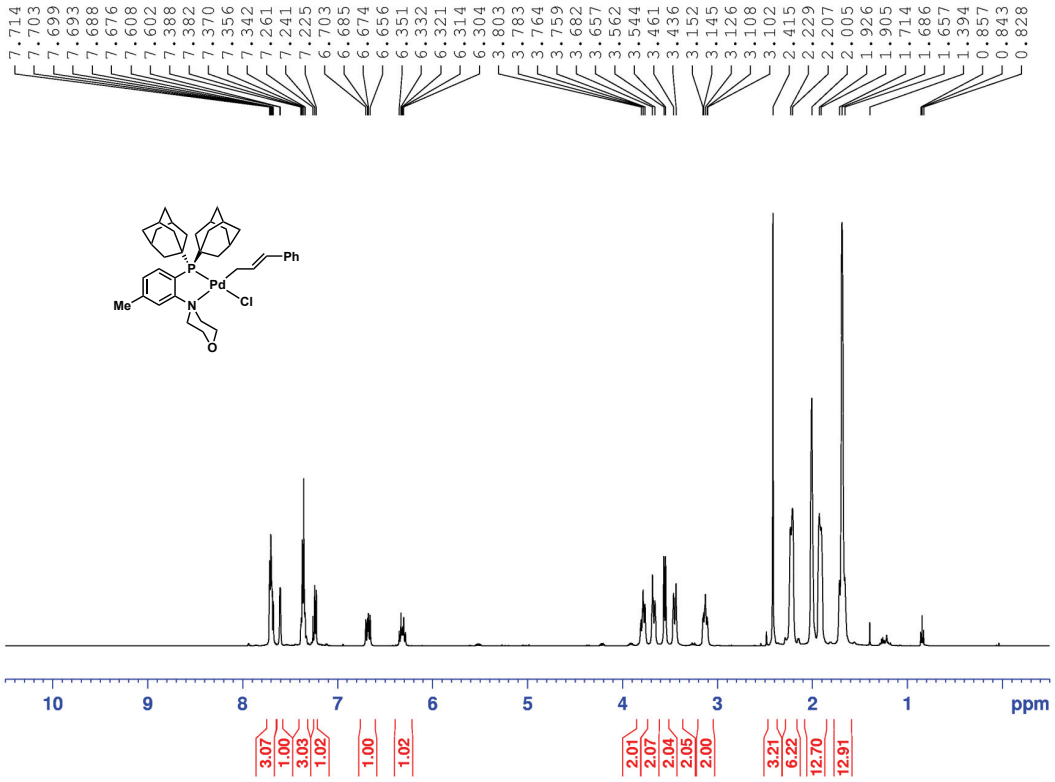

$^{13}C\{^{1}H\}$ spectrum of 3-33 ($CDCl_3$, 125.7 MHz, 300 K)

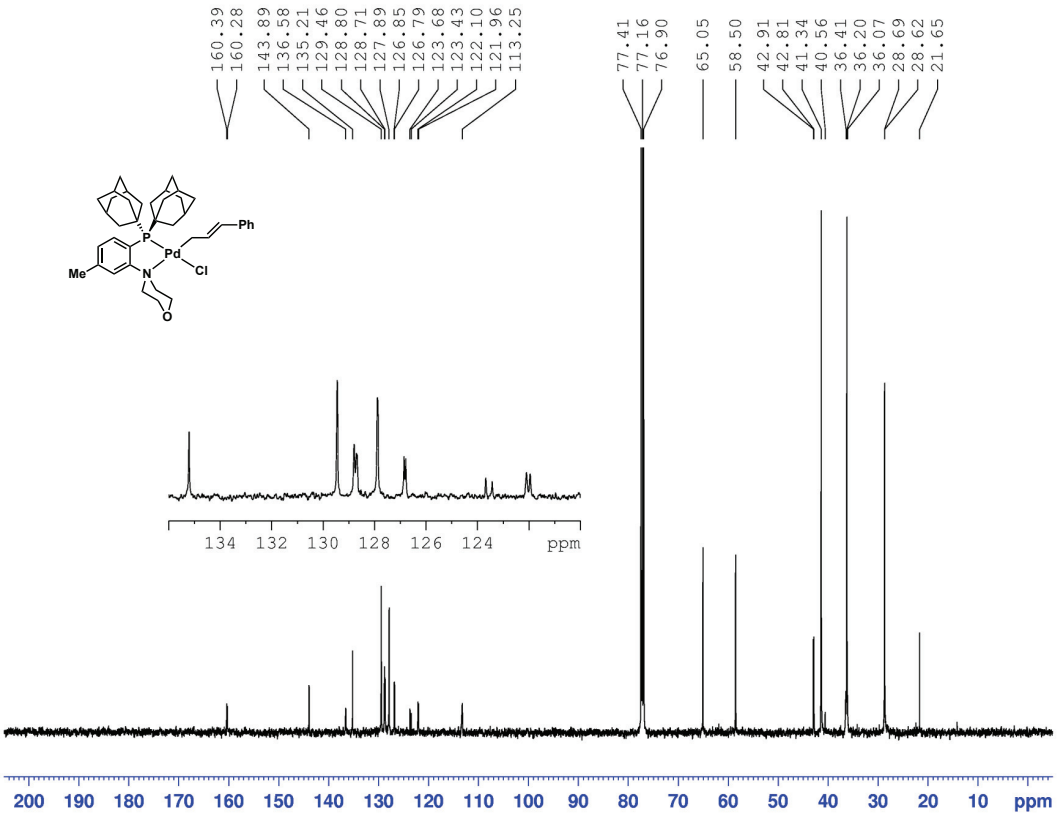

$^{31}P\{^{1}H\}$ NMR spectrum of 3-33 ($CDCl_3$, 121.5 MHz, 300 K)

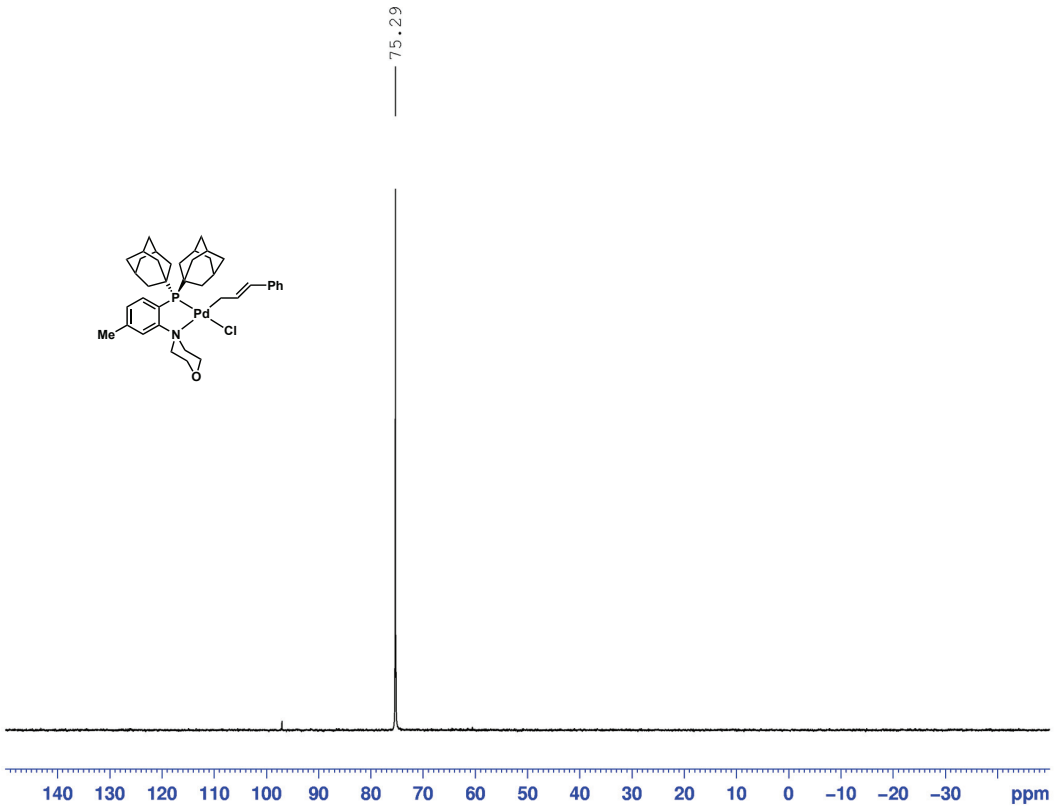

Chapter 3 Crystallographic Solution and Refinement Details

Crystallographic data were obtained at 173(2) K for **3-20**, **3-24**, **3-26**, **3-43·CH_2Cl_2**, **3-34**, and **3-35**, and at 296(2) K for **3-22** and **3-25**, on either a Bruker PLATFORM/SMART 1000 CCD diffractometer or a Bruker D8/APEX II CCD diffractometer using graphite-monochromated Mo K*a* (λ = 0.71073 Å) radiation. Unit cell parameters were determined and refined on all reflections. Data reduction and correction for Lorentz polarization were performed using Saint-plus,[127] and scaling and absorption correction were performed using the SADABS software package.[128] Structure solution by direct methods and least-squares refinement on F^2 were performed using the SHELXTL software suite.[129] Non-hydrogen atoms were refined with anisotropic displacement parameters, while hydrogen atoms were placed in calculated positions and refined with a riding model. Multi-scan absorption correction was employed in all cases.
In the case of **3-20**, non-merohedral twinning was found to exist in the crystal used for data collection, and therefore TWINABS was used to correct for absorption, and both components were indexed using CELL_NOW (Bruker AXS Inc., Madison, WI, 2004). The two domains are related by 179.8 degrees about the reciprocal axis [1.000 0.003 -0.001] and real axis [1.000 -0.003 0.027]. A single component HKLF 4 file was used for initial structure solution using direct methods, while integrated intensities from both components were written into an HKLF 5 file, which was used for solution refinement.

Compound **3-43** cocrystallized with one molecule of dichloromethane. Additionally, the cinnamyl group of **3-43** is disordered over two orientations which occupy nearly the same space; all but the metal-bound carbon (C31) and the para-carbon of the phenyl (C37) are modelled as a 59:41 positional disorder over two sites. The morpholine moiety of **3-35** exists in two conformations, which has been modelled as a 65:35 positional disorder of the oxygen atom and a neighbouring carbon atom over two sites, where the major component is the usual chair conformation. For **3-34**, significant voids filled with poorly ordered solvent exist in the lattice. These have been modelled using the SQUEEZE subroutine of the Platon software suite. The procedure extracted a total of 228 electrons from a volume of 618 $Å^3$, which may be attributed to three molecules of solvent (CH_2Cl_2 or diethyl ether) per asymmetric unit.

Crystal data and structure refinement details for 3-20, 3-22, and 3-24-3-26:

Compound	**3-20**	**3-22**	**3-24**	**3-25**	**3-26**
Empirical Formula	$C_{30}H_{42}NPS$	$C_{30}H_{41}FNOP$	$C_{29}H_{41}N_2OP$	$C_{29}H_{41}N_2OP$	$C_{32}H_{46}N_3O_3P$
Formula Weight	479.68	481.61	464.61	464.61	523.67
Temperature (K)	173(2)	296(2)	173(2)	296(2)	173(2)
Wavelength (Å)	0.71073	0.71073	0.71073	0.71073	0.71073
Crystal System	Monoclinic	Orthorhombic	Monoclinic	Orthorhombic	Triclinic
Space Group	P2(1)/n	P2(1)2(1)2(1)	P2(1)/c	P2(1)2(1)2(1)	P-1
a / Å	12.205(2)	7.9191(2)	9.9701(5)	7.9957(4)	10.4270(5)
b / Å	11.509(2)	15.0686(4)	16.9174(8)	14.9383(7)	11.0705(6)
c / Å	18.079(4)	21.0847(6)	15.3331(7)	20.8422(10)	12.8635(7)
α / °	90	90	90	90	96.2290(10)
β / °	92.59(3)	90	107.9710(10)	90	99.8300(10)
γ / °	90	90	90	90	109.9500(10)
V / $Å^3$	2537.0(9)	2516.03(12)	2460.0(2)	2489.4(2)	1352.79(12)
Z	4	4	4	4	2
ρ_{calc} / Mg m^{-3}	1.256	1.271	1.254	1.240	1.286
μ / mm^{-1}	0.210	0.141	0.137	0.135	0.137
Crystal Size / mm^3	0.53 x 0.44 x 0.23	0.34 x 0.23 x 0.11	0.43 x 0.39 x 0.27	0.40 x 0.12 x 0.07	0.53 x 0.19 x 0.13
Theta Range / °	1.97 to 26.45	1.66 to 27.52	2.78 to 26.37	1.68 to 27.51	1.63 to 26.41
Reflns. Collected	5212	47617	44130	22400	22533
Independent Reflns.	5212 [R(int) = 0.0000]	5805 [R(int) = 0.0367]	5040 [R(int) = 0.0348]	5729 [R(int) = 0.0481]	5532 [R(int) = 0.0335]
GOF on F^2	1.052	1.023	1.058	1.029	1.053
Final R indices [I > 2σ(I)] [a]	R_1 = 0.0458, wR_2 = 0.1101	R_1 = 0.0283, wR_2 = 0.0697	R_1 = 0.0497, wR_2 = 0.1236	R_1 = 0.0336, wR_2 = 0.0704	R_1 = 0.0379, wR_2 = 0.0920
R indices (all data) [a]	R_1 = 0.0624 wR_2 = 0.1187	R_1 = 0.0307, wR_2 = 0.0714	R_1 = 0.0577, wR_2 = 0.1303	R_1 = 0.0425 wR_2 = 0.0751	R_1 = 0.0469 wR_2 = 0.0981
Largest peak, hole (e$Å^{-3}$)	0.647 and -0.256	0.219 and -0.158	0.470 and -0.449	0.235 and -0.175	0.313 and -0.274
Absolute Structure Parameter	N/A	0.02(6)	N/A	-0.03(7)	N/A

[a] $R_1 = \Sigma| |F_o| - |F_c| |/\Sigma|F_o|$. $wR_2 = [\Sigma [w(F_o^2 - F_c^2)^2]/ \Sigma [w(F_o^2)^2]]^{1/2}$. $W = 1/[\sigma^2(F_o^2) + (mP)^2 + nP]$,

where $P = (F_o^2 + 2F_c^2)/3$.

Crystal data and structure refinement details for **3-34**, **3-35** and **3-43**:

Compound	**3-34**	**3-35**	**3-43**
Empirical Formula	$C_{40}H_{53}ClNOPPd$	$C_{39}H_{50}ClFNOPd$	$C_{40}H_{53}Cl_3NPPdS$
Formula Weight	736.65	740.62	823.61
Temperature (K)	173(2)	173(2)	173(2)
Wavelength (Å)	0.71073	0.71073	0.71073
Crystal System	Triclinic	Monoclinic	Monoclinic
Space Group	P-1	P2(1)/n	P2(1)/n
a / Å	10.0961(4)	10.3503(4)	18.6330(8)
b / Å	12.3233(5)	18.5899(8)	10.4416(4)
c / Å	18.9808(8)	17.4546(7)	19.3804(8)
α / °	75.1300(10)	90	90
β / °	87.3660(10)	96.5690(10)	100.1560(10)
γ / °	72.9320(10)	90	90
V / Å^3	2180.83(15)	3336.4(2)	3711.5(3)
Z	2	4	4
ρ_{calc} / Mg m^{-3}	1.122	1.474	1.474
μ / mm^{-1}	0.550	0.723	0.846
Crystal Size / mm^3	0.39 x 0.33 x 0.09	0.57 x 0.47 x 0.37	0.36 x 0.27 x 0.14
Theta Range / °	1.11 to 27.49°	1.61 to 27.52	1.40 to 27.50°
Reflns. Collected	19495	48071	32283
Independent Reflns.	9926 [R(int) = 0.0233]	7675 [R(int) = 0.0232]	8524 [R(int) = 0.0276]
GOF on F^2	1.085	1.022	1.084
Final R indices $[I > 2\sigma(I)]$ [a]	$R_1 = 0.0297$, $wR_2 = 0.0729$	$R_1 = 0.0220$, $wR_2 = 0.0573$	$R_1 = 0.0283$, $wR_2 = 0.0741$
R indices (all data) [a]	$R_1 = 0.0349$, $wR_2 = 0.0752$	$R_1 = 0.0241$, $wR_2 = 0.0585$	$R_1 = 0.0357$, $wR_2 = 0.0836$
Largest peak, hole (eÅ^{-3})	0.603 and -0.519	0.669 and -0.307	0.616 and -0.709

[a] $R_1 = \Sigma| |F_o| - |F_c| |/\Sigma|F_o|$. $wR_2 = [\Sigma [w(F_o^2 - F_c^2)^2]/ \Sigma [w(F_o^2)^2]]^{1/2}$. $w = 1/[\sigma^2(F_o^2) + (mP)^2 + nP]$, where $P = (F_o^2 + 2F_c^2)/3$.

References

(1) Hartwig, J. F. *Organotransition Metal Chemistry*; University Science Books: Sausalito, 2010.

(2) Shilov, A. E.; Shul'pin, G. B. *Chem. Rev.* **1997**, *97*, 2879.

(3) (a) Valente, C.; Calimsiz, S.; Hoi, K. H.; Mallik, D.; Sayah, M.; Organ, M. G. *Angew. Chem. Int. Ed.* **2012**, *51*, 3314. (b) Fortman, G. C.; Nolan, S. P. *Chem. Soc. Rev.* **2011**, *40*, 5151. (c) Wu, X.-F.; Anbarasan, P.; Neumann, H.; Beller, M. *Angew. Chem. Int. Ed.* **2010**, *49*, 9047.

(4) *Enzyme Catalysis in Organic Synthesis*; 3rd ed.; Wiley-VCH Verlag GmbH & Co. KGaA, 2012.

(5) (a) Anastas, P; Warner, J. *Green Chemistry: Theory and Practice*; Oxford University Press: Oxford, 1998. (b) Sheldon, R. A. *Chem. Soc. Rev.* **2012**, *41*, 1437.

(6) (a) Trost, B. *Science* **1991**, *254*, 1471. (b) Sheldon, R. A.; Arends, I. W. C. E.; Hanfeld, U. *Green Chemistry and Catalysis*; Wiley-VCH Verlag GmbH & Co. KGaA: Weinheim, 2007.

(7) Dunn, P. J. *Chem. Soc. Rev.* **2012**, *41*, 1452.

(8) Walsh, P. J.; Kozlowski, M. C. *Fundamentals of Asymmetric Catalysis*; University Science Books, 2009.

(9) (a) Knowles, W. S. *Angew. Chem. Int. Ed.* **2002**, *41*, 1998. (b) Knowles, W. S. *Acc. Chem. Res.* **1983**, *16*, 106.

(10) (a) Miyashita, A.; Yasuda, A.; Takaya, H.; Toriumi, K.; Ito, T.; Souchi, T.; Noyori, R. *J. Am. Chem. Soc.* **1980**, *102*, 7932. (b) Noyori, R. *Angew. Chem. Int. Ed.* **2002**, *41*, 2008.

(11) (a) Chauvin, Y. *Angew. Chem. Int. Ed.* **2006**, *45*, 3740. (b) Schrock, R. R. *Angew. Chem. Int. Ed.* **2006**, *45*, 3748. (c) Grubbs, R. H. *Angew. Chem. Int. Ed.* **2006**, *45*, 3760.

(12) (a) Calderon, N. *Acc. Chem. Res.* **1972**, *5*, 127. (b) Grubbs, R. H. *Tetrahedron* **2004**, *60*, 7117.

(13) Ivin, K. J.; Mol, J. C. *Olefin Metathesis and Metathesis Polymerization*; Academic Press: New York, 1997.

(14) Weissermel, K.; Arpe, H. J. *Industrial Organic Chemistry*; 3rd ed.; Wiley-VCH GmbH: Weinheim, 1997.

(15) Truett, W. L.; Johnson, D. R.; Robinson, I. M.; Montague, B. A. *J. Am. Chem. Soc.* **1960**, *82*, 2337.

(16) Banks, R. L.; Bailey, G. C. *Ind. Eng. Chem. Prod. Res. Dev.* **1964**, *3*, 170.

(17) Calderon, N.; Chen, H. Y.; Scott, K. W. *Tetrahedron Lett.* **1967**, *8*, 3327.

(18) Schrock, R.; Rocklage, S.; Wengrovius, J.; Rupprecht, G.; Fellmann, J. *J. Mol. Catal.* **1980**, *8*, 73.

(19) Grubbs, R. H.; Carr, D. D.; Hoppin, C.; Burk, P. L. *J. Am. Chem. Soc.* **1976**, *98*, 3478.

(20) (a) Sanford, M. S.; Ulman, M.; Grubbs, R. H. *J. Am. Chem. Soc.* **2001**, *123*, 749. (b) Sanford, M. S.; Love, J. A.; Grubbs, R. H. *J. Am. Chem. Soc.* **2001**, *123*, 6543.

(21) Astruc, D. *New J. Chem.* **2005**, *29*, 42.

(22) (a) Grubbs, R. H. *Handbook of Metathesis: Applications in Organic Synthesis*; Wiley-VCH: Weinheim, 2003. (b) Rosebrugh, L. E.; Herbert, M. B.; Marx, V. M.; Keitz, B. K.; Grubbs, R. H. *J. Am. Chem. Soc.* **2013**, *135*, 1276. (c) Occhipinti, G.; Hansen, F. R.; Törnroos, K. W.; Jensen, V. R. *J. Am. Chem. Soc.* **2013**, *135*, 3331.

(23) *Special-issue on Cross-Coupling*: Buchwald, S. L. *Acc. Chem. Res.* **2008**, *41*, 1439.

(24) (a) Diederich, F.; Stang, P. *Metal-catalyzed Cross-coupling Reactions*; Wiley-VCH: Weinheim, **2008**. (b) Miyaura, N.; Suzuki, A. *Chem. Rev.* **1995**, *95*, 2457. (c) Fleckenstein, C. A.; Plenio, H. *Chem. Soc. Rev.* **2010**, *39*, 694. (d) Beletskaya, I. P.; Cheprakov, A. V. *Organometallics* **2012**, *31*, 7753. (e) Fu, G. C. *Acc. Chem. Res.* **2008**, *41*, 1555. (f) Torborg, C.; Beller, M. *Adv. Synth. Catal.* **2009**, *351*, 3027. (g) Littke, A. F.; Fu, G. C. *Angew. Chem. Int. Ed.* **2002**, *41*, 4176.

(25) Nicolaou, K. C.; Bulger, P. G.; Sarlah, D. *Angew. Chem. Int. Ed.* **2005**, *44*, 4442.

(26) (a) Heck, R. F. *J. Org. Chem.* **1972**, *37*, 2320. (b) Heck, R. F. *J. Am. Chem. Soc.* **1968**, *90*, 5518.

(27) C. Nicolaou, K.; M. Ramanjulu, J.; Natarajan, S.; Brase, S.; Rubsam, F. *Chem. Commun.* **1997**, 1899.

(28) Klinkenberg, J. L.; Hartwig, J. F. *Angew. Chem. Int. Ed.* **2011**, *50*, 86.

(29) Kürti, L.; Czakó, B. *Strategic Applications of Named Reactions in Organic Synthesis*; Elsevier Academic Press: Burlington, MA, USA, 2005.

(30) Cornils, B.; Herrmann, W. A. *Applied Homogeneous Catalysis with Organometallic Compounds: A Comprehensive Handbook in Three Volumes*; Wiley-VCH Verlag GmbH: Weinheim, 2002.

(31) (a) Negishi, E.; de Meijere, A. *Handbook of Organopalladium Chemistry for Organic Synthesis: Volume 1 and 2*; Wiley, 2003. (b) Tasler, S.; Mies, J.; Lang, M. *Adv. Synth. Catal.* **2007**, *349*, 2286. (c) Cooper, T. W. J.; Campbell, I. B.; Macdonald, S. J. F. *Angew. Chem. Int. Ed.* **2010**, *49*, 8082.

(32) Surry, D. S.; Buchwald, S. L. *Chem. Sci.* **2011**, *2*, 27.

(33) (a) Lundgren, R. J.; Stradiotto, M. *Chem. Eur. J.* **2012**, *18*, 9758. (b) Lundgren, R. J.; Stradiotto, M. *Aldrichimica Acta* **2012**, *45*, 59. (c) Surry, D. S.; Buchwald, S. L. *Angew. Chem. Int. Ed.* **2008**, *47*, 6338. (d) Jiang, L.; Buchwald, S. L. In *Metal-Catalyzed Cross-Coupling Reactions*; Wiley-VCH Verlag GmbH: Weinheim, 2008.

(34) (a) Shelby, Q.; Kataoka, N.; Mann, G.; Hartwig, J. *J. Am. Chem. Soc.* **2000**, *122*, 10718. (b) Anderson, K. W.; Ikawa, T.; Tundel, R. E.; Buchwald, S. L. *J. Am. Chem. Soc.* **2006**, *128*, 10694. (c) Sergeev, A. G.; Schulz, T.; Torborg, C.; Spannenberg, A.; Neumann, H.; Beller, M. *Angew. Chem. Int. Ed.* **2009**, *48*, 7595. (d) Schulz, T.; Torborg, C.; Schäffner, B.; Huang, J.; Zapf, A.; Kadyrov, R.; Börner, A.; Beller, M. *Angew. Chem. Int. Ed.* **2009**, *48*, 918. (e) Chen, G.; Chan, A. S. C.; Kwong, F. Y. *Tetrahedron Lett.* **2007**, *48*, 473. (f) Monnier, F.; Taillefer, M. *Angew. Chem. Int. Ed.* **2008**, *47*, 3096.

(35) Hartwig, J. F. *Acc. Chem. Res.* **2008**, *41*, 1534.

(36) (a) Watson, D. A.; Su, M.; Teverovskiy, G.; Zhang, Y.; Garcia-Fortanet, J.; Kinzel, T.; Buchwald, S. L. *Science* **2009**, *325*, 1661. (b) Jin, Z.; Hammond, G. B.; Xu, B. *Aldrichimica Acta* **2012**, *45*, 67.

(37) (a) Fürstner, A. *Angew. Chem. Int. Ed.* **2009**, *48*, 1364. (b) Correa, A.; Garcia Mancheno, O.; Bolm, C. *Chem. Soc. Rev.* **2008**, *37*, 1108. (c) Sherry, B. D.; Fürstner, A. *Acc. Chem. Res.* **2008**, *41*, 1500.

(38) (a) Creutz, S. E.; Lotito, K. J.; Fu, G. C.; Peters, J. C. *Science* **2012**, *338*, 647. (b) Xia, N.; Taillefer, M. *Angew. Chem. Int. Ed.* **2009**, *48*, 337. (c) Monnier, F.; Taillefer, M. *Angew. Chem. Int. Ed.* **2009**, *48*, 6954. (d) Klapars, A.; Antilla, J. C.; Huang, X.; Buchwald, S. L. *J. Am. Chem. Soc.* **2001**, *123*, 7727.

(39) (a) Ikeda, S.-i. *Acc. Chem. Res.* **2000**, *33*, 511. (b) Montgomery, J. *Acc. Chem. Res.* **2000**, *33*, 467.

(40) Ullmann, F. *Ber. Dtsch. Chem. Ges.* **1903**, *36*, 2389.

(41) Goldberg, I. *Ber. Dtsch. Chem. Ges.* **1906**, *39*, 1691.

(42) Huffman, L. M.; Stahl, S. S. *J. Am. Chem. Soc.* **2008**, *130*, 9196.

(43) (a) Ley, S. V.; Thomas, A. W. *Angew. Chem. Int. Ed.* **2003**, *42*, 5400. (b) Hickman, A. J.; Sanford, M. S. *Nature* **2012**, ***484***, 177. (c) Yoshikai, N.; Nakamura, E. *Chem. Rev.* **2011**, *112*, 2339.

(44) Yao, B.; Wang, D.-X.; Huang, Z.-T.; Wang, M.-X. *Chem. Commun.* **2009**, 2899.

(45) (a) Chan, D. M. T.; Monaco, K. L.; Wang, R.-P.; Winters, M. P. *Tetrahedron Lett.* **1998**, *39*, 2933. (b) Evans, D. A.; Katz, J. L.; West, T. R. *Tetrahedron Lett.* **1998**, *39*, 2937. (c) Lam, P. Y. S.; Clark, C. G.; Saubern, S.; Adams, J.; Winters, M. P.; Chan, D. M. T.; Combs, A. *Tetrahedron Lett.* **1998**, *39*, 2941.

(46) Giri, R.; Hartwig, J. F. *J. Am. Chem. Soc.* **2010**, *132*, 15860.

(47) (a) Buchwald, S. L.; Mauger, C.; Mignani, G.; Scholz, U. *Adv. Synth. Catal.* **2006**, *348*, 23. (b) Blaser, H.-U.; Indolese, A.; Naud, F.; Nettekoven, U.; Schnyder, A. *Adv. Synth. Catal.* **2004**, *346*, 1583.

(48) Milstein, D.; Stille, J. K. *J. Am. Chem. Soc.* **1978**, *100*, 3636.

(49) Kosugi, M.; Kameyama, M.; Migita, T. *Chem. Lett.* **1983**, *12*, 927.

(50) Guram, A. S.; Buchwald, S. L. *J. Am. Chem. Soc.* **1994**, *116*, 7901.

(51) Paul, F.; Patt, J.; Hartwig, J. F. *J. Am. Chem. Soc.* **1994**, *116*, 5969.

(52) Guram, A. S.; Rennels, R. A.; Buchwald, S. L. *Angew. Chem. Int. Ed. Engl.* **1995**, *34*, 1348.

(53) Louie, J.; Hartwig, J. F. *Tetrahedron Lett.* **1995**, *36*, 3609.

(54) Louie, J.; Hartwig, J. F. *J. Am. Chem. Soc.* **1995**, *117*, 11598.

(55) Alcazar-Roman, L. M.; Hartwig, J. F. *Organometallics* **2002**, *21*, 491.

(56) Barrios-Landeros, F.; Carrow, B. P.; Hartwig, J. F. *J. Am. Chem. Soc.* **2009**, *131*, 8141.

(57) (a) Driver, M. S.; Hartwig, J. F. *J. Am. Chem. Soc.* **1997**, *119*, 8232. (b) Hartwig, J. F. *Inorg. Chem.* **2007**, *46*, 1936.

(58) (a) Shekhar, S.; Ryberg, P.; Hartwig, J. F. *Org. Lett.* **2006**, *8*, 851. (b) Shekhar, S.; Ryberg, P.; Hartwig, J. F.; Mathew, J. S.; Blackmond, D. G.; Strieter, E. R.; Buchwald, S. L. *J. Am. Chem. Soc.* **2006**, *128*, 3584.

(59) Wolfe, J. P.; Buchwald, S. L. *J. Org. Chem.* **1996**, *61*, 1133.

(60) (a) Wolfe, J. P.; Buchwald, S. L. *J. Org. Chem.* **1997**, *62*, 6066. (b) Widenhoefer, R. A.; Buchwald, S. L. *Organometallics* **1996**, *15*, 2755. (c) Louie, J.; Driver, M. S.; Hamann, B. C.; Hartwig, J. F. *J. Org. Chem.* **1997**, *62*, 1268. (d) Fors, B. P.; Davis, N. R.; Buchwald, S. L. *J. Am. Chem. Soc.* **2009**, *131*, 5766.

(61) Hamann, B. C.; Hartwig, J. F. *J. Am. Chem. Soc.* **1998**, *120*, 7369.

(62) Schlummer, B.; Scholz, U. *Adv. Synth. Catal.* **2004**, *346*, 1599.

(63) Wolfe, J. P.; Wagaw, S.; Marcoux, J.-F.; Buchwald, S. L. *Acc. Chem. Res* **1998**, *31*, 805.

(64) Ogata, T.; Hartwig, J. F. *J. Am. Chem. Soc.* **2008**, *130*, 13848.

(65) (a) So, C. M.; Zhou, Z.; Lau, C. P.; Kwong, F. Y. *Angew. Chem. Int. Ed.* **2008**, *47*, 6402. (b) So, C. M.; Kwong, F. Y. *Chem. Soc. Rev.* **2011**, *40*, 4963.

(66) Harris, M. C.; Huang, X.; Buchwald, S. L. *Org. Lett.* **2002**, *4*, 2885.

(67) (a) Fors, B. P.; Watson, D. A.; Biscoe, M. R.; Buchwald, S. L. *J. Am. Chem. Soc.* **2008**, *130*, 13552. (b) Biscoe, M. R.; Fors, B. P.; Buchwald, S. L. *J. Am. Chem. Soc.* **2008**, *130*, 6686. (c) Fors, B. P.; Krattiger, P.; Strieter, E.; Buchwald, S. L. *Org. Lett.* **2008**, *10*, 3505.

(68) (a) Anderson, K. W.; Tundel, R. E.; Ikawa, T.; Altman, R. A.; Buchwald, S. L. *Angew. Chem. Int. Ed.* **2006**, *45*, 6523. (b) Shen, Q.; Shekhar, S.; Stambuli, J. P.; Hartwig, J. F. *Angew. Chem. Int. Ed.* **2005**, *44*, 1371.

(69) (a) Shen, Q.; Hartwig, J. F. *J. Am. Chem. Soc.* **2006**, *128*, 10028. (b) Schulz, T.; Torborg, C.; Enthaler, S.; Schäffner, B.; Dumrath, A.; Spannenberg, A.; Neumann, H.; Börner, A.; Beller, M. *Chem. Eur. J.* **2009**, *15*, 4528. (c) Surry, D. S.; Buchwald, S. L. *J. Am. Chem. Soc.* **2007**, *129*, 10354. (d) Vo, G. D.; Hartwig, J. F. *J . Am. Chem. Soc.* **2009**, *131*, 11049.

(70) (a) Nishiyama, M.; Yamamoto, T.; Koie, Y. *Tetrahedron Lett.* **1998**, *39*, 617. (b) Yamamoto, T.; Nishiyama, M.; Koie, Y. *Tetrahedron Lett.* **1998**, *39*, 2367. (c) Hartwig, J. F.; Kawatsura, M.; Hauck, S. I.; Shaughnessy, K. H.; Alcazar-Roman, L. M. *J. Org. Chem.* **1999**, *64*, 5575. (d) Hill, L. L.; Moore, L. R.; Huang, R.; Craciun, R.; Vincent, A. J.; Dixon, D. A.; Chou, J.; Woltermann, C. J.; Shaughnessy, K. H. *J. Org. Chem.* **2006**, *71*, 5117. (e) Tewari, A.; Hein, M.; Zapf, A.; Beller, M. *Tetrahedron* **2005**, *61*, 9705. (f) Netherton, M. R.; Fu, G. C. *Org. Lett.* **2001**, *3*, 4295. (g) Kataoka, N.; Shelby, Q.; Stambuli, J. P.; Hartwig, J. F. *J. Org. Chem.* **2002**, *67*, 5553.

(71) (a) Shen, Q.; Ogata, T.; Hartwig, J. F. *J. Am. Chem. Soc.* **2008**, *130*, 6586. (b) Shen, Q.; Hartwig, J. F. *Org. Lett.* **2008**, *10*, 4109.

(72) (a) Reddy, C. V.; Kingston, J. V.; Verkade, J. G. *J. Org. Chem.* **2008**, *73*, 3047. (b) Singer, R. A.; Doré, M.; Sieser, J. E.; Berliner, M. A. *Tetrahedron Lett.* **2006**, *47*, 3727. (c) Rataboul, F.; Zapf, A.; Jackstell, R.; Harkal, S.; Riermeier, T.; Monsees, A.; Dingerdissen, U.; Beller, M. *Chem. Eur. J.* **2004**, *10*, 2983. (d) Harkal, S.; Rataboul, F.; Zapf, A.; Fuhrmann, C.; Riermeier, T.; Monsees, A.; Beller, M. *Adv. Synth. Catal.* **2004**, *346*, 1742. (e) Ackermann, L.; Born, R. *Angew. Chem. Int. Ed.* **2005**, *44*, 2444. (f) Chung, K. H.; So, C. M.; Wong, S. M.; Luk, C. H.; Zhou, Z.; Lau, C. P.; Kwong, F. Y. *Synlett* **2012**, *23*, 1181. (g) Wong, S. M.; So, C. M.; Chung, K. H.; Lau, C. P.; Kwong, F. Y. *Eur. J. Org. Chem.* **2012**, *2012*, 4172. (h) Kwong, F. Y.; Chan, A. S. C. *Synlett* **2008**, *2008*, 1440. (i) Lavery, C. B.; McDonald, R.; Stradiotto, M. *Chem. Commun.* **2012**, *48*, 7277.

(73) Huser, M.; Youinou, M.-T.; Osborn, J. A. *Angew. Chem. Int. Ed. Engl.* **1989**, *28*, 1386.

(74) Ehrentraut, A.; Zapf, A.; Beller, M. *J. Mol. Catal. A: Chem.* **2002**, *182,* 515.

(75) Zapf, A.; Beller, M. *Chem. Commun.* **2005**, 431.

(76) Dumrath, A.; Lübbe, C.; Neumann, H.; Jackstell, R.; Beller, M. *Chem. Eur. J.* **2011**, *17*, 9599.

(77) Huang, X.; Anderson, K. W.; Zim, D.; Jiang, L.; Klapars, A.; Buchwald, S. L. *J. Am. Chem. Soc.* **2003**, *125*, 6653.

(78) Charles, M. D.; Schultz, P.; Buchwald, S. L. *Org. Lett.* **2005**, *7*, 3965.

(79) Dooleweerdt, K.; Fors, B. P.; Buchwald, S. L. *Org. Lett.* **2010**, *12*, 2350.

(80) (a) Herrmann, W. A.; Elison, M.; Fischer, J.; Köcher, C.; Artus, G. R. J. *Chem. Eur. J* **1996**, *2*, 772. (b) Herrmann, W. A.; Elison, M.; Fischer, J.; Köcher, C.; Artus, G. R. J. *Angew. Chem. Int. Ed. Eng.* **1995**, *34*, 2371.

(81) Organ, M. G.; Abdel-Hadi, M.; Avola, S.; Dubovyk, I.; Hadei, N.; Kantchev, E. A. B.; O'Brien, C. J.; Sayah, M.; Valente, C. *Chem. Eur. J.* **2008**, *14*, 2443.

(82) Driver, M. S.; Hartwig, J. F. *J. Am. Chem. Soc.* **1996**, *118*, 7217.

(83) Wolfe, J. P.; Wagaw, S.; Buchwald, S. L. *J . Am. Chem. Soc.* **1996**, *118*, 7215.

(84) Marcoux, J.-F.; Wagaw, S.; Buchwald, S. L. *J. Org. Chem.* **1997**, *62*, 1568.

(85) Birkholz, M.-N.; Freixa, Z.; van Leeuwen, P. W. N. M. *Chem. Soc. Rev.* **2009**, *38*, 1099.

(86) Sadighi, J. P.; Harris, M. C.; Buchwald, S. L. *Tetrahedron Lett.* **1998**, *39*, 5327.

(87) Guari, Y.; van Strijdonck, G. P. F.; Boele, M. D. K.; Reek, J. N. H.; Kamer, P. C. J.; van Leeuwen, P. W. N. M. *Chem. Eur. J.* **2001**, *7*, 475.

(88) Blaser, H.-U.; Brieden, W.; Pugin, B.; Spindler, F.; Studer, M.; Togni, A. *Top. Catal.* **2002**, *19*, 3.

(89) Lundgren, R. J.; Sappong-Kumankumah, A.; Stradiotto, M. *Chem. Eur. J.* **2010**, *16*, 1983.

(90) Aubin, Y.; Fischmeister, C.; Thomas, C. M.; Renaud, J.-L. *Chem. Soc. Rev.* **2010**, *39*, 4130.

(91) Klinkenberg, J. L.; Hartwig, J. F. *J. Am. Chem. Soc.* **2010**, *132*, 11830.

(92) Tsvelikhovsky, D.; Buchwald, S. L. *J. Am. Chem. Soc.* **2011**, *133*, 14228.

(93) Lundgren, R. J.; Peters, B. D.; Alsabeh, P. G.; Stradiotto, M. *Angew. Chem. Int. Ed.* **2010**, *49*, 4071.

(94) Lundgren, R. J.; Hesp, K. D.; Stradiotto, M. *Synlett* **2011**, 2443.

(95) Robinson, B. *Chem. Rev.* **1963**, *63*, 373.

(96) (a) Cellier, P. P.; Spindler, J.-F.; Taillefer, M.; Cristau, H.-J. *Tetrahedron Lett.* **2003**, *44*, 7191. (b) Lee, K.-S.; Lim, Y.-K.; Cho, C.-G. *Tetrahedron Lett.* **2002**, *43*, 7463. (c) Ellames, G. J.; Gibson, J. S.; Herbert, J. M.; McNeill, A. H. *Tetrahedron* **2001**, *57*, 9487. (d) Alonso, F.; Radivoy, G.; Yus, M. *Tetrahedron* **2000**, *56*, 8673.

(97) Lundgren, R. J.; Stradiotto, M. *Angew. Chem. Int. Ed.* **2010**, *49*, 8686.

(98) Goedert, M.; Spillantini, M. G. *Science* **2006**, *314*, 777.

(99) (a) Hamley, I. W. *Chem. Rev.* **2012**, *112*, 5147. (b) Kepp, K. P. *Chem. Rev.* **2012**, *112*, 5193.

(100) Hardy, J.; Selkoe, D. J. *Science* **2002**, *297*, 353.

(101) Dr. Donald Weaver and Dr. Mark Reed, Halifax, Nova Scotia.

(102) Yoshida, H.; Yanai, H.; Namiki, Y.; Fukatsu-Sasaki, K.; Furutani, N.; Tada, N. *CNS Drug Rev.* **2006**, *12*, 9.

(103) (a) Markesbery, W. R. *Free Radical Biol. Med.* **1997**, *23*, 134. (b) Yan, Y. F.; Gong, K.; Ma, T.; Zhang, L. H.; Zhao, N. M.; Zhang, X. F.; Tang, P. F.; Gong, Y. D. *Neurosci. Lett.* **2012**, *531*, 160.

(104) Allen, C. F. H. *Org. Synth.* **1943**, *2*, 228.

(105) Coleman, G. H. *Org. Synth.* **1941**, *1*, 442.

(106) Nakagawa, H.; Ohyama, R.; Kimata, A.; Suzuki, T.; Miyata, N. *Bioorg. Med. Chem. Lett.* **2006**, *16*, 5939.

(107) Huang, Y.-Y.; Lin, H.-C.; Cheng, K.-M.; Su, W.-N.; Sung, K.-C.; Lin, T.-P.; Huang, J.-J.; Lin, S.-K.; Wong, F. F. *Tetrahedron* **2009**, *65*, 9592.

(108) (a) Horton, D. A.; Bourne, G. T.; Smythe, M. L. *Chem. Rev.* **2003**, *103*, 893. (b) Hajduk, P. J.; Bures, M.; Praestgaard, J.; Fesik, S. W. *J. Med. Chem.* **2000**, *43*, 3443.

(109) Pande, M. A.; Samant, S. D. *Recyclable Catalysis* **2012**, *1*, 6.

(110) Chalifour, R. J.; McLaughlin, R. W.; Lavoie, L.; Morissette, C.; Tremblay, N.; Boulé, M.; Sarazin, P.; Stéa, D.; Lacombe, D.; Tremblay, P.; Gervais, F. *J. Biol. Chem.* **2003**, 34874.

(111) (a) LeVine III, H. *Anal. Biochem.* **2006**, *356*, 265. (b) LeVine III, H.; Ding, Q.; Walker, J. A.; Voss, R. S.; Augelli-Szafran, C. E. *Neurosci. Lett.* **2009**, *465*, 99.

(112) Auburn, P. R.; Mackenzie, P. B.; Bosnich, B. *J. Am. Chem. Soc.* **1985**, *107*, 2033.

(113) Kubota, Y.; Nakada, S.; Sugi, Y. *Synlett* **1998**, 183.

(114) Mojtahedi, M. M.; Javadpour, M.; Abaee, M. S. *Ultrason. Sonochem.* **2008**, *15*, 828.

(115) Duffy, K. J.; Darcy, M. G.; Delorme, E.; Dillon, S. B.; Eppley, D. F.; Erickson-Miller, C.; Giampa, L.; Hopson, C. B.; Huang, Y.; Keenan, R. M.; Lamb, P.; Leong, L.; Liu, N.; Miller, S. G.; Price, A. T.; Rosen, J.; Shah, R.; Shaw, T. N.; Smith, H.; Stark, K. C.; Tian, S.-S.; Tyree, C.; Wiggall, K. J.; Zhang, L.; Luengo, J. I. *J. Med. Chem.* **2001**, *44*, 3730.

(116) Xu, X.-H.; Wang, X.; Liu, G.-k.; Tokunaga, E.; Shibata, N. *Org. Lett.* **2012**, *14*, 2544.

(117) Alsabeh, P. G.; Lundgren, R. J.; McDonald, R.; Johansson Seechurn, C. C. C.; Colacot, T. J.; Stradiotto, M. *Chem. Eur. J.* **2013**, *19*, 2131.

(118) (a) Hansch, C.; Leo, A.; Taft, R. W. *Chem. Rev.* **1991**, *91*, 165. (b) Hammett, L. P. *J. Am. Chem. Soc.* **1937**, *59*, 96.

(119) Murata, M.; Buchwald, S. L. *Tetrahedron* **2004**, *60*, 7397.

(120) Fürstner, A.; Kennedy, J. W. J. *Chem. Eur. J.* **2006**, *12*, 7398.

(121) Castanet, A.-S.; Colobert, F.; Broutin, P.-E. *Tetrahedron Lett.* **2002**, *43*, 5047.

(122) Adjabeng, G.; Brenstrum, T.; Wilson, J.; Frampton, C.; Robertson, A.; Hillhouse, J.; McNulty, J.; Capretta, A. *Org. Lett.* **2003**, *5*, 953.

(123) Farrugia, L. J. *J. Appl. Crystallogr.* **1997**, *30*, 565.

(124) (a) Mann, B. E. *J. Magn. Reson.* **1976**, 17. (b) Led, J. J.; Gesmar, H. *J. Magn. Reson.* **1982**, 444. (c) Blacquiere, J. M.; Higman, C. S.; McDonald, R.; Fogg, D. E. J. *J. Am. Chem. Soc.* **2011**, 14054.

(125) Beller, M.; Ehrentraut, A.; Fuhrmann, C.; Zapf, A., US Patent 20040068131.

(126) Hansen, H. M.; Lysen, M.; Begtrup, M.; Kristensen, J. L. *Tetrahedron* **2005**, *61*, 9955.

(127) *SAINT-Plus, Version 7.23a; Data Reduction and Correction Program. Bruker AXS Inc., Madison, WI.* **2004**.

(128) Sheldrick, G. M. *SADABS, Area-Detector Absorption Correction, v2.10, Universität Göttingen (Germany)* **1999**.

(129) Sheldrick, G. M. *Acta. Crystallogr.* **2008**, 112.